

An Orally Bioavailable, Indole-3-glyoxylamide Based Series of Tubulin Polymerization Inhibitors Showing Tumor Growth Inhibition in a Mouse Xenograft Model of Head and Neck Cancer

Helen E. Colley,^{*,†,∇} Munita Muthana,^{‡,∇} Sarah J. Danson,[§] Lucinda V. Jackson,^{||} Matthew L. Brett,^{||} Joanne Harrison,^{||} Sean F. Coole,^{||} Daniel P. Mason,^{||} Luke R. Jennings,[†] Melanie Wong,^{⊥,∇} Vamshi Tulasi,[⊥] Dennis Norman,[⊥] Peter M. Lockey,[⊥] Lynne Williams,[‡] Alexander G. Dossetter,[#] Edward J. Griffen,^{#,∇} and Mark J. Thompson^{*,||,∇}

[†]School of Clinical Dentistry, University of Sheffield, 19 Claremont Crescent, Sheffield S10 2TA, U.K.

[‡]Department of Oncology, The University of Sheffield, Medical School, Beech Hill Road, Sheffield S10 2RX, U.K.

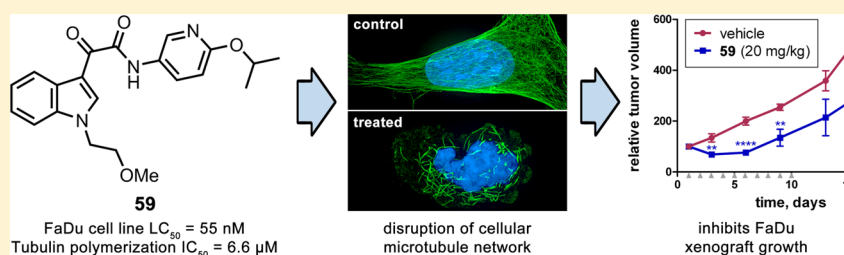
[§]Academic Unit of Clinical Oncology and Sheffield Experimental Medicine Centre, Weston Park Hospital, Whitham Road, Sheffield S10 2SJ, U.K.

^{||}Department of Chemistry, University of Sheffield, Brook Hill, Sheffield S3 7HF, U.K.

[⊥]Charles River, 8–9 Spire Green Centre, Harlow, Harlow, Essex CM19 5TR, U.K.

[#]MedChemica Limited, Ebenezer House, Rycroft, Newcastle-Under-Lyme, Staffordshire ST5 2BE, U.K.

Supporting Information



ABSTRACT: A number of indole-3-glyoxylamides have previously been reported as tubulin polymerization inhibitors, although none has yet been successfully developed clinically. We report here a new series of related compounds, modified according to a strategy of reducing aromatic ring count and introducing a greater degree of saturation, which retain potent tubulin polymerization activity but with a distinct SAR from previously documented libraries. A subset of active compounds from the reported series is shown to interact with tubulin at the colchicine binding site, disrupt the cellular microtubule network, and exert a cytotoxic effect against multiple cancer cell lines. Two compounds demonstrated significant tumor growth inhibition in a mouse xenograft model of head and neck cancer, a type of the disease which often proves resistant to chemotherapy, supporting further development of the current series as potential new therapeutics.

INTRODUCTION

Microtubule-targeting agents (MTAs) are a major class of cancer chemotherapeutic drugs^{1,2} that have enjoyed decades of clinical success in the treatment of a wide range of cancers. These agents bind to heterodimers of α - and β -tubulin, the building blocks of cellular microtubules, and in doing so interfere with normal microtubule dynamics. Depending on their exact binding site, MTAs can stabilize or destabilize microtubules, but in either event, disruption of normal function results and ultimately leads to apoptosis. The precise mechanism of action of MTAs used in the clinic is still incompletely understood, and as such continues to be investigated and debated.^{3–6} Although it had long been assumed that MTAs are effective against cancers solely through interruption of mitosis, on which their effect is certainly important,^{7,8} more recent evidence points toward a multi-

faceted mode of action arising from interaction with microtubules throughout the cell cycle.^{7,9–11}

Despite the advances in treatment MTAs have undoubtedly offered, existing agents suffer from some significant drawbacks¹² which often compromise clinical efficacy and can lead to treatment failure. Drug resistance (either innate or acquired) is a serious problem,^{13–16} and adverse toxicities such as peripheral neuropathy^{17,18} (PN) can prove dose-limiting, indicative of a narrow therapeutic window.

The search for novel agents in the class has therefore been intensive^{19,20} and whereas the more recent approvals, such as vinflunine,²¹ eribulin,^{22–24} ixabepilone,^{25,26} and the antibody–drug conjugate trastuzumab emtansine,²⁷ have proven

Received: August 25, 2015

Published: November 18, 2015

beneficial for a limited number of indications, not all clinical studies have demonstrated improved efficacy, and classical MTA-associated adverse reactions,^{28–30} including PN,^{31–33} are still encountered with these newer agents. It is worth noting that eribulin in particular has shown evidence of an improved safety profile and promise for wider application³⁴ although drug resistance has also been encountered with this agent.³⁵ Overall, in spite of some welcome benefits, the newer MTAs have seemingly failed to displace their older counterparts to a significant degree, at least to date. Although they are expected to gain broader use in the future, it remains an important goal for the field to develop novel agents which can demonstrate the same broad spectrum of efficacy as the more established drugs while offering significant progress in overcoming resistance and minimizing unmanageable toxicity.

To this end, many novel small-molecule MTAs have been reported in recent years,^{36–39} some with promising preclinical or early clinical data, although the challenge of demonstrating superior clinical performance over existing agents is considerable. Nonetheless, such compounds include indibulin **1** and rosabulin **2** (Figure 1), two experimental drugs with high structural similarity for which a novel tubulin binding site has been claimed.^{40,41}

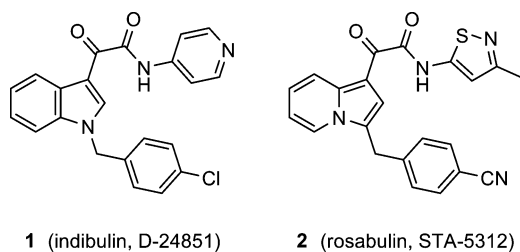


Figure 1. Structures of glyoxylamide-based tubulin polymerization inhibitors that have progressed to clinical trials.

Little has been published regarding **2**, and its development appears to have been abandoned following phase I clinical trials.^{41,42} Compound **1** showed *in vivo* efficacy and early evidence of improved therapeutic window,⁴³ suggested to be a consequence of it targeting a novel binding site on tubulin.⁴⁰ It has persisted in phase I clinical development for a number of years, with the primary issue apparently being low exposure,^{44,45} in turn likely due to its poor aqueous solubility. Although both **1** and **2** have encountered problems in the clinic, the fact remains that they were promising preclinical agents, and the issues subsequently encountered for **1** do not seem insurmountable.

In the light of an intriguing report⁴⁶ suggesting indole-3-glyoxylamides unsubstituted at N1 can still make effective tubulin polymerization inhibitors, we supposed that exploring modifications of **1** and **2** at this locus would be a viable starting point for the development of new potential MTAs. The initial focus of the present work was replacement of the *p*-chlorobenzyl group of **1**, aiming first to improve aqueous solubility through the dual strategy of reducing aromatic ring count and increasing saturation. The benefits in terms of compound developability of both minimizing the number of aromatic rings⁴⁷ and increasing the count of *sp*³ carbon atoms^{48–50} are gaining appreciation as a result of several studies supporting such rationale over recent years. Solubility prediction by either direct calculation or matched molecular

pair analysis (MMPA) is shown to justify such an approach in the present context.

Tubulin polymerization inhibitors identified during this study were first applied in models of head and neck cancer (HNC), a disease in which existing MTAs have shown promise for improved treatment outcomes if the common problems of toxicity and drug resistance can be overcome.^{51–56}

HNC is the sixth most common cancer worldwide and is of particular concern due to rising incidence over the past two decades. Treatment is often some combination of surgery, radiotherapy, and chemotherapy, but overall survival rates have not significantly improved in many years and response rates to typical first-line chemotherapy regimens, usually a combination of 5-FU and cisplatin, are problematically low (around 30%).^{51,57} More recently, targeted therapies have been introduced⁵⁸ in an effort to improve treatment of HNC, most notably the EGFR-targeted monoclonal antibody cetuximab, which was approved in 2008 for use in locally advanced or metastatic/recurrent HNC. Other targeted therapies remain under investigation in HNC, including antiangiogenic agents, PI3K/Akt/mTOR inhibitors, and p53 gene replacement therapy.^{58–60} Whereas such targeted approaches have certainly benefited some patients, their overall impact on HNC treatment has been mixed,^{59–62} and personalized or combination therapy will likely prove necessary to maximize clinical success of these targeted drugs;^{60,61} thus, more effective general first-line chemotherapy treatments are still much needed. Given the limited but promising data on the potential of MTAs in HNC, appropriate disease models therefore represent a useful context for the testing and development of new agents in the class.

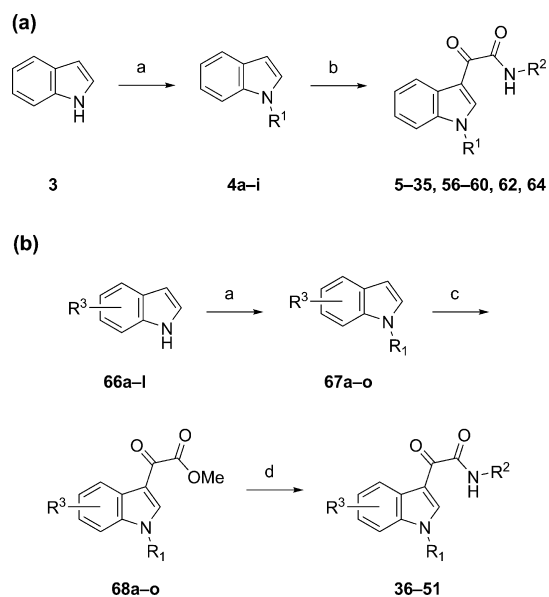
RESULTS AND DISCUSSION

Solubility Prediction Studies. To test our initial assumptions regarding modifications to **1**, directly calculated solubilities were determined for some of the first-generation analogues planned initially and detailed in the SAR study below (**5–13**, **17**, **18**, **32**, and **33**; Tables 1–3). Direct calculation of aqueous solubility is known to represent a considerable challenge, although several methods now exist with accuracy to well within an order of magnitude for most small molecules.⁶³ The compounds specified above were evaluated by the method of Tetko et al.⁶⁴ using the web-based ALOGPS 2.1 program,⁶⁵ which estimated at least an order of magnitude improvement in solubility over **1** in each case (Supporting Information, Table S11). Given such direct prediction of solubility is acknowledged as a difficult problem, an alternative method was applied to further validate our proposed structural modifications to **1**. A matched pairs approach was employed that has previously shown promise in providing guidance when seeking to optimize molecular properties.⁶⁶ The database of solubility transformations curated by MedChemica⁶⁷ was used to give an historical view of how different chemical changes have influenced measured solubility in order to set reasonable bounds on what effects should be expected. The chemical changes were identified using a matched pair finding approach combining that of Hussein and Rea⁶⁸ with that of Warner et al.,⁶⁹ which captures both the group being changed and essentially⁷⁰ the local chemical environment around the change. The data associated with each chemical change in its local environment was then recalled from the database and the recovered values used to construct a solubility network (see Supporting Information, Figure S16 and accompanying

legend). Results of the matched pair analysis were in agreement with those from direct calculation above, predicting at least an order of magnitude increase in solubility for analogues of 1 replacing the *p*-chlorobenzyl group with simple aliphatic substituents. Addition of a methoxy-group to the pyridine ring, as was ultimately found necessary to recover activity, was predicted to cause a small compromise in solubility although these analogues (8–10; Table 1) were still expected to be much more soluble than 1.

Chemistry. Glyoxylamides derived from *N*-substituted indoles 4 were prepared using a straightforward two-step, one-pot procedure essentially as described previously (Scheme 1a).⁷¹ However, for derivatization of intermediates 67

Scheme 1. General Synthetic Routes to the Indole-3-glyoxylamide Screening Libraries, Using Either (a) a One-Pot Procedure, or (b) a Two-Step Route Suitable for Modified Indoles^a



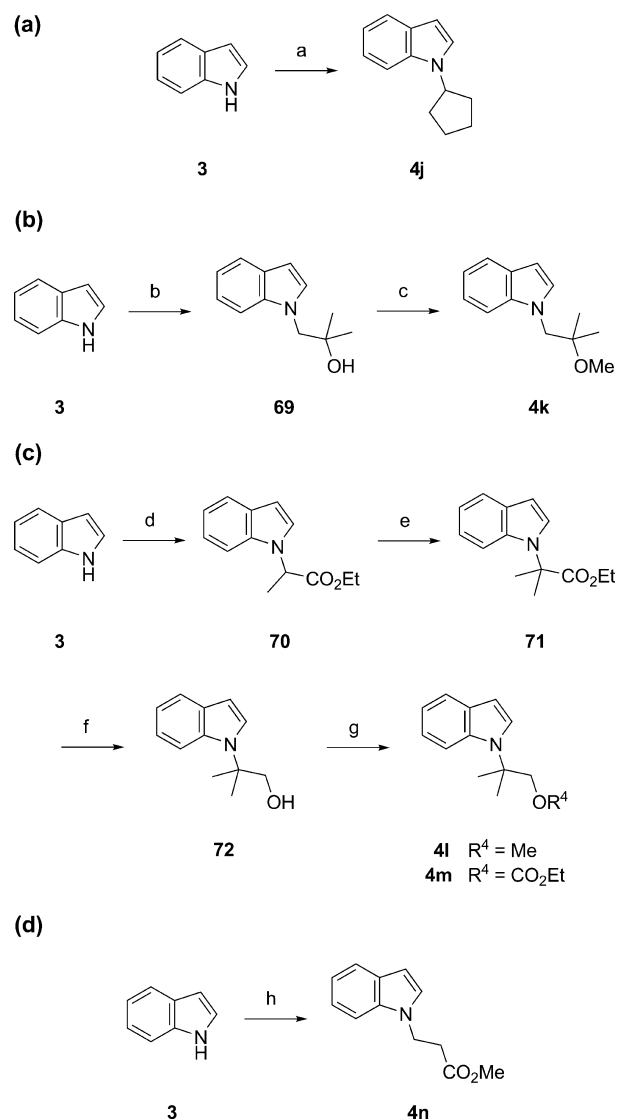
^aReagents and conditions: (a) NaH, R¹-X, DMF or THF, 6–83%; (b) (i) oxalyl chloride, THF, 3 h, (ii) R²-NH₂, DIPEA, DMAP (catalytic), THF, 18 h, 20–78%; (c) methyl chlorooxoacetate, AlCl₃, CH₂Cl₂, 0 °C, 7–86%; (d) R²-NH₂, 30 mol % TBD, toluene, 85 °C, 18 h, 5–58%. For the sake of clarity, individual structures of 4a–i (Table S8) and modified indoles 66a–l (Table S9) and their *N*-alkylated derivatives 67a–o (Table S10) are provided in the Supporting Information.

containing modifications at indole positions 4–7, this approach was surprisingly found to be unsuitable, in contrast to earlier examples where similar substrates unsubstituted at N1 (i.e., R¹ = H) gave the expected products, albeit in reduced yields.⁷¹ In the present study, when compounds of general structure 67 were reacted as outlined in Scheme 1a (with or without heating to 50 °C in the first step to promote reaction with oxalyl chloride); no significant formation of the expected indole-3-glyoxylamide products was observed as evidenced by HPLC or LC-MS, yet little of the starting indoles remained, suggesting degradation of these starting materials had occurred. Addition of DIPEA to the first step of the process, reaction with oxalyl chloride, to prevent strongly acidic conditions from developing only appeared to suppress reaction of the indole derivative with the latter. Thus, an alternative route was employed (Scheme

1b) via glyoxylate ester intermediates 67, formed using a Friedel–Crafts reaction with methyl chlorooxoacetate. This transformation has been shown effective with the less reactive azaindole derivatives,⁷² as also proved the case in our hands, and was easily adapted for substituted indoles with acceptable yields. The resulting ester intermediates were then readily converted into the desired glyoxylamides via direct amidation catalyzed by 1,5,7-triazabicyclo[4.4.0]dec-5-ene (TBD).⁷³

Some *N*-substituted indole derivatives not accessible through direct *N*-alkylation were also required, and these were approached by various other methods as appropriate (Scheme 2). 1-Cyclopentylindole 4j was prepared by reaction with cyclopentylboronic acid using conditions reported for prepara-

Scheme 2. Preparation of *N*-Substituted Indole Intermediates Accessed via Other Routes^a

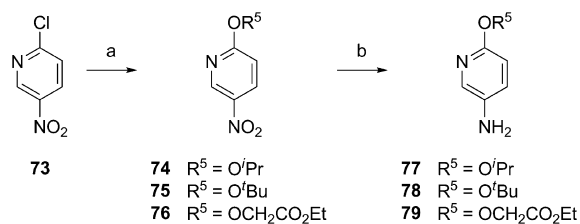


^aReagents and conditions: (a) cyclopentylboronic acid, NaHMDS, 10 mol % Cu(OAc)₂, DMAP, toluene, 95 °C, 18 h, 34%; (b) isobutene oxide, NaH, DMF, 24 h, 74%; (c) MeI, NaH, THF, 24 h, 52%; (d) ethyl 2-bromopropionate, NaH, DMF, 40 °C, 18 h, 74%; (e) LDA, MeI, THF, –78 °C → rt, 18 h, 86%; (f) LiAlH₄, THF, –78 °C → rt, 18 h, 78%; (g) MeI, NaH, THF, 3 h, 79% (4l) or ethyl bromoacetate, NaH, DMF, 20 h, 29% (4m); (h) methyl acrylate, 50 mol % DBU, MeCN, 50 °C, 12 h, 43%.

tion of the cyclopropyl derivative from the requisite boronic acid.⁷⁴ Ring-opening of isobutene oxide by indole anion⁷⁵ followed by *O*-methylation furnished intermediate **4k**. Tertiary alkyl derivatives **4l** and **4m** were accessed by *O*-alkylation of **72**, which in turn was synthesized in three steps from indole **3** utilizing methodology already reported for some substituted indole starting materials.⁷⁶ Finally, **4n** was prepared by an aza-Michael reaction between indole and methyl acrylate.⁷⁷ Glyoxylamide synthesis from these additional intermediates **4j–n** was performed according to the general method outlined above (Scheme 1a).

Variation of the glyoxylamide N-substituent R² (Scheme 1) was mostly achieved through the use of commercially available starting materials, although some such analogues required in-house synthesis of the amine precursors, R²-NH₂ (Scheme 3).

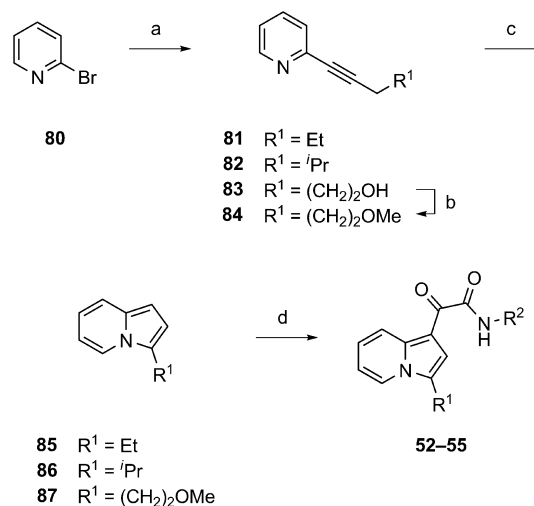
Scheme 3. Preparation of 5-Aminopyridines with Varied 2-Alkoxy Substituents^a



^aReagents and conditions: (a) R⁵-OH, NaH, ^tPrOH or DMF or THF, 44–65%; (b) H₂, Pd-C, MeOH, 62–95%.

Nucleophilic aromatic substitution of 2-chloro-5-nitropyridine **73** with alkoxides followed by hydrogenolysis of the nitro-group⁷⁸ provided easy access to intermediates **77–79** for use in glyoxylamide syntheses. A small number of analogues exchanging the indole core for indolizine, as found in model compound **2**, were also evaluated. 3-Alkylindolizines **85–87** were prepared from 2-bromopyridine in two steps by a known route^{79,80} comprising Sonogashira cross-coupling followed by a copper(I)-mediated cyclization. For the most part, this sequence proceeded smoothly, with the exception of intermediate **84**, whose synthesis proved surprisingly challenging. Sonogashira reaction between 2-bromopyridine **80** and pent-4-yn-1-ol readily afforded alcohol **83**, but initial attempts at *O*-methylation in THF were unsuccessful, giving none of the desired product and seemingly resulting in intramolecular reaction between the generated alkoxide and the alkyne (data not shown). Attempts to convert **83** into 3-(2-hydroxyethyl)-indolizine resulted in similar mixtures with no formation of the expected product. Methylation under modified conditions in DMF at 0 °C did provide a low yield of **84**, but its isolation from the product mixture formed was not straightforward so these shortcomings inspired an alternative approach whereby pent-4-yn-1-ol was first methylated to give 5-methoxypent-1-yne. Because this intermediate is somewhat volatile (lit.⁸¹ bp 107–115 °C), the crude material was used without extensive purification and reacted with 2-bromopyridine under the usual conditions (Scheme 4). This completed an alternative route to **84**, which although still low-yielding, proved operationally simpler and more amenable to scale than the earlier method. Once in hand, the 3-alkylindolizine intermediates **84–86** were successfully elaborated into the desired glyoxylamides by the same two-step, one-pot procedure used for the majority of the indole derivatives (Scheme 1a).

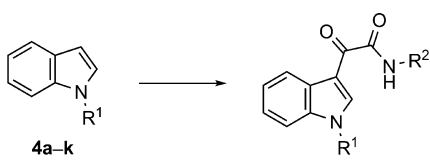
Scheme 4. Synthesis of Analogues Replacing the Indole System with an Indolizine Core^a



^aReagents and conditions: (a) R¹CH₂C≡CH, 2 mol % PdCl₂(PPh₃)₂, 4 mol % PPh₃, 4 mol % CuI, TEA, 18 h, 63–78%; (b) MeI, NaH, DMF, 0 °C, 3.5 h, 27%; (c) CuCl, DMA/TEA (7:1), 130 °C, 31–55%; (d) (i) oxalyl chloride, THF, 0 °C, 3 h, (ii) R²-NH₂, DIPEA, DMAP, THF, 18 h, 20–66%.

Primary Screening and Elucidation of SAR. Test compounds were first assessed for cytotoxicity against FaDu, an EGFR inhibitor insensitive⁸² HNC cell line derived from squamous cell carcinoma of the pharynx. Screens consisted of a 72 h end point MTT assay, and LC₅₀ values were determined for compounds showing cytotoxic activity at or below 10 μM. Analogues of **1** replacing the *p*-chlorobenzyl group at N1 with various simple alkyl groups showed a loss of cytotoxic activity (compounds **5–7**, Table 1); however, introduction of a methoxy-group adjacent to the pyridine ring nitrogen rescued activity (**8–10**), and switching the positions of these structural features, as in analogues **11–13**, was found to result in a further order of magnitude improvement in potency.

The foregoing results inspired synthesis of a wider range of analogues to investigate the SAR with respect to variation of both R¹ and R². First, systematic changes to the R² group revealed some clear trends in activity (Table 2). Removal of the pyridyl nitrogen (N to CH; **14** and **15**) resulted in a modest compromise to cytotoxic potency of no more than a 3-fold change, whereas in contrast, the inactivity of **16** indicated the *p*-methoxy group is essential for activity. Introduction of a second ring nitrogen at the *meta*-position of the aromatic group (pyrimidines **17** and **18**) showed the same modest reduction in potency as the aniline compounds, whereas introduction of a second ring nitrogen at the *ortho*-position (pyridazine **19**) proved highly detrimental to activity. A change of *p*-methoxy to ethoxy was tolerated with a 2-fold increase in LC₅₀ (compound **20**), whereas introduction of a second methoxy-substituent, as in **21**, was not. Replacement of the *p*-methoxy group with either trifluoromethoxy or trifluoromethyl was found severely detrimental to cytotoxic activity (compare **22** and **23** with **14** and **15**, and **24** and **25** with **12** and **13**, respectively). Exchanging the pyridine ring of **12** for a five-membered heterocycle, in analogous fashion to compound **2**, also proved unproductive. In sum, although the R² variations explored at this stage did not lead to improvement in cytotoxic potency in

Table 1. Cytotoxic Potencies of First-Generation Compounds in the Present Library^a


4	R ¹	Product	R ²	LC ₅₀ ± SEM ^b (FaDu), μM
- ^c		1		0.032 ± 0.003
4a		5		> 10
4b		6		> 10
4c		7		> 10
4a		8		4.18 ± 0.26
4b		9		1.75 ± 0.20
4c		10		0.235 ± 0.032
4a		11		0.219 ± 0.044
4b		12		0.085 ± 0.006
4c		13		0.017 ± 0.002

^aAn expanded form of this Table, including yields, is included in the Supporting Information (Table S1). ^bReported mean and SEM values represent the results of at least three independent experiments. ^cCompound **1** was sourced commercially.

any case, a number of changes were identified that are tolerated without seriously compromising activity.

In contrast, variation of the R¹ group did lead to the sought-after improvement in cytotoxic potency (Table 3). Changing the isopropyl group of **12** to *sec*-butyl slightly improved activity, although cyclopentyl **29** or isobutyl **30** substituents resulted in a 4-fold drop-off. Exchanging the oxygen atom in the 2-methoxyethyl substituent of **13** for a methylene group, as in *n*-butyl analogue **31**, caused no change in potency, indicating that the shape, rather than polarity, of this R¹ group is the major determinant of activity. Another change to **13**, introducing an additional methyl group α - to indole N1, resulted in the most potent compound in the series, **32**, with an LC₅₀ against FaDu of 12 nM. Other analogues of **13**, with a ring bridging the side chain oxygen atom, differed markedly in activity. Tetrahydrofuran compound **33** was essentially as potent as its parent, whereas oxetane analogue **34** was unexpectedly compromised by more than an order of magnitude. Introducing a tertiary center β - to N1, as in *gem*-dimethyl compound **35**, was not tolerated at all. Taken together, cytotoxicity data for this set of analogues are suggestive of a common binding pocket for the R¹ side chain. Although simple, linear R¹ chains give rise to some of the most potent compounds, a degree of further

Table 2. Cytotoxicity Data for Second-Generation Analogues Designed to Interrogate SAR at R² Position of the Parent Structure^a

4	R ¹	Product	R ²	LC ₅₀ ± SEM ^b (FaDu), μM
4b		14		0.181 ± 0.011
4c		15		0.059 ± 0.004
4b		16		> 10
4b		17		0.171 ± 0.013
4c		18		0.055 ± 0.002
4b		19		2.27 ± 0.24
4b		20		0.175 ± 0.010
4b		21		> 10
4b		22		8.93 ± 0.76
4c		23		0.487 ± 0.073
4b		24		> 10
4c		25		> 10
4b		26		10.4 ± 0.9
4b		27		> 10

^aAn expanded form of this Table, including yields, is included in the Supporting Information (Table S2). ^bReported mean and SEM values represent the results of at least three independent experiments (except **24**, *n* = 2).

substitution is tolerable or even beneficial, whereas too much substitution severely compromises or abolishes the observed activity.

The final set of compounds prepared for initial SAR studies focused on variation at indole positions 4–7 (Table 4). These analogues **36**–**51** retained the core structure of compounds **12** or **13** (except for **39**, R² = 4-methoxyphenyl) with systematically varied modifications at C4 to C7: chloro- or methoxy-substitution, or a switch to an azindole (i.e., ring CH to N). The majority of these changes were not tolerated and abolished cytotoxic activity, which was particularly unexpected in the case of azindoles **47**–**49** given such a small structural change. For analogues introducing an additional group, only chloro-substitution at C4 or C6 gave any retention of activity, albeit with at least a 20-fold increase in LC₅₀. The single useful modification identified in this series was a change from indole to 7-azindole, with **50** and **51** showing similar potency to their parent compounds, **12** and **13**, respectively.

Evaluation and Early Optimization of in Vitro PK Properties. A selection of the most promising compounds was

Table 3. Cytotoxicity Data for Second-Generation Analogues Designed to Interrogate SAR at R¹ Position of the Parent Structure^a

4	R ¹	Product	R ²	LC ₅₀ ± SEM ^b (FaDu), μM
4f		28		0.068 ± 0.005
4j		29		0.370 ± 0.037
4h		30		0.317 ± 0.032
4d		31		0.018 ± 0.003
4g		32		0.012 ± 0.001
4i		33		0.031 ± 0.003
4o		34		0.686 ± 0.097
4k		35		> 10

^aAn expanded form of this Table, including yields, is included in the Supporting Information (Table S3). ^bReported mean and SEM values represent the results of at least three independent experiments.

screened for solubility, microsomal stability, and Caco-2 permeability in an initial effort to identify likely ADME liabilities. Aqueous solubility thresholds for **12**, **13**, and **32** were estimated to be in the region of 10 μM by HPLC (cf. **1**, ≤ 1 μM) although reproducibility was difficult, thought to be due to approaching the detection limit by UV, such that these measurements were not considered reliable. Results from dynamic light scattering (DLS) experiments (see Supporting Information, Figure S6 and accompanying text) were more supportive of a solubility threshold of 10 μM or higher for several compounds, including thresholds of at least 20, 80, and 40 μM, respectively, for **12**, **13**, and **32**. Taken together, it appeared as anticipated that considerable improvement had already been realized over **1**, which in contrast was seen to form large aggregates at 10 μM by DLS with some evidence for aggregate formation at 1 μM (markedly raised count rate).

Caco-2 permeability data (Table 5) for selected compounds were predictive of good intestinal absorption, i.e. P_{app} (A → B) > 10 × 10⁻⁶ cm s⁻¹, with no evidence of active efflux (P_{app} ratio < 2). Mouse microsomal half-lives, estimated by extrapolation from 30 min assay end point values (Table S6), did prove a concern, however, indicating rapid clearance would likely be an issue in vivo. Metabolism was previously identified⁴⁴ as a possible contributing factor to the suboptimal pharmacokinetics of **1**, making this issue all the more important to address in the present series of related compounds.

A further selection of analogues was subsequently designed and synthesized in an attempt to address the shortcomings with respect to metabolic stability. It had not been possible to extract conclusive trends from the first round of data, although the R¹ group did appear to influence stability (noting $t_{1/2}$ order **32** > **13** > **12**); thus, exchange of the indole for an indolizine core heterocycle, replacing the C–N bond linking the R¹ substituent with a C–C bond, was attempted but unfortunately did not prove advantageous. Indolizine analogues **53** and **54** proved

Table 4. Synthesis and Evaluation of Further Analogues, Modified at Indole Positions 4–7^a

R ³ modification	R ¹	Indole 67	Product	LC ₅₀ ± SEM ^b (FaDu), μM
4-Cl		67a	36	2.13 ± 0.35
5-Cl		67b	37^c	> 10
5-Cl		67c	38	> 10
5-Cl		67b	39^{c,d}	> 10
6-Cl		67d	40	1.77 ± 0.08
7-Cl		67e	41	10.2 ± 0.8
4-OMe		67f	42	7.78 ± 0.15
5-OMe		67g	43	> 10
5-OMe		67h	44	> 10
6-OMe		67i	45	> 10
7-OMe		67j	46	> 10
4-aza		67k	47	> 10
5-aza		67l	48	> 10
6-aza		67m	49	> 10
7-aza		67n	50	0.126 ± 0.010
7-aza		67o	51	0.027 ± 0.002

^aAn expanded form of this Table, including yields, is included in the Supporting Information (Table S4). ^bReported mean and SEM values represent the results of at least three independent experiments. ^cCompounds **37** and **39** were synthesized according to Scheme 1a, in turn meaning intermediate **68b** was not synthesized. ^dThe R² group in **39** is 4-methoxyphenyl, not 2-methoxy-5-pyridyl as in all the other examples.

equally as metabolically unstable as their indole counterparts **12** and **13**, if not more so, and also suffered from a small but notable drop-off in cytotoxic potency. Alternatively, introducing a tertiary center α- to N1, as in **57**, did not offer any improvement either.

In contrast, adding extra bulk to the methoxy-substituent of the R² group to block metabolism at this site greatly improved stability, conferring an order of magnitude increase in half-life without adversely compromising cytotoxic potency (compare **59** with **13**). However, adding further substitution at this site did negatively affect activity (compare *tert*-butyl derivative **60**). A related modification to the methoxy-group in the R¹ substituent resulted in modest stabilization (comparing **56** with **13**), but in this case the penalty in cytotoxic activity was too severe to consider it a useful change.

Matched pair analysis for prediction of solubility, as described above, anticipated a modest but acceptable compromise for representative compounds introducing more bulky hydrophobic groups in an attempt to block metabolism

Table 5. Assessment and Preliminary Optimization of Selected in Vitro PK Properties

	Core	R ¹	R ²	LC ₅₀ ± SEM ^b (FaDu), μM	MLM t _{1/2} , min	Caco-2 P _{app} (A→B) ^c	P _{app} ratio ^d
12	indole 4b			0.085 ± 0.006	5	19.8	1.4
13	indole 4c			0.017 ± 0.002	11	32.0	1.2
17	indole 4b			0.171 ± 0.013	5	39.8	1.0
32	indole 4g			0.012 ± 0.001	16	33.6	1.1
33	indole 4i			0.031 ± 0.003	34	35.0	0.7
52	indolizine 85			0.110 ± 0.016	–	–	–
53	indolizine 86			0.160 ± 0.021	< 5	–	–
54	indolizine 87			0.036 ± 0.003	6	–	–
55	indolizine 87			0.758 ± 0.045	–	–	–
56	indole 4e			0.211 ± 0.018	23	–	–
57	indole 4l			0.137 ± 0.010	16	–	–
58	indole 4b			0.408 ± 0.036	66	–	–
59	indole 4c			0.055 ± 0.004	99	15.2 ^e	0.9
60	indole 4c			0.858 ± 0.102	–	–	–
61	indole 4m			> 10	–	–	–
62	indole 4n			0.168 ± 0.026	–	–	–
63	indole 4n			> 10	–	–	–
64	indole 4c			> 10	–	–	–
65	indole 4c			> 10	–	–	–

^aAn expanded form of this Table, including yields, is included in the Supporting Information (Table S5). ^bReported mean and SEM values represent the results of at least three independent experiments. ^cP_{app} values are quoted as ×10⁶ cm⁻¹; values quoted are the mean of two independent experiments, which were in good agreement in every case. ^dP_{app} ratio = P_{app} (B → A)/P_{app} (A → B). ^eRecovery was <50% in the Caco-2 assay with 59, indicating potential issues with solubility or binding to cellular proteins/lipids under the assay conditions, which may reduce the accuracy of the result.

(56, 57, 60; Supporting Information, Figure S17). These predictions were indeed reflected in the DLS measurements referred to earlier (Supporting Information Figure S6). Other analogues prepared specifically with the aim of improving solubility included 61, 63, and 65, and although all three compounds appeared fully soluble up to 200 μM by DLS (Supporting Information, Figure S6a,b), introduction of the carboxylic acid group abolished cytotoxicity in every case.

Targeting of Tubulin. A subset of cytotoxic compounds from the initial SAR study was evaluated further to confirm their presumed mode-of-action, inhibition of tubulin polymer-

ization (Figure 2). GTP-promoted microtubule assembly from purified porcine brain tubulin was followed by measuring changes in optical density (OD₃₄₀) of the solution over a period of 60 min following initiation of reaction, according to a well-established protocol.⁸³ Increasing concentrations of 12, 32, 33 (Figure 2a), 51, 57, and 59 were found to suppress the polymerization reaction in a dose-dependent manner. Assay end point values, expressed relative to vehicle control, were considered indicative of extent of reaction, and a secondary plot of these results against inhibitor concentration permitted derivation of IC₅₀ values (Figure 2b; full dose–response plots

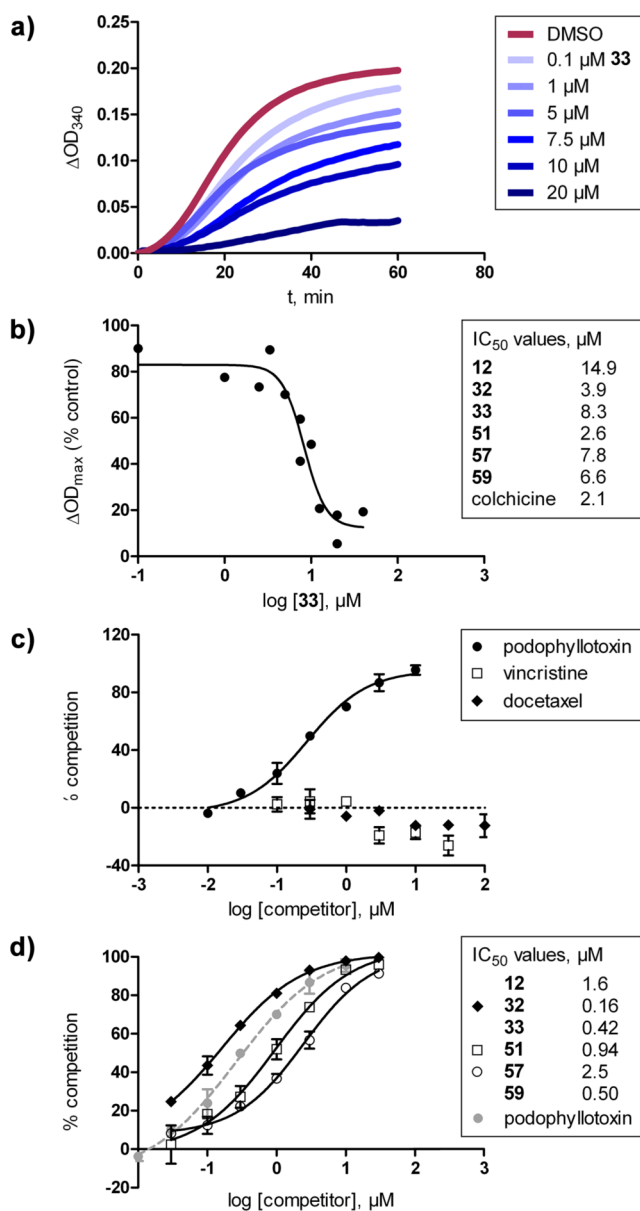


Figure 2. (a) Tubulin polymerization time-course plots following changes in OD_{340} of reaction mixtures in the presence of increasing concentrations of 33 (blue lines) compared to vehicle control (red line). (b) Secondary plots of reaction end point data allow determination of IC_{50} for inhibition of tubulin polymerization by 33 and other compounds as indicated. Data from multiple experiments was plotted as individual data points, as shown, and fit globally. (c) Competition for tubulin binding between [³H]-colchicine (at 0.1 μM) and vincristine, docetaxel, or podophyllotoxin shows only the latter competes with binding at the colchicine site, as expected. (d) The same six compounds listed in (b) above all compete for binding at the colchicine site with IC_{50} values as shown, with representative results graphed for 32, 51, 57, and podophyllotoxin (positive control).

for all six compounds, and colchicine used as a positive control, are included in the Supporting Information, Figure S1). In contrast, compounds 11 and 13 unexpectedly showed no inhibition in the polymerization assay, alongside 1, for which such a result has already been reported⁴⁰ (Supporting Information, Figure S2). Earlier work⁴⁰ on 1 suggested it does not inhibit the polymerization of post-translationally modified tubulin (acetylated on Lys40 of the α -subunit) from

mature animal brain, such as would be expected in a commercially sourced preparation, and an unmodified sample derived from infant animal brain is required to see inhibition. This observation, among others, led the authors to conclude the compound binds to an unprecedented site in the vicinity of Lys40 of α -tubulin. The apparent inactivity of 1 in the present tubulin polymerization assays was therefore anticipated, but similar results for 11 and 13 seemed unusual given the positive results for closely related analogues.

To investigate further, the above set of compounds, together with 10, 23, 50, and 57, was tested in an alternative tubulin polymerization assay which relies on the fluorescence of DAPI when incorporated into growing microtubules,⁸⁴ as opposed to detecting polymer growth through changes in OD_{340} . Under these conditions, inhibition was now observed for all library compounds, including 11 and 13 (Supporting Information, Figures S2,S3). Where results were obtained in both assays, there was qualitative evidence for agreement between the relative IC_{50} values (Supporting Information, Figure S4), although the very small sample size precludes any firm evidence of a correlation. Similarly, the trend in potencies obtained in both polymerization assays (particularly the fluorescence-based method, with the larger number of compounds screened) is in good general agreement with that seen earlier in cellular cytotoxicity activities, suggesting interaction with tubulin was a major factor leading to the observed toxic phenotype (see Supporting Information, Figure S5 and accompanying legend). It is worth noting that although 1 did not show inhibition of tubulin polymerization in the absorbance-based assay, as stated above, there was some evidence of activity using the fluorescence-based method (Supporting Information, Figure S2), although results between experiments were inconsistent. It is thus not possible to reach a conclusion either way regarding inhibition by 1, although it seemed plausible to suggest that obtaining a clear result was compromised by the poor solubility of the compound. To investigate this possibility further and assess whether the initial results for 11 and 13 described above might likewise be linked to solubility issues, DLS experiments were carried out to look for evidence of aggregation over a concentration range relevant to the inhibition assays (Supporting Information, Figure S6a,b). Extensive aggregation was seen for 1 at 10 μM , forming particles of approximately 1 μm in diameter, with some evidence for aggregate formation at 1 μM as already noted above. In contrast, most compounds evaluated from the present library showed no obvious evidence of aggregation at 10 μM , which was true of the subset evaluated in both the tubulin polymerization assays and the DLS screen (11–13, 32, 33, 53, 57, and 59). It seems apparent that 11 and 13 are not appreciably different in solubility to other representative library members which did display tubulin polymerization inhibition in both assays, suggesting the observed inactivity of the former in the OD_{340} -based assay is due to an as yet unknown property of these compounds (because both seem fully soluble over the concentration range used). In contrast, the DLS results lend support to the idea that, in the case of 1, poor compound solubility may indeed interfere with the reliability of these assay readouts.

Having gained evidence that compounds from the current series do interact directly with tubulin, it was considered important to elucidate their binding site. There are three well-characterized binding domains on tubulin, the colchicine, *Vinca* alkaloid, and taxane binding sites, all located on the β -subunit, and most (but not all) established MTAs bind at or close to

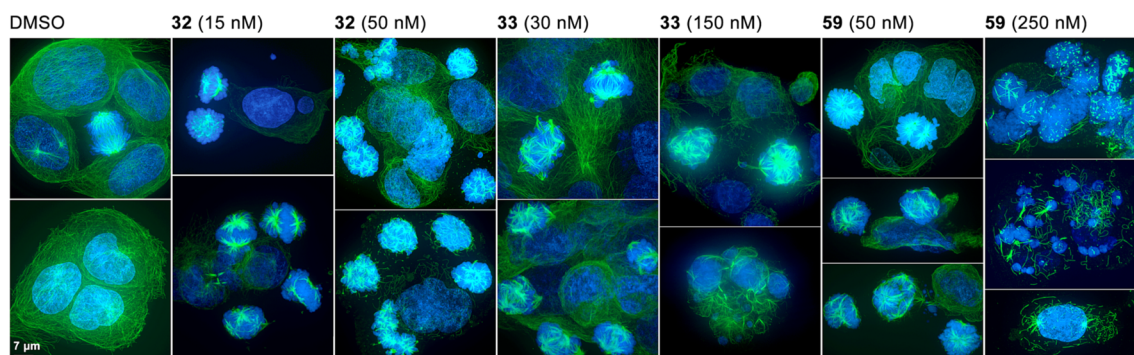


Figure 3. Representative images of fixed FaDu cells stained for α -tubulin (green) and DNA (blue) after treatment as indicated for 24 h. Control cells (DMSO-treated) show a well-structured microtubule network and are dividing normally, with mitotic cells in anaphase (center) and prophase (left) clearly visible in the upper-left panel. In contrast, cells treated with active tubulin polymerization inhibitors showed multiple mitotic defects, most notably formation of multipolar spindles, and compound **59** appeared especially destructive to the microtubule network at high concentration. Images in all panels are to the same scale. An enlarged version of these images is provided in the Supporting Information for improved clarity (Figure S13).

one of them. Taxane domain ligands are known to act as microtubule stabilizers, whereas drug binding to the *Vinca* alkaloid or colchicine sites destabilizes microtubules. Given that actives from the current series inhibit tubulin polymerization, binding at either the colchicine or *Vinca* domains was anticipated. Evaluation of test compounds at all sites was probed by competition with tritium-labeled standards (colchicine, vinblastine, or paclitaxel), looking for dose-dependent displacement of radioactivity from the protein with increasing test compound concentration. The same set of compounds evaluated in the tubulin polymerization assays was screened for binding. Results at the colchicine site proved the most conclusive, with the assay first validated using competition of [^3H]-colchicine with podophyllotoxin, a known binder at this site⁸⁵ (Figure 2c). As expected, no competition with [^3H]-colchicine was observed with either vincristine or docetaxel. All test compounds gave positive results, with selected IC_{50} values presented in Figure 2d together with dose–response plots for **32**, **51**, and **57** (see Supporting Information for dose–response plots for all compounds, Figure S7). Good correlation between FaDu cytotoxicity (LC_{50} values) and IC_{50} for competition with [^3H]-colchicine seems apparent (Supporting Information, Figure S8), although as applies to the polymerization assay results above, a firm conclusion cannot be drawn from existing data given the small sample size. Evaluation of **1** again proved problematic (Figure S9): a partial competition curve was obtained up to a point where binding leveled off, suggesting a solubility threshold could have been reached. It is informative to consider this result in the light of previous data⁸⁶ reporting that [^3H]-**1** was readily displaced from tubulin by excess colchicine, whereas in the reciprocal experiment, [^3H]-colchicine binding was only partially competed by excess **1**. Considering all aspects together, these results could be interpreted to mean that **1** binds to the colchicine site with good affinity but its poor solubility hinders accurate assessment of this binding, especially where the compound must be present in excess. It remains to be said that binding of **1** to the colchicine site is necessarily assessed independently of that at the other proposed site on the α -subunit, suggesting the compound could be a dual site binder to tubulin.

In our experience, evaluation of the same 12 library compounds as above at the *Vinca* alkaloid and taxane binding sites proved unexpectedly difficult (for a more detailed analysis, see Supporting Information, Figures S10–S12 and accompany-

ing legends). Briefly, at the *Vinca* site, docetaxel was found to compete with [^3H]-vinblastine binding just as well as vincristine, whereas at the taxane site, vincristine competed with [^3H]-paclitaxel binding with an IC_{50} only 2-fold higher than that for docetaxel (Supporting Information, Figure S10). These observations limited the confidence with which clear results could be drawn from the data; however, none of the compounds showed any obvious evidence of binding at the taxane domain in agreement with their activity as inhibitors, rather than promoters, of tubulin polymerization. At the *Vinca* site, some (but not all) of the test compounds displayed IC_{50} values close to that of vincristine, suggesting the intriguing possibility that these members of the library are capable of binding tubulin at both the colchicine and *Vinca* alkaloid domains (Supporting Information, Figure S12); however, given the difficulties encountered with the assay this can only be considered a preliminary finding, deserving further investigation in due course.

In sum, a small set of compounds from the cytotoxicity-led SAR study was found to inhibit tubulin polymerization through binding at the colchicine site, with good general agreement between potency in both assays and the earlier LC_{50} data. Attention was next focused on whether the expected phenotype for destabilization of microtubules is seen at the cellular level.

To visualize the effect of **32**, **33**, and **59** on the microtubule network, FaDu cells were treated with two concentrations of each compound for 24 h then fixed and stained for α -tubulin and DNA (Figure 3). Concentrations were chosen corresponding to approximately 1 \times and 5 \times the cytotoxic LC_{50} (72 h end point); after exposure for 24 h, the majority of the cell population will be in mitotic arrest at the higher of these concentrations (as discussed later; see Figure 4).

All three compounds proved able to induce mitotic spindle defects at low concentration, and in particular, several cells with multipolar spindles were seen with **33** and **59**. It is also clear that a high concentration of each compound caused extensive damage to the microtubule network. Comparison of the images suggests there may be some differences in the cellular phenotype produced by each compound, perhaps indicating subtle variation in their precise mode of action. This observation could form the basis of future investigations to understand the effects of compounds from this series in cells in more detail. In the present context though, it is clear that the three compounds tested caused obvious defects in the

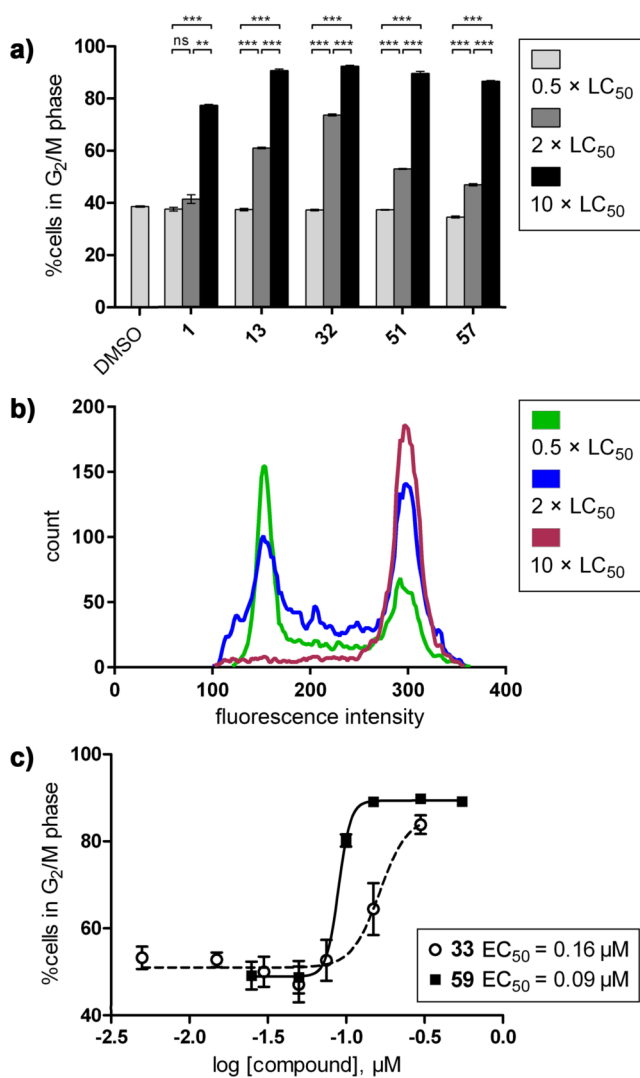


Figure 4. (a) Exposure of FaDu cells to increasing concentrations of the compounds indicated, for 24 h, caused dose-dependent cell cycle arrest in the G₂/M phase; for comparisons, ns = $P > 0.05$, ** = $P < 0.01$, *** = $P < 0.001$. (b) Representative histograms for the three concentrations of 57 (cell count versus DNA staining intensity) showing the clear shift in cell cycle distribution upon compound treatment; DMSO control (not shown) was essentially identical to the 0.5 × LC₅₀ (green) plot. (c) A more detailed dose–response analysis for compounds 33 and 59 provided EC₅₀ values for the observed mitotic arrest.

microtubule network of FaDu cells at concentrations consistent with the cytotoxic potencies determined earlier. Because the compounds have also been shown to interact directly with purified tubulin, these results do appear to confirm engagement of the same target in cells as the basis of their cytotoxic action.

A small set of the most potent compounds was also assessed by flow cytometry for their effect on the cell cycle distribution of proliferating FaDu cells (Figure 4). As can be seen clearly, all compounds induced accumulation of the majority of the population at G₂/M phase after 24 h exposure. Using multiple concentrations of 33 and 59 allowed dose–response curves to be plotted and EC₅₀ values derived for this mitotic arrest, and these values are approximately 5-fold or 2-fold higher, respectively, than the LC₅₀ values for cytotoxicity (72 h end point). This does suggest mitotic arrest as the primary cause of cell death in the latter assays, although a direct comparison at

equivalent end points is not possible because all cells are dead by 72 h (compromising analysis by flow cytometry), whereas meaningful LC₅₀ values cannot be obtained at 24 h (because viability is only partially reduced by this stage, typically by only 40–50% even at the top of the dose–response concentration range). It appears that G₂/M accumulation results relatively soon after treatment, within the first 18–24 h, and a prolonged period of cell cycle arrest is entered, as is typical with MTAs,⁸⁷ before ultimate cell death, which is not extensive until around 48 h (data not shown).

Thus, it was established that representative compounds from the current series cause disruption of the cellular microtubule network and induce cell cycle arrest in mitosis, consistent with their tubulin polymerization inhibition properties.

Evaluation in Other Cell Models. It was also considered important to evaluate some of the most potent compounds more widely, including cell lines representing other cancer types. The additional lines used were SCC-4 (squamous cell carcinoma of the tongue), SK-MEL-28 (malignant melanoma), SH-SY5Y (neuroblastoma), and MES-SA (uterus sarcoma). A multidrug-resistant derivative of the latter, MES-SA/Dx5, was also used because it is known to express very high levels of P-glycoprotein (P-gp).^{88,89} When used in combination, these two lines therefore represent a useful tool to evaluate the propensity of test compounds for efflux-mediated resistance.

Screening against the additional cell lines was carried out with a selection of six compounds (13, 32, 33, 51, 57, and 59), spanning an order of magnitude range of LC₅₀ from the FaDu screen (12–137 nM), alongside 1 for comparison (Figure 5). The observed cytotoxic activities, together with the trend in potency, remained very similar across all lines (Figure 5a; see also Supporting Information, Figure S14). The multidrug-resistant cell line MES-SA/Dx5 showed significant cross-resistance to vinblastine, paclitaxel, and colchicine as expected, but not to 1 or the present test compounds (Figure 5b), suggesting the latter are not substrates for efflux by P-gp. Further support for this assumption is provided by the bidirectional Caco-2 assay results discussed above (Table 5). Efflux can also occur by the Caco-2 cell line and may be mediated by any of multiple transporters including P-gp, BCRP/ABCG2, MRP1, and MRP2.^{90–92} Hence, the fact an efflux ratio of less than 2 was observed for 12, 13, 17, 32, 33, and 59 suggests these compounds are not good substrates for any of the transporters characterized in Caco-2.

The present series of compounds appears to possess general cytotoxic activity against cancer cell lines and does not seem susceptible to active efflux based on results from two cell lines expressing transporter proteins commonly associated with multidrug resistance.

A further priority was to evaluate selected compounds from the series in a suitable 3D cell culture model. Whereas 2D (monolayer) culture provides a convenient platform for initial screening experiments, it is not a representative model of a clinical tumor; thus, 3D cell culture models are increasingly being developed and applied to better assess the potential for in vivo activity of preclinical compounds.⁹³ The simplest such 3D model is the multicellular tumor spheroid (MCTS), a valuable screening tool which may be formed from either a single cell type or cocultured cells.⁹⁴ The FaDu cell line employed for primary screening in this study readily forms monocultured MCTS,⁹⁵ permitting the effect of compounds 32, 33, and 59 on these spheroids to be monitored in a time- and dose-dependent fashion (Figure 6). FaDu MCTS are an established and well-

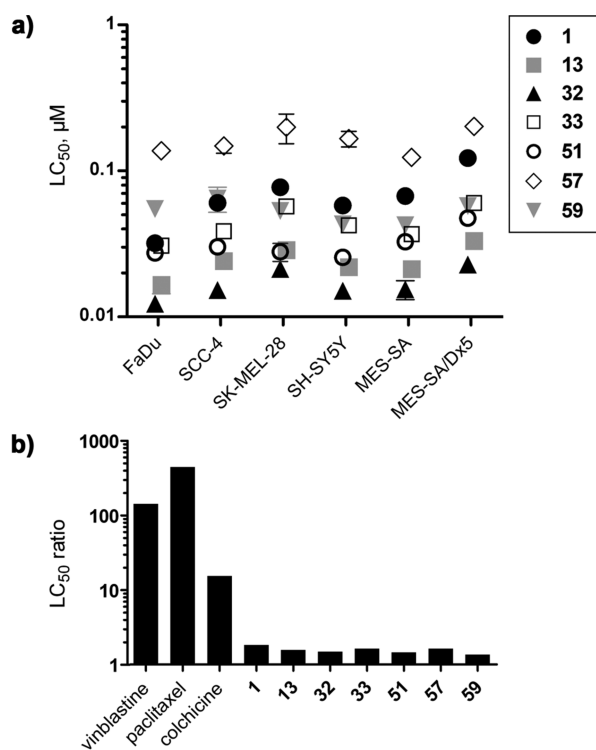


Figure 5. (a) Distribution of cytotoxicity LC₅₀ values for the compounds indicated across a range of cell lines representing different cancer types. (b) Ratio of LC₅₀ values for various compounds between the multidrug-resistant cell line MES-SA/Dx5 and its parent line, MES-SA. Varying degrees of resistance are seen to vinblastine, paclitaxel, and colchicine but not to 1 or a selection of members from the present series. The cytotoxicity data used in making both these graphs are tabulated in full (mean, SEM, n) in the Supporting Information (Table S7a,b).

characterized model of HNC solid tumors that have been widely employed.^{94–96}

An effect on normal spheroid growth was not evident until 2–3 days after dosing, but from this point onward, an ongoing dispersion of cells from the spheroid was seen (Figure 6a), assumed to be due to the cytotoxic effect of the compounds inducing progressive cell death. As shown for 59 (Figure 6b), the extent of this effect was dose-dependent at the experiment end point (7 days post dosing), and size measurements taken at regular intervals allowed time-course plots of spheroid volume to be made (also for 59; Figure 6c). This revealed that at concentrations high enough to ultimately reduce the spheroid volume (>0.1 µM), it takes several days before the toxic effect of the compound is sufficient to outweigh new cell growth, emphasizing the requirement for continued drug exposure *in vivo*. Measurements taken at the 7 day end point over a range of concentrations allowed dose–response plots to be constructed for all three test compounds and EC₅₀ values for spheroid disruption to be derived (Figure 6d). Combined results from two such independent experiments were compared with the 2D cytotoxic potencies determined earlier (Figure 6e).

Compounds 32 and 59 demonstrated good agreement between duplicate experiments, with a 3D potency approximately 3- or 2-fold higher, respectively, than the requisite result in 2D culture. In contrast, more variation was seen in 3D experiments with 33 for reasons which were not immediately clear, but 3D results were nonetheless well within an order of magnitude of those seen in 2D. Hence, all three compounds did

show efficacy in the 3D MCTS model at concentrations similar to those observed in the earlier FaDu monolayer screens, without any prohibitive dropoff in activity. There is certainly scope for higher-content screening using MCTS which could be exploited in the future as part of more detailed mode-of-action studies, but for the purposes of the current work, it was satisfactory to note successful translation of activity to a 3D model for representative compounds in the existing series.

Mouse Xenograft Study. Two compounds, 33 and 59, were selected for a preliminary *in vivo* efficacy study in a mouse model of HNC using xenografts of the FaDu cell line. In addition to the positive results for both in the FaDu MCTS model described above, these compounds were chosen because they were the only candidates with both LC₅₀ < 100 nM from the primary cytotoxicity screen and a microsomal half-life of at least 30 min. Given concerns over the still suboptimal solubility of the series, oral dosing was chosen since earlier data suggested moderate to good absorption by this route (Table 5). Mice with established xenografts were dosed once daily for a period of 10 days as shown (Figure 7), and a significant inhibition of tumor growth was seen initially in all treatment groups.

An unexpected feature of the results is the apparent partial recovery in tumor volume before the end of the dosing period (comparing measurements between days 6 and 9), although numerical analysis revealed this difference is only statistically significant in the group receiving 59 at 10 mg/kg. There are a number of possible explanations for this observation, and particularly in the absence of accompanying pharmacokinetic data, any interpretation would be speculative at best. The FaDu cell line does overexpress BCRP/ABCG2,⁸² so even though there is no reason to assume acquired resistance is developing to the current test compounds, the above results do emphasize the importance that the potential for new drugs to activate mechanisms of resistance be appropriately investigated at an early stage of development. On a more encouraging note, treatment with 33 appeared to result in poor tumor growth even after administration had ceased.

CONCLUSIONS

A library of modified indole-3-glyoxylamides has been reported, capable of inhibiting tubulin polymerization and displaying cancer cell cytotoxicity with a well-defined SAR. Furthermore, two compounds from the series displayed evidence for efficacy in a mouse xenograft model of HNC. This study builds on previous work by others which has already established a range of compounds of the indole-3-glyoxylamide class, such as 1 and 2, as promising tubulin polymerization inhibitors. Other members of the class have been investigated preclinically,^{97–99} including 88–91 (Figure 8) arising from an SAR study¹⁰⁰ published shortly after the disclosure of 1, with both 90 and 91 reportedly demonstrating *in vivo* activity.

Given the apparent failure of 2 in the clinic, and the difficulties encountered in attempting to develop 1, we hypothesized as the basis of the present work that the physicochemical and PK properties of such compounds might be improved by removing the benzylic group at N1 common to existing compounds in the class and replacing it with aliphatic substituents. This current study details first steps in such a direction, establishing that compounds modified thus are capable of retaining potent activity, albeit with a subtly different but distinct SAR suggestive of changes in binding pose. The desired improvement in solubility as compared to 1 looks to have been realized successfully.

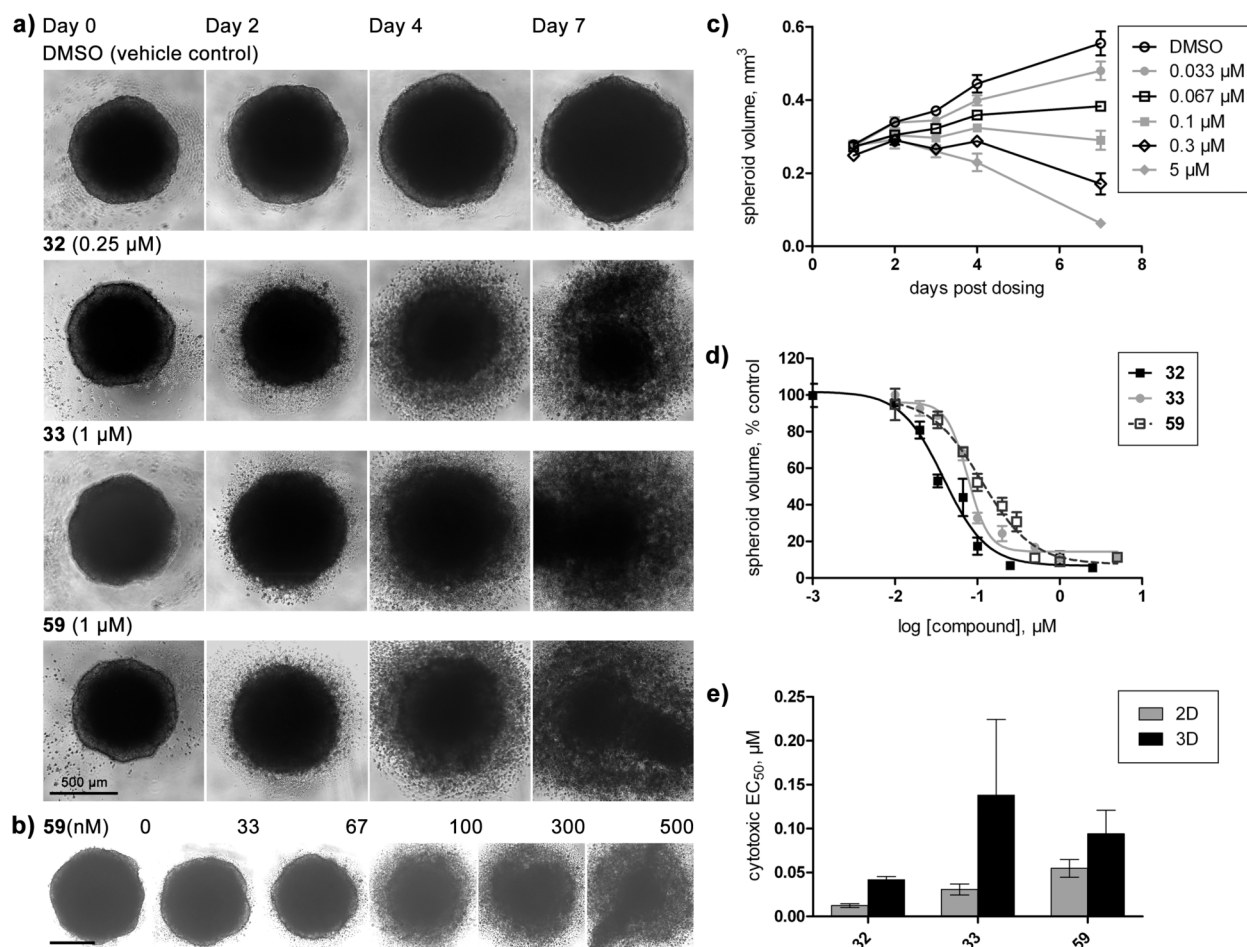


Figure 6. Effect of compounds **32**, **33**, and **59** on multicellular tumor spheroids (MCTS) formed from the FaDu cell line. (a) Images captured at 0, 2, 4, and 7 days postdosing demonstrate ongoing toxicity toward treated MCTS, whereas untreated controls show continued growth over the same time period; scale bar (lower left panel) 500 μm . (b) Images of MCTS treated with increasing concentrations of **59** captured 7 days postdosing, with enhanced brightness to emphasize the fragmentation of spheroids which is induced in a dose-dependent manner; scale bar (leftmost panel) 500 μm . (c) Time-course plots of average volume at selected concentrations of **59** again show dose-dependent toxicity toward FaDu MCTS. (d) Representative dose–response plots at end point (7 days postdosing) allow EC_{50} determination for spheroid disruption; values derived from these data are 39 nM (**32**), 77 nM (**33**), and 113 nM (**59**). (e) Comparison of 3D cytotoxic potencies (mean \pm SEM) with values from 2D (monolayer) screening reported earlier (Table 5).

Although the reported library has been established as a workable hit series, further optimization of PK properties is evidently necessary, although the present results suggest this is achievable. A better-defined SAR, aspects of which remain unexplored, is ideally necessary to help inform this undertaking. A more detailed understanding of the compounds' mode of action at the cellular level is also important, especially to interrogate and direct improvement of their selectivity for the desired target, tubulin. In the context of the MTA drug class, selectivity is a critical consideration given that a narrow therapeutic window remains arguably the most significant drawback of the existing agents in clinical use. Compounds with superior therapeutic window are urgently required, and evidence for such was probably the most appealing aspect of preclinical data for **1**. Efforts to assess and optimize the therapeutic window must therefore be a priority in the identification and development of potential new MTAs likely to be of clinical value, arising either from this series or elsewhere.

EXPERIMENTAL SECTION

Chemistry. General Procedures. Reactions were run under an inert atmosphere of N_2 unless stated otherwise. Anhydrous solvents were obtained from an in-house “Grubbs” system and stored under N_2 until use. All other solvents and reagents were obtained from commercial sources and used as supplied. NMR spectra were recorded at the frequencies listed, and ^{13}C NMR spectra were recorded with complete proton decoupling. J values are reported in Hz. Melting points were determined using a Gallenkamp melting point apparatus in capillary tubes and are uncorrected. Analytical HPLC was carried out using a C_{18} 5 μm column (4.6 mm \times 250 mm) and a gradient of 5–100% MeCN/water over 20 or 25 min (holding at 100% for 5 min), with UV detection at 254 nm and a flow rate 1.0 mL min^{-1} . Purity of all screening compounds was determined to be >95% by HPLC; a tabulated list of purities is included in the Supporting Information. Where required, preparative HPLC was performed using a C_{18} 5 μm column (19 mm \times 250 mm) with UV detection at 254 nm and a flow rate between 15–20 mL min^{-1} , using a gradient specified in each case. Dynamic light scattering measurements were carried out using the Malvern Instruments Zetasizer Nano ZS system, equipped with a 4 mW He–Ne laser at 633 nm, as described.¹⁰¹ To our knowledge, the compound series presented here is free of obvious interference motifs (“PAINS”), and the presence of a well-defined SAR

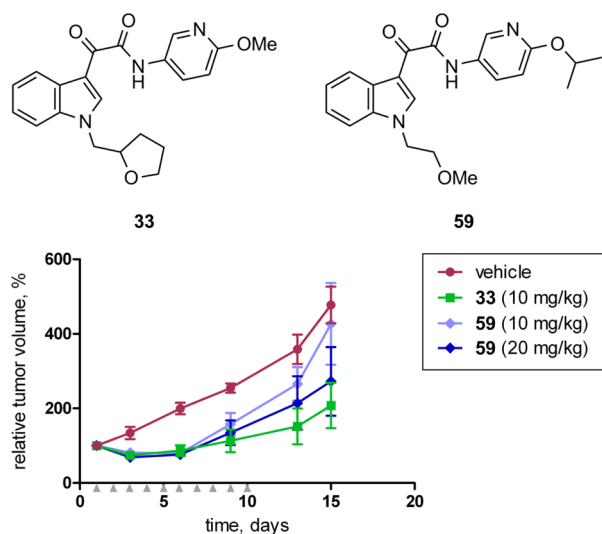


Figure 7. Compounds 33 and 59 were administered by oral gavage at the doses indicated, once daily for 10 days (gray arrowheads), and produced a significant reduction in tumor growth relative to the control group. This effect was statistically significant ($P < 0.05$) in all treatment groups at days 3, 6, and 9, and significant at the $P < 0.0001$ level at day 6 in all cases. Only 33 exerted a sustained effect beyond the dosing period ($P < 0.01$ at days 13 and 15). Detailed plots of tumor volume, body weight, and survival for each treatment group, including results with vinblastine as a comparator/control drug, are presented in the Supporting Information (Figure S15).

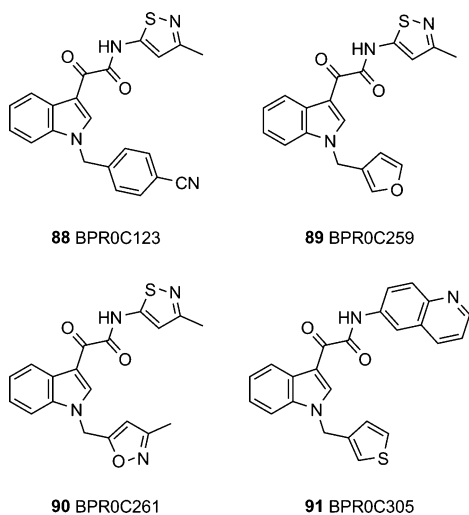


Figure 8. Some other indole-3-glyoxylamides with reported in vitro or in vivo antitumor activity. Note 88 is the indole analogue of 2.

(with respect to both tubulin interaction and cytotoxicity) provides good evidence against nonspecific modes of action.¹⁰²

2-Isopropoxyethyl 4-Methylbenzenesulfonate (Precursor to 4e). 2-Isopropoxyethanol (1.15 mL, 1.05 g, 10 mmol) and triethylamine (1.53 mL, 1.11 g, 11 mmol) were dissolved in anhydrous CH_2Cl_2 and the solution cooled to 0 °C before addition of *p*-toluenesulfonyl chloride (2.10 g, 11 mmol). The mixture was stirred at 0 °C for 30 min then at rt overnight. The reaction was quenched by addition of satd NH_4Cl then diluted with water and extracted with CH_2Cl_2 (3×20 mL). The combined extracts were dried over Na_2SO_4 , filtered, and evaporated to give a colorless oil which was purified by flash chromatography on silica gel, eluted with 1:1 CH_2Cl_2 /hexane \rightarrow $\text{CH}_2\text{Cl}_2 \rightarrow$ 1:4 EtOAc/ CH_2Cl_2 , affording the title compound as colorless oil (1.46 g, 57%). δ_{H} (400 MHz, $\text{DMSO}-d_6$) 7.78 (d, 2H, $J = 8.0$), 7.48 (d, 2H, $J = 8.0$), 4.08 (t, 2H, $J = 4.5$), 3.52–3.45 (m, 3H),

2.40 (s, 3H), 1.00 (d, 6H, $J = 6.0$). δ_{C} (101 MHz, $\text{DMSO}-d_6$) 145.3, 133.8, 130.6, 128.1, 71.4, 70.9, 65.5, 22.3, 21.5. m/z (ES) 281 ($[\text{M} + \text{Na}]^+$). HRMS, found 281.0817 ($\text{C}_{12}\text{H}_{18}\text{NaO}_4\text{S}$ requires 281.0824).

1-Methoxypropan-2-yl 4-Methylbenzenesulfonate (Precursor to 4g). 1-Methoxypropan-2-ol (4.9 mL, 4.5 g, 50 mmol) was dissolved in anhydrous THF (250 mL) then the solution cooled to 0 °C. Sodium hydride (60% dispersion in mineral oil, 2.3 g, 58 mmol) was added portionwise over 10 min, followed 5 min later by the addition of *p*-toluenesulfonyl chloride (11.0 g, 58 mmol) and DMAP (50 mg). After 30 min at 0 °C, the mixture was warmed to 40 °C and maintained at this temperature for 24 h. The reaction was quenched by addition of satd NH_4Cl then the mixture evaporated under vacuum. The residue was partitioned between Et_2O and water, the layers separated, and the aqueous phase extracted again with Et_2O . The combined organic extracts were washed with water then brine, dried over Na_2SO_4 , filtered, and evaporated, yielding a thick, yellow oil. Purification by flash column chromatography on silica gel, eluted with 50 \rightarrow 75 \rightarrow 100% CH_2Cl_2 /hexane then 1% MeOH/ CH_2Cl_2 , afforded the title compound as a yellow oil (7.3 g, 60%) which was stored at -20 °C until further use. δ_{H} (400 MHz, $\text{DMSO}-d_6$) 7.79 (d, 2H, $J = 8.0$), 7.47 (d, 2H, $J = 8.0$), 4.66 (ddd, 1H, $J = 3.5, 6.0, 12.5$), 3.37–3.27 (m, 2H), 3.13 (s, 3H), 2.42 (s, 3H), 1.14 (d, 3H, $J = 6.0$). δ_{C} (101 MHz, $\text{DMSO}-d_6$) 145.1, 134.2, 130.4, 128.0, 78.8, 74.3, 58.7, 21.5, 17.4. m/z (ES) 245 ($[\text{M} + \text{H}]^+$). HRMS, found 245.0845 ($\text{C}_{11}\text{H}_{17}\text{O}_4\text{S}$ requires 245.0848).

Oxetan-2-ylmethyl 4-Methylbenzenesulfonate (precursor to 4o). A stirred solution of oxetane-2-methanol (0.95 g, 10.8 mmol) in CH_2Cl_2 (30 mL) was cooled to 0 °C then triethylamine (1.65 mL, 1.20 g, 11.8 mmol) and *p*-toluenesulfonyl chloride (2.26 g, 11.8 mmol) were added successively, followed by a small amount of DMAP. The mixture was maintained at 4 °C overnight then poured into water, extracted, and the layers separated. The aqueous layer was extracted with additional CH_2Cl_2 then the combined organic solutions washed with water, dried over Na_2SO_4 , filtered, and evaporated, giving a pale-yellow oil. Flash column chromatography, eluted with 15 \rightarrow 30 \rightarrow 45% EtOAc/hexane, afforded the title compound as a crystalline white solid (2.11 g, 81%). δ_{H} (400 MHz, CDCl_3) 7.84 (d, 2H, $J = 8.0$), 7.37 (d, 2H, $J = 8.0$), 4.98–4.91 (m, 1H), 4.66–4.59 (m, 1H), 4.56–4.49 (m, 1H), 4.17 (d, 2H, $J = 4.0$), 2.78–2.67 (m, 1H), 2.64–2.53 (m, 1H), 2.47 (s, 3H). δ_{C} (101 MHz, CDCl_3) 144.9, 132.9, 129.9, 128.0, 78.6, 72.0, 69.0, 23.4, 21.7. m/z (ES) 243 ($[\text{M} + \text{H}]^+$). HRMS, found 243.0694 ($\text{C}_{11}\text{H}_{15}\text{O}_4\text{S}$ requires 243.0691); mp 55–58 °C (lit.¹⁰³ 58–59 °C).

Typical Procedure for Synthesis of *N*-Alkyl Intermediates 4a–i, 4o, and 67a–o. Indole, or the relevant indole derivative, was dissolved in anhydrous DMF (or THF if specified) at a concentration between 0.25–0.5 M, then the solution cooled to 0 °C. Alkylating agent (1.2 equiv unless stated otherwise) was added, then sodium hydride (60% dispersion in mineral oil, 1.2 equiv) was added in small portions over a period of 10–15 min. Once addition was complete, the reaction mixture was stirred at 0 °C for 30 min then continued at rt (unless stated otherwise) for a duration specified in each case. The reaction was quenched by cautious, dropwise addition of water or satd NH_4Cl , then evaporated to dryness. The residue was partitioned between EtOAc or Et_2O and water and extracted, then the aqueous layer extracted with a second portion of organic solvent. The combined extracts were washed three times with water, once with brine, dried over Na_2SO_4 , filtered, and evaporated to afford the crude product which was purified by flash column chromatography on silica gel as indicated for each case, then dried and stored at -20 °C until further use.

1-Ethyl-1*H*-indole 4a. Prepared from indole (1.17 g, 10 mmol) and bromoethane (1.35 mL, 1.97 g, 18 mmol), reacting overnight at 30 °C. Column eluent 5 \rightarrow 10 \rightarrow 20% CH_2Cl_2 /hexane. Product obtained as a colorless oil (1.12 g, 77%). δ_{H} (400 MHz, $\text{DMSO}-d_6$) 7.55 (d, 1H, $J = 8.0$), 7.46 (dd, 1H, $J = 0.5, 8.0$), 7.38 (d, 1H, $J = 3.0$), 7.14 (dt, 1H, $J = 1.0, 7.0$), 7.02 (dt, 1H, $J = 1.0, 7.0$), 6.43 (dd, 1H, $J = 0.5, 3.0$), 4.19 (q, 2H, $J = 7.0$), 1.35 (t, 3H, $J = 7.0$). δ_{C} (101 MHz, $\text{DMSO}-d_6$) 135.8, 128.6, 128.3, 121.4, 120.9, 119.2, 110.1, 100.9, 40.7, 15.9; m/z (ES)

146 ($[M + H]^+$). HRMS, found 146.0970 ($C_{10}H_{12}N$ requires 146.0970). HPLC purity 98.4%.

1-Isopropyl-1H-indole 4b. Prepared from indole (2.93 g, 25 mmol) and 2-iodopropane (3.0 mL, 5.1 g, 30 mmol), reacting at rt for 90 min. Column eluent 5 \rightarrow 10 \rightarrow 20% CH_2Cl_2 /hexane. Product obtained as a colorless oil (1.67 g, 42%). δ_H (400 MHz, $DMSO-d_6$) 7.55 (d, 1H, $J = 7.5$), 7.51–7.46 (m, 2H), 7.15–7.10 (m, 1H), 7.01 (t, 1H, $J = 7.5$), 6.45 (d, 1H, $J = 3.0$), 4.74 (septet, 1H, $J = 6.5$), 1.45 (d, 6H, $J = 6.5$). δ_C (101 MHz, $DMSO-d_6$) 135.6, 128.6, 125.0, 121.3, 120.9, 119.3, 110.2, 101.2, 46.8, 23.0. m/z (ES) 160 ($[M + H]^+$). HRMS, found 160.1120 ($C_{11}H_{14}N$ requires 160.1126). HPLC purity 99.5%.

1-(2-Methoxyethyl)-1H-indole 4c. Prepared from indole (2.34 g, 20 mmol) and 2-bromoethyl methyl ether (2.26 mL, 3.34 g, 24 mmol), reacting at rt for 30 min. Column eluent 20 \rightarrow 30 \rightarrow 40 \rightarrow 60% CH_2Cl_2 /hexane. Title compound is a viscous, pale-yellow oil (2.90 g, 83%). δ_H (250 MHz, $DMSO-d_6$) 7.58–7.45 (m, 2H), 7.34 (d, 1H, $J = 3.0$), 7.17–7.09 (m, 1H), 7.06–6.98 (m, 1H), 6.42 (dd, 1H, $J = 0.5, 3.0$), 4.32 (t, 2H, $J = 5.0$), 3.64 (t, 2H, $J = 5.0$), 3.21 (s, 3H). δ_C (62.8 MHz, $DMSO-d_6$) 136.4, 129.4, 128.6, 121.4, 120.8, 119.3, 110.3, 101.0, 71.5, 58.5, 45.8. m/z (ES) 176 ($[M + H]^+$). HRMS, found 176.1077 ($C_{11}H_{14}NO$ requires 176.1075). HPLC purity 99.4%.

1-Butyl-1H-indole 4d. Prepared from indole (1.17 g, 10 mmol) and 1-bromobutane (1.29 mL, 1.64 g, 12 mmol), reacting at rt for 30 min. Column eluent 5 \rightarrow 10 \rightarrow 20% CH_2Cl_2 /hexane. Product obtained as a pale-yellow oil (1.43 g, 83%). δ_H (400 MHz, $CDCl_3$) 7.70 (dt, 1H, $J = 1.0, 8.0$), 7.42 (dd, 1H, $J = 0.5, 8.0$), 7.30–7.25 (m, 1H), 7.19–7.14 (m, 2H), 6.55 (dd, 1H, $J = 0.5, 3.0$), 4.18 (t, 2H, $J = 7.0$), 1.92–1.84 (m, 2H), 1.41 (sextet, 2H, $J = 7.5$), 1.03 (t, 3H, $J = 7.5$). δ_C (101 MHz, $CDCl_3$) 136.0, 128.6, 127.8, 121.3, 121.0, 119.2, 109.4, 100.9, 46.2, 32.4, 20.2, 13.8. m/z (ES) 174 ($[M + H]^+$). HRMS, found 174.1276 ($C_{12}H_{16}N$ requires 174.1283). HPLC purity 99.9%.

1-(2-Isopropoxyethyl)-1H-indole 4e. Prepared from indole (469 mg, 4 mmol) and 2-isopropoxyethyl-4-methylbenzenesulfonate (1.14 g, 4.4 mmol) in THF, reacting at rt overnight. Column eluent 50 \rightarrow 60 \rightarrow 100% toluene/hexane. Title compound obtained as a yellow oil (387 mg, 50%). δ_H (400 MHz, $DMSO-d_6$) 7.55 (d, 1H, $J = 8.0$), 7.49 (d, 1H, $J = 8.0$), 7.36 (d, 1H, $J = 3.0$), 7.12 (t, 1H, $J = 8.0$), 6.99 (t, 1H, $J = 8.0$), 6.42 (d, 1H, $J = 3.0$), 4.29 (t, 2H, $J = 5.5$), 3.68 (t, 2H, $J = 5.5$), 3.48 (septet, 1H, $J = 6.0$), 1.00 (d, 6H, $J = 6.0$). δ_C (101 MHz, $DMSO-d_6$) 136.3, 129.5, 128.5, 121.3, 120.8, 119.3, 110.3, 100.8, 71.4, 66.9, 46.4, 22.4. m/z (ES) 204 ($[M + H]^+$). HRMS, found 204.1385 ($C_{13}H_{18}NO$ requires 204.1388).

1-sec-Butyl-1H-indole 4f. Prepared from indole (2.34 g, 20 mmol) and 2-iodobutane (2.76 mL, 4.42 g, 24 mmol), reacting at rt for 6 h. Column eluent 5 \rightarrow 10 \rightarrow 20% CH_2Cl_2 /hexane. Product obtained as a thick, colorless oil (0.20 g, 6%). δ_H (250 MHz, $DMSO-d_6$) 7.56–7.47 (m, 2H), 7.44 (d, 1H, $J = 3.0$), 7.14–7.06 (m, 1H), 7.03–6.95 (m, 1H), 6.46 (d, 1H, $J = 3.0$), 4.49 (sextet, 1H, $J = 7.0$), 1.92–1.72 (m, 2H), 1.43 (d, 3H, $J = 7.0$), 0.70 (t, 3H, $J = 7.0$). δ_C (62.8 MHz, $DMSO-d_6$) 136.2, 128.4, 125.4, 121.2, 120.8, 119.2, 110.3, 101.3, 52.7, 29.9, 21.2, 11.1. m/z (ES) 174 ($[M + H]^+$). HRMS, found 174.1275 ($C_{12}H_{16}N$ requires 174.1283).

1-(1-Methoxypropan-2-yl)-1H-indole 4g. Prepared from indole (2.75 g, 23.5 mmol) and 1-methoxypropan-2-yl 4-methylbenzenesulfonate (6.0 mL, 6.9 g, 28 mmol), reacting at 55 °C overnight. Column eluent 40 \rightarrow 50 \rightarrow 67 \rightarrow 100% toluene/hexane then 10% CH_2Cl_2 /toluene. Title compound obtained as a pale-yellow oil (3.11 g, 70%). δ_H (250 MHz, $DMSO-d_6$) 7.57–7.44 (m, 3H), 7.12 (dt, 1H, $J = 1.5, 7.5$), 7.05–6.97 (m, 1H), 6.45 (d, 1H, $J = 3.0$), 4.87–4.72 (m, 1H), 3.71–3.54 (m, 2H), 3.20 (s, 3H), 1.43 (d, 3H, $J = 7.0$). δ_C (62.8 MHz, $DMSO-d_6$) 136.2, 128.5, 125.8, 121.3, 120.8, 119.4, 110.3, 101.4, 75.6, 58.8, 50.6, 18.0. m/z (ES) 190 ($[M + H]^+$). HRMS, found 190.1224 ($C_{12}H_{16}NO$ requires 190.1232). HPLC purity 99.4%.

1-Isobutyl-1H-indole 4h. Prepared from indole (2.34 g, 20 mmol) and 1-iodo-2-methylpropane (2.76 mL, 4.42 g, 24 mmol), reacting at rt for 1 h. Column eluent 5 \rightarrow 10 \rightarrow 20% CH_2Cl_2 /light petroleum. Product obtained as a thick, colorless oil (0.54 g, 16%). δ_H (400 MHz, $DMSO-d_6$) 7.55 (d, 1H, $J = 8.0$), 7.46 (dd, 1H, $J = 0.5, 8.0$), 7.33 (d, 1H, $J = 3.0$), 7.14–7.09 (m, 1H), 7.03–6.98 (m, 1H), 6.43 (dd, 1H, $J = 0.5, 3.0$), 3.96 (d, 2H, $J = 7.5$), 2.17–2.05 (m, 1H), 0.84 (d, 6H, $J =$

6.5). δ_C (101 MHz, $DMSO-d_6$) 136.4, 129.5, 128.5, 121.3, 120.8, 119.2, 110.4, 100.7, 53.3, 29.6, 20.4. m/z (ES) 174 ($[M + H]^+$). HRMS, found 174.1275 ($C_{12}H_{16}N$ requires 174.1283). HPLC purity 99.6%.

1-(Tetrahydrofuran-2-yl)methyl-1H-indole 4i. Prepared from indole (2.34 g, 20 mmol) and tetrahydrofurfuryl bromide (2.70 mL, 3.96 g, 24 mmol), reacting at rt for 2 h. Column eluent 20 \rightarrow 40 \rightarrow 60 \rightarrow 80% CH_2Cl_2 /hexane. Product obtained as a pale-pink oil (1.33 g, 33%). δ_H (400 MHz, $CDCl_3$) 7.68 (d, 1H, $J = 8.0$), 7.42 (d, 1H, $J = 8.0$), 7.29–7.22 (m, 2H), 7.17–7.12 (m, 1H), 6.55 (d, 1H, $J = 3.0$), 4.33–4.19 (m, 3H), 3.91–3.85 (m, 1H), 3.82–3.76 (m, 1H), 2.03–1.94 (m, 1H), 1.92–1.73 (m, 2H), 1.66–1.56 (m, 1H). δ_C (101 MHz, $CDCl_3$) 136.5, 128.7, 128.5, 121.5, 120.9, 119.3, 109.5, 101.4, 78.1, 68.3, 50.1, 29.1, 25.7. m/z (ES) 202 ($[M + H]^+$). HRMS, found 202.1225 ($C_{13}H_{16}NO$ requires 202.1232). HPLC purity 99.8%.

1-(Oxetan-2-ylmethyl)-1H-indole 4o. Indole (426 mg, 3.64 mmol) was dissolved in DMF (10 mL) and the solution cooled to 0 °C. Sodium hydride (60% dispersion in mineral oil, 160 mg, 4.00 mmol) was added in portions over 5 min, then after another 5 min stirring, oxetan-2-ylmethyl 4-methylbenzenesulfonate (0.97 g, 4.00 mmol) was added. The reaction was allowed to continue for 3 h, after which it was deemed essentially complete by TLC. It was quenched by dropwise addition of satd NH_4Cl then extracted between EtOAc and water. The aqueous layer was extracted with further EtOAc then the combined organic extracts washed three times with water and once with brine. The solution was dried over Na_2SO_4 , filtered, and evaporated, giving an oil which was purified by flash column chromatography on silica gel, eluted with 10 \rightarrow 20 \rightarrow 33 \rightarrow 45% EtOAc/hexane, to provide the title compound as a colorless oil (530 mg, 78%). δ_H (400 MHz, $CDCl_3$) 7.69 (dt, 1H, $J = 1.0, 8.0$), 7.41 (dd, 1H, $J = 1.0, 8.0$), 7.31–7.23 (m, 2H), 7.18–7.13 (m, 1H), 6.59 (dd, 1H, $J = 1.0, 3.0$), 5.23–5.15 (m, 1H), 4.67–4.59 (m, 1H), 4.42–4.32 (m, 3H), 2.72–2.62 (m, 1H), 2.42–2.32 (m, 1H). δ_C (101 MHz, $CDCl_3$) 136.7, 128.8, 128.5, 121.6, 121.0, 119.4, 109.4, 101.7, 81.1, 68.5, 51.3, 24.6. m/z (ES) 188 ($[M + H]^+$). HRMS, found 188.1084 ($C_{12}H_{14}NO$ requires 188.1075). HPLC purity 99.0%.

4-Chloro-1-isopropyl-1H-indole 67a. Prepared from 4-chloroindole (3.03 g, 20 mmol) and 2-iodopropane (2.4 mL, 4.1 g, 24 mmol), reacting at rt overnight. Column eluent 5 \rightarrow 10 \rightarrow 20% CH_2Cl_2 /hexane. Title compound obtained as a pale-yellow oil (2.04 g, 53%). δ_H (400 MHz, $CDCl_3$) 7.34–7.28 (m, 2H), 7.18–7.12 (m, 2H), 6.66 (d, 1H, $J = 3.0$), 4.69 (septet, 1H, $J = 7.0$), 1.56 (d, 6H, $J = 7.0$). δ_C (101 MHz, $CDCl_3$) 136.3, 127.3, 126.2, 124.2, 121.8, 119.0, 108.2, 99.9, 47.6, 22.8. m/z (ES) 194 (100%; $[M(^{35}Cl) + H]^+$), 196 (30%; $[M(^{37}Cl) + H]^+$). HRMS, found 194.0741 ($C_{11}H_{13}ClN$ requires 194.0737). HPLC purity 99.5%.

5-Chloro-1-isopropyl-1H-indole 67b. Prepared from 5-chloroindole (3.78 g, 25 mmol) and 2-iodopropane (3.0 mL, 5.1 g, 30 mmol), reacting at rt for 2 h. Column eluent 5 \rightarrow 10 \rightarrow 20% CH_2Cl_2 /hexane. Title compound obtained as a viscous, colorless oil (2.46 g, 51%). δ_H (250 MHz, $DMSO-d_6$) 7.58 (d, 1H, $J = 2.0$), 7.56–7.48 (m, 2H), 7.11 (dd, 1H, $J = 2.0, 9.0$), 6.44 (d, 1H, $J = 3.0$), 4.73 (septet, 1H, $J = 6.5$), 1.43 (d, 6H, $J = 6.5$). δ_C (62.8 MHz, $DMSO-d_6$) 134.1, 129.7, 126.8, 124.0, 121.2, 120.0, 111.8, 101.1, 47.3, 22.9. m/z (ES) 194 (100%; $[M(^{35}Cl) + H]^+$), 196 (30%; $[M(^{37}Cl) + H]^+$). HRMS, found 194.0734 ($C_{11}H_{13}ClN$ requires 194.0737). HPLC purity 99.4%.

5-Chloro-1-(2-methoxyethyl)-1H-indole 67c. Prepared from 5-chloroindole (1.32 g, 8.7 mmol) and 2-bromoethyl methyl ether (0.98 mL, 1.45 g, 10.5 mmol), reacting in THF at rt overnight. Column eluent 5 \rightarrow 10 \rightarrow 20% CH_2Cl_2 /toluene. Product obtained as a colorless oil (1.07 g, 59%). δ_H (400 MHz, $DMSO-d_6$) 7.59 (d, 1H, $J = 2.0$), 7.52 (d, 1H, $J = 9.0$), 7.43 (d, 1H, $J = 3.0$), 7.12 (dd, 1H, $J = 2.0, 9.0$), 6.42 (dd, 1H, $J = 0.5, 3.0$), 4.33 (t, 2H, $J = 5.5$), 3.63 (t, 2H, $J = 5.5$), 3.20 (s, 3H). δ_C (101 MHz, $DMSO-d_6$) 134.9, 131.2, 129.6, 124.1, 121.3, 119.9, 112.0, 100.8, 71.5, 58.5, 46.0. m/z (ES) 210 (100%; $[M(^{35}Cl) + H]^+$), 212 (25%; $[M(^{37}Cl) + H]^+$). HRMS, found 210.0694 ($C_{11}H_{13}ClNO$ requires 210.0686). HPLC purity 99.4%.

6-Chloro-1-isopropyl-1H-indole 67d. Prepared from 6-chloroindole (3.03 g, 20 mmol) and 2-iodopropane (2.4 mL, 4.1 g, 24 mmol), reacting at rt for 48 h. Column eluent 5 \rightarrow 10 \rightarrow 20% CH_2Cl_2 /hexane.

Product obtained as a colorless oil (1.88 g, 49%). δ_{H} (400 MHz, CDCl_3) 7.56 (d, 1H, $J = 8.5$), 7.42–7.40 (m, 1H), 7.25 (d, 1H, $J = 3.5$), 7.10 (dd, 1H, $J = 2.0, 8.5$), 6.53 (dd, 1H, $J = 0.5, 3.5$), 4.63 (septet, 1H, $J = 6.5$), 1.56 (d, 6H, $J = 6.5$). δ_{C} (101 MHz, CDCl_3) 135.9, 127.3, 127.1, 124.3, 121.8, 120.0, 109.5, 101.4, 47.3, 22.7. m/z (ES) 194 (100%; $[\text{M}^{(35)\text{Cl}} + \text{H}]^+$), 196 (35%; $[\text{M}^{(37)\text{Cl}} + \text{H}]^+$). HRMS, found 194.0730 ($\text{C}_{11}\text{H}_{13}\text{ClN}$ requires 194.0737). HPLC purity 98.7%.

7-Chloro-1-isopropyl-1H-indole 67e. Prepared from 7-chloroindole (1.52 g, 10 mmol) and 2-iodopropane (1.2 mL, 2.0 g, 12 mmol), reacting at rt overnight. Column eluent 0 \rightarrow 1 \rightarrow 2.5 \rightarrow 5 \rightarrow 10% CH_2Cl_2 /hexane. Product obtained as a colorless oil (0.50 g, 26%). δ_{H} (400 MHz, CDCl_3) 7.55 (dd, 1H, $J = 1.0, 8.0$), 7.34 (d, 1H, $J = 3.5$), 7.19 (dd, 1H, $J = 1.0, 8.0$), 7.02 (t, 1H, $J = 8.0$), 6.58 (d, 1H, $J = 3.5$), 5.75 (septet, 1H, $J = 6.5$), 1.56 (d, 6H, $J = 6.5$). δ_{C} (101 MHz, CDCl_3) 131.8, 131.1, 124.9, 123.6, 119.9, 119.7, 116.5, 102.2, 47.9, 23.9. m/z (ES) 194 (100%; $[\text{M}^{(35)\text{Cl}} + \text{H}]^+$), 196 (35%; $[\text{M}^{(37)\text{Cl}} + \text{H}]^+$). HRMS, found 194.0731 ($\text{C}_{11}\text{H}_{13}\text{ClN}$ requires 194.0737). HPLC purity 99.1%.

4-Methoxy-1-isopropyl-1H-indole 67f. Prepared from 4-methoxyindole (1.25 g, 8.5 mmol) and 2-iodopropane (1.02 mL, 1.73 g, 10.2 mmol), reacting at rt overnight. Column eluent 10 \rightarrow 20 \rightarrow 30 \rightarrow 35% CH_2Cl_2 /hexane. Title compound obtained as a slightly opaque, colorless oil (0.61 g, 38%). δ_{H} (400 MHz, CDCl_3) 7.24–7.16 (m, 2H), 7.06 (d, 1H, $J = 8.5$), 6.68 (t, 1H, $J = 3.0$), 6.57 (d, 1H, $J = 7.5$), 4.69 (septet, 1H, $J = 6.5$), 4.01 (s, 3H), 1.56 (d, 6H, $J = 6.5$). δ_{C} (101 MHz, CDCl_3) 153.5, 137.0, 122.1, 122.0, 119.1, 103.1, 99.1, 98.4, 55.3, 47.3, 22.8. m/z (ES) 190 ($[\text{M} + \text{H}]^+$). HRMS, found 190.1235 ($\text{C}_{12}\text{H}_{16}\text{NO}$ requires 190.1232). HPLC purity 88.7%.

5-Methoxy-1-isopropyl-1H-indole 67g. Prepared from 5-methoxyindole (1.55 g, 10.5 mmol) and 2-iodopropane (1.26 mL, 2.14 g, 12.6 mmol), reacting at rt overnight. Column eluent 10 \rightarrow 20 \rightarrow 25 \rightarrow 33 \rightarrow 40% CH_2Cl_2 /hexane. Product initially obtained as an oil which crystallized on standing to give an off-white solid (0.72 g, 36%). δ_{H} (400 MHz, CDCl_3) 7.31 (d, 1H, $J = 9.0$), 7.24 (d, 1H, $J = 3.0$), 7.14 (d, 1H, $J = 2.5$), 6.92 (dd, 1H, $J = 2.5, 9.0$), 6.48 (d, 1H, $J = 3.0$), 4.66 (septet, 1H, $J = 7.0$), 3.89 (s, 3H), 1.55 (d, 6H, $J = 7.0$). δ_{C} (101 MHz, CDCl_3) 153.9, 130.9, 128.9, 124.1, 111.6, 110.2, 102.6, 100.7, 55.9, 47.2, 22.8. m/z (ES) 190 ($[\text{M} + \text{H}]^+$). HRMS, found 190.1240 ($\text{C}_{12}\text{H}_{16}\text{NO}$ requires 190.1232). HPLC purity 96.6%; mp 65–66 °C.

5-Methoxy-1-(2-methoxyethyl)-1H-indole 67h. Prepared from 5-methoxyindole (1.47 g, 10 mmol) and 2-bromoethyl methyl ether (1.13 mL, 1.67 g, 12 mmol), reacting in THF at 35 °C overnight. Column eluent 5 \rightarrow 10 \rightarrow 17.5 \rightarrow 20% EtOAc/hexane. Title compound obtained as a pale-yellow oil (1.36 g, 66%). δ_{H} (400 MHz, $\text{DMSO}-d_6$) 7.37 (d, 1H, $J = 9.0$), 7.29 (d, 1H, $J = 3.0$), 7.05 (d, 1H, $J = 2.5$), 6.77 (dd, 1H, $J = 2.5, 9.0$), 6.33 (dd, 1H, $J = 0.5, 3.0$), 4.28 (t, 2H, $J = 5.5$), 3.75 (s, 3H), 1.55 (d, 2H, $J = 5.5$), 3.21 (s, 3H). δ_{C} (101 MHz, $\text{DMSO}-d_6$) 153.9, 131.6, 129.9, 128.9, 111.5, 111.0, 102.5, 100.6, 71.6, 58.5, 55.8, 45.9. m/z (ES) 206 ($[\text{M} + \text{H}]^+$). HRMS, found 206.1188 ($\text{C}_{12}\text{H}_{16}\text{NO}_2$ requires 206.1181). HPLC purity 99.3%.

6-Methoxy-1-isopropyl-1H-indole 67i. Prepared from 6-methoxyindole (1.55 g, 10.5 mmol) and 2-iodopropane (1.26 mL, 2.14 g, 12.6 mmol), reacting at 35 °C overnight. Column eluent 20 \rightarrow 30 \rightarrow 40% CH_2Cl_2 /hexane. Product obtained as a pale-yellow oil (0.72 g, 36%) which crystallized slowly on storage at -20 °C. δ_{H} (400 MHz, CDCl_3) 7.54 (d, 1H, $J = 8.5$), 7.16 (d, 1H, $J = 3.0$), 6.88 (d, 1H, $J = 2.0$), 6.82 (dd, 1H, $J = 2.0, 8.5$), 6.49 (d, 1H, $J = 3.0$), 4.63 (septet, 1H, $J = 6.5$), 3.92 (s, 3H), 3.28 (d, 6H, $J = 6.5$). δ_{C} (101 MHz, CDCl_3) 156.0, 136.2, 122.9, 122.4, 121.5, 109.1, 101.1, 93.4, 55.8, 46.9, 22.7. m/z (ES) 190 ($[\text{M} + \text{H}]^+$). HRMS, found 190.1237 ($\text{C}_{12}\text{H}_{16}\text{NO}$ requires 190.1232). HPLC purity 98.2%. mp 30–31 °C.

7-Methoxy-1-isopropyl-1H-indole 67j. Prepared from 7-methoxyindole (1.63 mL, 1.84 g, 12.5 mmol) and 2-iodopropane (1.5 mL, 2.6 g, 15 mmol), reacting at rt overnight. Column eluent 2.5 \rightarrow 5 \rightarrow 10% EtOAc/hexane. Title compound obtained as a slightly opaque, colorless oil (0.92 g, 39%) which crystallized slowly on storage at -20 °C. δ_{H} (400 MHz, CDCl_3) 7.31–7.25 (m, 2H), 7.05 (t, 1H, $J = 8.0$), 6.69 (d, 1H, $J = 8.0$), 6.54 (d, 1H, $J = 3.0$), 5.51 (septet, 1H, $J = 6.5$), 4.00 (s, 3H), 1.54 (d, 6H, $J = 6.5$). δ_{C} (101 MHz, CDCl_3) 147.7,

130.7, 125.5, 123.7, 119.5, 113.8, 102.4, 101.6, 55.4, 48.9, 24.0. m/z (ES) 190 ($[\text{M} + \text{H}]^+$). HRMS, found 190.1236 ($\text{C}_{12}\text{H}_{16}\text{NO}$ requires 190.1232). HPLC purity 94.8%. mp 36–38 °C.

1-Isopropyl-1H-pyrrolo[3,2-b]pyridine 67k. Prepared from 4-azaindole (1.18 g, 10 mmol) and 2-iodopropane (1.20 mL, 2.04 g, 12 mmol), reacting at rt for 90 min. Column eluent 2.5 \rightarrow 5 \rightarrow 7.5% MeOH/ CH_2Cl_2 . Product obtained as a pale-pink oil (0.56 g, 35%). δ_{H} (400 MHz, CDCl_3) 8.47 (dd, 1H, $J = 1.0, 4.5$), 7.67 (dt, 1H, $J = 1.0, 8.5$), 7.46 (d, 1H, $J = 3.5$), 7.11 (dd, 1H, $J = 4.5, 8.5$), 6.73 (d, 1H, $J = 3.5$), 4.66 (septet, 1H, $J = 6.5$), 1.55 (d, 6H, $J = 6.5$). δ_{C} (101 MHz, CDCl_3) 147.0, 143.1, 128.4, 127.0, 116.5, 116.0, 102.3, 47.6, 22.7. m/z (ES) 161 ($[\text{M} + \text{H}]^+$). HRMS, found 161.1072 ($\text{C}_{10}\text{H}_{13}\text{N}_2$ requires 161.1079). HPLC purity 98.0%.

1-Isopropyl-1H-pyrrolo[3,2-c]pyridine 67l. Prepared from 5-azaindole (2.95 g, 25 mmol) and 2-iodopropane (3.0 mL, 5.1 g, 30 mmol), reacting at rt for 2 h. Column eluent 0 \rightarrow 5 \rightarrow 10 \rightarrow 12.5% MeOH/ CH_2Cl_2 . Product obtained as a pale-orange oil (1.78 g, 44%) which crystallized on standing to give an off-white solid. δ_{H} (250 MHz, $\text{DMSO}-d_6$) 8.81 (d, 1H, $J = 1.0$), 8.18 (d, 1H, $J = 6.0$), 7.59 (d, 1H, $J = 3.0$), 7.51 (d, 1H, $J = 6.0$), 6.62–6.59 (m, 1H), 4.77 (septet, 1H, $J = 6.5$), 1.44 (d, 6H, $J = 6.5$). δ_{C} (62.8 MHz, $\text{DMSO}-d_6$) 143.7, 140.3, 138.9, 126.6, 125.5, 105.8, 100.9, 47.4, 22.8. m/z (ES) 161 ($[\text{M} + \text{H}]^+$). HRMS, found 161.1077 ($\text{C}_{10}\text{H}_{13}\text{N}_2$ requires 161.1079). HPLC purity 99.7%. mp 71–72 °C.

1-Isopropyl-1H-pyrrolo[2,3-c]pyridine 67m. Prepared from 6-azaindole (2.95 g, 25 mmol) and 2-iodopropane (3.0 mL, 5.1 g, 30 mmol), reacting at rt for 75 min. Column eluent 0 \rightarrow 5 \rightarrow 10% MeOH/ CH_2Cl_2 . Title compound obtained as a yellow oil (1.88 g, 47%) which crystallized slowly, forming a waxy, off-white solid on storage at -20 °C. δ_{H} (250 MHz, $\text{DMSO}-d_6$) 8.92 (s, 1H), 8.11 (d, 1H, $J = 5.5$), 7.72 (s, 1H, $J = 3.0$), 7.51 (dd, 1H, $J = 1.0, 5.0$), 6.50 (dd, 1H, $J = 1.0, 3.0$), 4.89 (septet, 1H, $J = 6.5$), 1.48 (d, 6H, $J = 6.5$). δ_{C} (62.8 MHz, $\text{DMSO}-d_6$) 138.3, 133.7, 132.85, 132.78, 129.1, 115.3, 100.6, 47.8, 23.1. m/z (ES) 161 ($[\text{M} + \text{H}]^+$). HRMS, found 161.1083 ($\text{C}_{10}\text{H}_{13}\text{N}_2$ requires 161.1079). HPLC purity 99.5%. mp 35–36 °C.

1-Isopropyl-1H-pyrrolo[2,3-b]pyridine 67n. Prepared from 7-azaindole (2.95 g, 25 mmol) and 2-iodopropane (3.0 mL, 5.1 g, 30 mmol), reacting at rt for 2.5 h. Column eluent 33 \rightarrow 50 \rightarrow 67 \rightarrow 100% CH_2Cl_2 /hexane then 1 \rightarrow 2% MeOH/ CH_2Cl_2 . Title compound obtained as a slightly cloudy, colorless oil (2.20 g, 55%). δ_{H} (400 MHz, $\text{DMSO}-d_6$) 8.24 (dd, 1H, $J = 1.5, 4.5$), 7.94 (dd, 1H, $J = 1.5, 8.0$), 7.66 (d, 1H, $J = 3.5$), 7.07 (dd, 1H, $J = 4.5, 8.0$), 6.48 (d, 1H, $J = 3.5$), 5.10 Hz (septet, 1H, $J = 7.0$), 1.46 (d, 6H, $J = 7.0$). δ_{C} (101 MHz, $\text{DMSO}-d_6$) 146.9, 142.5, 128.8, 126.0, 120.6, 116.0, 99.6, 45.5, 22.9. m/z (ES) 161 ($[\text{M} + \text{H}]^+$). HRMS, found 161.1077 ($\text{C}_{10}\text{H}_{13}\text{N}_2$ requires 161.1079). HPLC purity 89.6%.

1-(2-Methoxyethyl)-1H-pyrrolo[2,3-b]pyridine 67o. Prepared from 7-azaindole (1.18 g, 10 mmol) and 2-bromoethyl methyl ether (1.13 mL, 1.67 g, 12 mmol), reacting at rt for 5 h. Column eluent 0 \rightarrow 1 \rightarrow 2 \rightarrow 4 \rightarrow 5% MeOH/ CH_2Cl_2 . Product obtained as a pale-yellow oil (1.16 g, 66%). δ_{H} (400 MHz, CDCl_3) 8.33 (dd, 1H, $J = 1.5, 4.5$), 7.92 (dd, 1H, $J = 1.5, 8.0$), 7.35 (d, 1H, $J = 3.0$), 7.07 (dd, 1H, $J = 4.5, 8.0$), 6.47 (d, 1H, $J = 3.0$), 4.50 (t, 2H, $J = 5.0$), 3.77 (t, 2H, $J = 5.0$), 3.35 (s, 3H). δ_{C} (101 MHz, CDCl_3) 147.4, 142.6, 129.0, 128.7, 120.7, 115.7, 99.3, 71.7, 58.9, 44.3. m/z (ES) 177 ($[\text{M} + \text{H}]^+$). HRMS, found 177.1023 ($\text{C}_{10}\text{H}_{13}\text{N}_2\text{O}$ requires 177.1028). HPLC purity 98.2%.

1-Cyclopentyl-1H-indole 4k. Indole (2.57 g, 21.9 mmol), DMAP (7.70 g, 65.7 mmol), cyclopentylboronic acid (5.00 g, 43.9 mmol), and Cu(OAc) $_2$ (0.40 g, 2.2 mmol) were added to a flame-dried, 3-neck flask equipped with a reflux condenser. Anhydrous toluene (40 mL) was introduced via cannula, then sodium hexamethyldisilazane (0.6 M solution in toluene, 36.5 mL, 21.9 mmol) was added to the resultant deep-blue suspension. A stream of dry air was introduced, bubbling through the reaction mixture, which was then heated to 95 °C and maintained at this temperature overnight. EtOAc (100 mL) and 1 M HCl (200 mL) were added and the mixture shaken thoroughly then vacuum filtered. The layers were separated and the aqueous phase extracted once more with EtOAc. The combined extracts were then dried over MgSO_4 , filtered, and evaporated, leaving a thick-brown oil, which was purified by flash column chromatography on silica gel,

eluted with 5 → 10 → 15% CH₂Cl₂/light petroleum, yielding the title compound as a pale-yellow oil (1.37 g, 34%). δ_{H} (400 MHz, DMSO-*d*₆) 7.56–7.48 (m, 2H), 7.44 (d, 1H, *J* = 3.0), 7.15–7.10 (m, 1H), 7.05–6.99 (m, 1H), 6.44 (d, 1H, *J* = 3.0), 4.87 (quintet, 1H, *J* = 7.0), 2.18–2.08 (m, 2H), 1.90–1.78 (m, 4H), 1.77–1.65 (m, 2H). δ_{C} (101 MHz, DMSO-*d*₆) 136.3, 128.7, 125.7, 121.3, 120.8, 119.4, 110.5, 101.2, 56.6, 32.6, 24.1. *m/z* (ES) 186 ([M + H]⁺). HRMS, found 186.1274 (C₁₁H₁₆N requires 186.1283). HPLC purity 98.8%.

1-(1H-Indol-1-yl)-2-methylpropan-2-ol 69. A solution of indole (2.81 g, 24 mmol) in anhydrous DMF (90 mL) was cooled to 0 °C, then sodium hydride (60% dispersion in mineral oil, 0.96 g, 24 mmol) added in small portions over 15 min. After a further 10 min stirring at 0 °C, isobutene oxide (533 μ L, 433 mg, 6 mmol) was added dropwise and stirring continued for an additional 50 min, at which point the cooling was removed. The reaction mixture was stirred at rt for 5.5 h at rt then 4 h at 30 °C, followed by addition of more isobutene oxide (89 μ L, 72 mg, 1 mmol), after which stirring was continued at 30 °C overnight. The reaction was quenched by dropwise addition of brine, then evaporated under vacuum. The resultant orange slurry was partitioned between Et₂O and water (~100 mL each). AcOH (0.2 mL) was added, then the mixture extracted and the layers separated. The aqueous phase was extracted again with Et₂O and the combined extracts washed three times with brine, dried over MgSO₄, filtered, and evaporated. Further purification was carried out by flash column chromatography on silica gel, eluted with 0 → 1 → 2% MeOH/CH₂Cl₂, affording the title compound as a pale-pink oil (0.98 g, 74%). δ_{H} (400 MHz, DMSO-*d*₆) 7.55–7.50 (m, 2H), 7.33 (d, 1H, *J* = 3.0), 7.12–7.07 (m, 1H), 6.98 (dt, 1H, *J* = 1.0, 7.5), 6.42 (dd, 1H, *J* = 0.5, 3.0), 4.66 (s, 1H), 4.07 (s, 2H), 1.09 (s, 6H). δ_{C} (101 MHz, DMSO-*d*₆) 137.3, 130.6, 128.1, 121.1, 120.5, 119.0, 111.1, 100.6, 70.9, 56.6, 27.9. *m/z* (ES) 190 ([M + H]⁺). HRMS, found 190.1237 (C₁₂H₁₆NO requires 190.1232). HPLC purity 99.4%.

1-(2-Methoxy-2-methylpropyl)-1H-indole 4k. Alcohol **69** (874 mg, 4.62 mmol) was dissolved in anhydrous THF (100 mL) at 0 °C, then sodium hydride (60% dispersion in mineral oil, 231 mg, 5.77 mmol) added in portions over 5 min. Methyl iodide (359 μ L, 819 mg, 5.77 mmol) was introduced 10 min later, then the reaction mixture stirred at 0 °C for 4.5 h then rt for 4.5 h. TLC analysis (3:1 CH₂Cl₂/hexane) indicated reaction was incomplete, so additional methyl iodide (72 μ L, 165 mg, 1.16 mmol) was added and stirring continued at 35 °C overnight. The reaction was then quenched by dropwise addition of satd NH₄Cl, evaporated to dryness and the residue extracted between EtOAc and water. The aqueous phase was extracted again with EtOAc, and the combined organic extracts washed with satd NH₄Cl, dried over MgSO₄, filtered, and evaporated. The oily residue was purified by flash column chromatography on silica gel, eluted with 10 → 20 → 33 → 50% CH₂Cl₂/hexane, giving the title compound as a viscous, pale-yellow oil (492 mg, 52%). δ_{H} (250 MHz, DMSO-*d*₆) 7.56–7.49 (m, 2H), 7.27 (d, 1H, *J* = 3.0), 7.11 (dt, 1H, *J* = 1.0, 7.0), 6.99 (dt, 1H, *J* = 1.0, 7.0), 6.43 (dd, 1H, *J* = 1.0, 3.0), 4.15 (s, 2H), 3.16 (s, 3H), 1.07 (s, 6H). δ_{C} (62.8 MHz, DMSO-*d*₆) 137.4, 130.4, 128.1, 121.3, 120.6, 119.1, 111.0, 100.9, 75.9, 53.9, 49.5, 22.8. *m/z* (ES) 204 ([M + H]⁺). HRMS, found 204.1384 (C₁₃H₁₈NO requires 204.1388). HPLC purity 99.3%.

Ethyl 2-(1H-Indol-1-yl)propanoate 70. Indole (5.86 g, 50 mmol) was dissolved in anhydrous DMF (175 mL) and the solution cooled to 0 °C, after which sodium hydride (60% dispersion in mineral oil, 2.20 g, 55 mmol) was added portionwise over 15 min. Stirring was continued for a further 15 min, then ethyl 2-bromopropionate (7.14 mL, 9.96 g, 55 mmol) was added. The reaction was then maintained at 40 °C for 5 h and continued at rt overnight before being quenched by careful, dropwise addition of water. The mixture was evaporated under vacuum and the residue extracted with Et₂O and water. The aqueous layer was extracted a second time with Et₂O then the combined extracts washed twice with water and twice with brine before drying over Na₂SO₄ and evaporating to leave an orange oil. This crude material was subjected to flash column chromatography on silica gel, eluted with 20 → 33 → 50 → 65% CH₂Cl₂/hexane, to provide the title compound as a somewhat cloudy, pale-yellow oil (8.03 g, 74%). δ_{H} (400 MHz, DMSO-*d*₆) 7.56 (d, 1H, *J* = 8.0), 7.47 (d, 1H, *J* = 3.0),

7.43 (d, 1H, *J* = 8.0), 7.16–7.11 (m, 1H), 7.07–7.02 (m, 1H), 6.50 (dd, 1H, *J* = 0.5, 3.0), 5.46 (q, 1H, *J* = 7.5), 4.12 (q, 2H, *J* = 7.0), 1.73 (d, 3H, *J* = 7.5), 1.15 (t, 3H, *J* = 7.0). δ_{C} (101 MHz, DMSO-*d*₆) 171.6, 136.3, 128.6, 126.9, 121.7, 120.9, 119.8, 110.2, 102.1, 61.5, 53.5, 17.7, 14.5. *m/z* (ES) 218 ([M + H]⁺). HRMS, found 218.1189 (C₁₃H₁₆NO₂ requires 218.1181). HPLC purity 98.1%.

Ethyl 2-(1H-Indol-1-yl)-2-methylpropanoate 71. A solution of intermediate **70** (7.93 g, 36.5 mmol) in dry THF (100 mL) was cooled to –78 °C, then LDA (2.0 M solution in THF, 22 mL, 44 mmol) was added over 10 min. The mixture was stirred at –78 °C for 45 min, at which point methyl iodide (3.77 mL, 8.60 g, 60.6 mmol) was added, then the reaction continued and allowed to warm slowly to rt overnight before being quenched by dropwise addition of satd NH₄Cl then EtOH (~5 mL each). After an additional 30 min stirring, the mixture was evaporated under vacuum and the residue extracted with Et₂O and water. The aqueous layer was extracted again with Et₂O and the combined organic solutions washed twice with brine, dried over MgSO₄, filtered, and evaporated to give a viscous orange oil. Additional purification by flash column chromatography on silica gel, eluted with 20 → 30 → 40 → 50 → 60% CH₂Cl₂/hexane, gave the title compound as a pale-yellow oil which crystallized on standing to a greasy, off-white solid (7.22 g, 86%). δ_{H} (400 MHz, DMSO-*d*₆) 7.58 (dt, 1H, *J* = 1.0, 8.0), 7.52 (d, 1H, *J* = 3.5), 7.13–7.09 (m, 2H), 7.07–7.00 (m, 1H), 6.47 (d, 1H, *J* = 3.5), 4.12 (q, 2H, *J* = 7.0), 1.81 (s, 6H), 1.06 (t, 3H, *J* = 7.0). δ_{C} (101 MHz, DMSO-*d*₆) 173.7, 135.1, 129.8, 126.0, 121.6, 121.3, 119.7, 111.4, 101.2, 61.8, 60.9, 25.9, 14.3. *m/z* (ES) 232 ([M + H]⁺). HRMS, found 232.1332 (C₁₄H₁₈NO₂ requires 232.1338). HPLC purity 97.9%.

2-(1H-Indol-1-yl)-2-methylpropan-1-ol 72. A solution of ester **71** (7.12 g, 30.8 mmol) in anhydrous THF (85 mL) was added over 15 min to a suspension of LiAlH₄ (1.28 g, 33.9 mmol) in the same solvent (40 mL) at –78 °C (some exotherm observed over the addition period). The reaction temperature was brought back down to –78 °C then stirring continued overnight, allowing for gradual warming to rt. The mixture was cooled to –78 °C once more then quenched by very cautious, dropwise addition of satd NH₄Cl, after which it was allowed to warm slowly to rt once more. The solvent was removed by evaporation under vacuum, then the residue extracted with Et₂O and water. The mixture was filtered under vacuum to remove suspended solids, then the layers separated and the aqueous phase extracted with more Et₂O. The combined organic extracts were washed with water then brine, dried over Na₂SO₄, filtered, and evaporated. Purification by flash column chromatography on silica gel, eluted with 0 → 1 → 2 → 3% MeOH/CH₂Cl₂, afforded the title compound as a yellow oil which slowly crystallized on standing to a pale-yellow solid (4.56 g, 78%). δ_{H} (400 MHz, DMSO-*d*₆) 7.69–7.64 (m, 1H), 7.56–7.51 (m, 1H), 7.43 (d, 1H, *J* = 3.5), 7.10–7.05 (m, 1H), 7.02–6.97 (m, 1H), 6.38 (dd, 1H, *J* = 1.0, 3.5), 5.08 (t, 1H, *J* = 4.5), 3.82 (d, 2H, *J* = 4.5), 1.62 (s, 6H). δ_{C} (101 MHz, DMSO-*d*₆) 135.1, 130.3, 127.6, 121.0, 120.7, 118.9, 113.7, 100.1, 67.6, 60.1, 25.2. *m/z* (ES) 190 ([M + H]⁺). HRMS, found 190.1232 (C₁₂H₁₆NO requires 190.1232), HPLC purity 99.3%, mp 68–71 °C.

1-(1-Methoxy-2-methylpropan-2-yl)-1H-indole 4l. Sodium hydride (60% dispersion in mineral oil, 248 mg, 6.2 mmol) was added in portions over 5 min to a solution of alcohol **72** (1.01 g, 4.97 mmol) in anhydrous THF (50 mL) at 0 °C. After 5 min more, methyl iodide (467 μ L, 1.06 g, 7.5 mmol) was added. The mixture was stirred at 0 °C for 30 min then rt for 3 h and quenched by dropwise addition of satd NH₄Cl. The mixture was evaporated under vacuum, extracted with Et₂O and water, the aqueous phase re-extracted with Et₂O, and the combined extracts dried over Na₂SO₄, filtered, and evaporated. Flash column chromatography on silica gel, eluted with 20 → 30 → 40% CH₂Cl₂/hexane, provided the title compound as a colorless oil (856 mg, 79%). δ_{H} (400 MHz, DMSO-*d*₆) 7.71–7.68 (m, 1H), 7.54 (d, 1H, *J* = 8.0), 7.37 (d, 1H, *J* = 3.5), 7.11–7.06 (m, 1H), 7.03–6.98 (m, 1H), 6.39 (dd, 1H, *J* = 0.5, 3.5), 3.75 (s, 2H), 3.18 (s, 3H), 1.65 (s, 6H). δ_{C} (101 MHz, DMSO-*d*₆) 135.0, 130.2, 127.5, 121.1, 120.9, 119.1, 113.6, 100.4, 78.2, 59.00, 58.97, 25.5. *m/z* (ES) 204 ([M + H]⁺). HRMS, found 204.1381 (C₁₃H₁₈NO requires 204.1388). HPLC purity 99.6%.

Ethyl 2-(2-(1H-Indol-1-yl)-2-methylpropoxy)acetate 4m. Ethyl bromoacetate (665 μL , 1.00 g, 6.0 mmol) and alcohol **72** (945 mg, 5.0 mmol) were dissolved in dry DMF, then sodium hydride (60% dispersion in mineral oil, 0.24 g, 6.0 mmol) was added slowly, in small portions, over 40 min. After stirring overnight at rt, additional ethyl bromoacetate (277 μL , 417 mg, 2.5 mmol) was added, followed by sodium hydride (60% dispersion in mineral oil, 100 mg, 2.5 mmol) over 30 min. The mixture was stirred at rt for a further 2 h then quenched by dropwise addition of satd NH_4Cl and evaporated under vacuum. The residue was extracted with EtOAc and satd NH_4Cl (100 mL each), then the aqueous layer extracted three more times with EtOAc. The combined organic extracts were then washed twice with water, then brine, dried over Na_2SO_4 , filtered, and concentrated under vacuum. Flash column chromatography on silica gel was carried out, eluted with 20 \rightarrow 33 \rightarrow 50% CH_2Cl_2 /toluene, affording the title compound as an orange gum (400 mg, 29%). δ_{H} (400 MHz, CDCl_3) 7.65 (t, 2H, $J = 8.5$), 7.42 (d, 1H, $J = 3.0$), 7.21–7.15 (m, 1H), 7.15–7.09 (m, 1H), 6.51 (d, 1H, $J = 3.0$), 4.19 (q, 2H, $J = 7.0$), 3.99 (s, 2H), 3.95 (s, 2H), 1.82 (s, 6H), 1.27 (t, 3H, $J = 7.0$). δ_{C} (101 MHz, CDCl_3) 168.6, 133.0, 128.4, 124.4, 119.4, 118.9, 117.1, 111.1, 98.7, 66.6, 59.0, 56.9, 23.4, 12.3. m/z (ES) 276 ($[\text{M} + \text{H}]^+$). HRMS, found 276.1610 ($\text{C}_{16}\text{H}_{22}\text{NO}_3$ requires 276.1600). HPLC purity 92.0%. Additional material from mixed column fractions was further purified by preparative HPLC, using a gradient of 40–70% MeCN/water, to give an additional portion of the title compound as a thick, orange-brown oil (40 mg, 3%; combined yield 440 mg, 32%).

Methyl 3-(1H-Indol-1-yl)propanoate 4n. Methyl acrylate (1.35 mL, 1.29 g, 15 mmol) and DBU (772 μL , 5 mmol) were added to a solution of indole (1.17 g, 10 mmol) in anhydrous MeCN (50 mL). The mixture was heated at 50 $^\circ\text{C}$ for 6 h, rt for 48 h, then 50 $^\circ\text{C}$ for 6 h and evaporated to dryness. EtOAc and water (50 mL) each were added, and after the residue had fully dissolved, the aqueous layer was adjusted to pH 6 with 1 M HCl and the mixture extracted. The aqueous layer was extracted with additional EtOAc (3 \times 30 mL), then the combined organic solutions washed twice with water, then brine, dried over Na_2SO_4 , filtered, and evaporated. Flash column chromatography on silica gel, eluted with 50 \rightarrow 67 \rightarrow 100% toluene/hexane, yielded the title compound as an oil (865 mg, 43%). δ_{H} (400 MHz, CDCl_3) 7.66 (dt, 1H, $J = 1.0, 8.0$), 7.38 (dd, 1H, $J = 0.5, 8.5$), 7.32–7.12 (m, 3H), 4.49 (t, 2H, $J = 7.0$), 3.70 (s, 3H), 2.86 (t, 2H, $J = 7.0$). δ_{C} (101 MHz, CDCl_3) 171.7, 135.6, 128.7, 128.0, 121.7, 121.1, 119.5, 109.1, 101.6, 52.0, 41.9, 34.8. m/z (ES) 204 ($[\text{M} + \text{H}]^+$). HRMS, found 204.1033 ($\text{C}_{12}\text{H}_{14}\text{NO}_2$ requires 204.1025). HPLC purity 97.8%.

2-Isopropoxy-5-nitropyridine 74. Sodium hydride (60% dispersion in mineral oil, 2.40 g, 60 mmol) was added in portions to anhydrous propan-2-ol (150 mL), then stirring of the suspension continued for 30 min. 2-Chloro-5-nitropyridine (9.51 g, 60 mmol) was then added and the reaction allowed to continue for 1 h before quenching by cautious, dropwise addition of water. The mixture was then evaporated under vacuum and the residue purified by flash column chromatography on silica gel, eluted with 1:19 EtOAc/hexane, affording the title compound as pale-yellow crystals (8.6 g, 64%). δ_{H} (400 MHz, $\text{DMSO}-d_6$) 9.25 (d, 1H, $J = 3.0$), 8.45 (dd, 1H, $J = 3.0, 9.0$), 6.96 (d, 1H, $J = 9.0$), 5.37 (septet, 1H, $J = 6.0$), 1.34 (d, 6H, $J = 6.0$). δ_{C} (101 MHz, $\text{DMSO}-d_6$) 166.7, 145.2, 139.5, 135.1, 112.2, 70.6, 22.0. m/z (ES) 183 ($[\text{M} + \text{H}]^+$). HRMS, found 183.0762 ($\text{C}_8\text{H}_{11}\text{N}_2\text{O}_3$ requires 183.0770). mp 47–50 $^\circ\text{C}$.

2-tert-Butoxy-5-nitropyridine 75. 2-Chloro-5-nitropyridine (2.38 g, 15 mmol) and *tert*-butanol (3.6 mL, 45 mmol) were dissolved in dry DMF (20 mL), then sodium hydride (60% dispersion in mineral oil, 0.72 g, 18 mmol) added slowly in small portions. During the addition, the reaction mixture was cooled in ice to control the observed exotherm. After addition was complete, stirring was continued at rt for 4 h, then water added dropwise to quench the reaction. The mixture was evaporated under vacuum and the residue purified by flash column chromatography on silica gel, eluted with 2 \rightarrow 4 \rightarrow 6 \rightarrow 10% EtOAc/hexane, to give the title compound as a dark-brown oil (1.34 g, 46%). δ_{H} (400 MHz, CDCl_3) 9.06 (d, 1H, $J = 3.0$), 8.30 (dd, 1H, $J = 3.0, 9.0$), 6.71 (d, 1H, $J = 9.0$), 1.65 (s, 9H). δ_{C} (101 MHz, CDCl_3) 167.3,

144.3, 138.6, 133.4, 113.0, 82.8, 28.4. m/z (GC-MS, EI) 196 (M^+). HRMS, found 196.0838 ($\text{C}_9\text{H}_{12}\text{N}_2\text{O}_3$ requires 196.0842). HPLC purity 91.9%.

Ethyl 2-(5-Nitropyridin-2-yloxy)acetate 76. Sodium hydride (60% dispersion in mineral oil, 0.80 g, 20 mmol) was added in small portions, slowly over 1.75 h, to a solution of 2-chloro-5-nitropyridine (3.18 g, 20 mmol) and ethyl glycolate (1.58 mL, 1.73 g, 16.6 mmol) in anhydrous THF (100 mL). After stirring at rt for 2 h more, the reaction was carefully quenched by dropwise addition of water, then the mixture evaporated under vacuum. The residue was partitioned between EtOAc and water, the layers separated, and the aqueous phase extracted with additional EtOAc. The combined extracts were washed with brine, dried over Na_2SO_4 , filtered, and evaporated, then the residue purified by flash column chromatography on silica gel, eluted with 5 \rightarrow 10 \rightarrow 15 \rightarrow 20% EtOAc/hexane, to provide the title compound as a pale-yellow solid (2.96 g, 65%). δ_{H} (400 MHz, CDCl_3) 9.05 (d, 1H, $J = 3.0$), 8.43 (dd, 1H, $J = 3.0, 9.0$), 7.01 (d, 1H, $J = 9.0$), 5.01 (s, 2H), 4.27 (q, 2H, $J = 7.0$), 1.31 (t, 3H, $J = 7.0$). δ_{C} (101 MHz, CDCl_3) 168.1, 165.7, 144.4, 134.4, 111.4, 63.5, 61.5, 14.1. m/z (ES) 227 ($[\text{M} + \text{H}]^+$). HRMS, found 227.0675 ($\text{C}_9\text{H}_{11}\text{N}_2\text{O}_5$ requires 227.0668). HPLC purity 99.2%. mp 51–52 $^\circ\text{C}$.

Hydrogenation of Nitro-compounds 74–76 to Amines 77–79: General Procedure. A 0.1 M solution of the nitro-compound in MeOH was hydrogenated over 10% Pd/C, using a ThalesNano H-Cube reactor in full H_2 mode at a flow rate of 0.5 mL min^{-1} . Evaporation of the solvent and further drying under vacuum gave the amine products, which were used without further purification.

6-Isopropoxy-pyridin-3-amine 77. Hydrogenation of **74** (767 mg, 4.2 mmol) gave the title compound as a peach-colored oil (397 mg, 62%). δ_{H} (400 MHz, $\text{DMSO}-d_6$) 7.49 (d, 1H, $J = 3.0$), 6.97 (dd, 1H, $J = 3.0, 9.0$), 6.46 (d, 1H, $J = 9.0$), 4.71 (septet, 1H, $J = 6.0$), 1.21 (d, 6H, $J = 6.0$). δ_{C} (101 MHz, $\text{DMSO}-d_6$) 166.7, 145.2, 139.5, 135.1, 112.2, 70.6, 20.1. m/z (ES) 153 ($[\text{M} + \text{H}]^+$). HRMS, found 153.1022 ($\text{C}_8\text{H}_{13}\text{N}_2\text{O}_3$ requires 153.1028).

6-tert-Butoxy-pyridin-3-amine 78. Hydrogenation of **75** (640 mg, 3.86 mmol) gave the title compound as a brown solid (475 mg, 88%). δ_{H} (400 MHz, CDCl_3) 7.70 (d, 1H, $J = 3.0$), 6.99 (dd, 1H, $J = 3.0, 9.0$), 6.58 (d, 1H, $J = 9.0$), 3.27 (br s, 2H), 1.49 (s, 9H). δ_{C} (101 MHz, CDCl_3) 156.9, 137.2, 133.5, 126.5, 115.0, 78.9, 28.9. m/z (ES) 167 ($[\text{M} + \text{H}]^+$). HRMS, found 167.1188 ($\text{C}_9\text{H}_{15}\text{N}_2\text{O}$ requires 167.1184). HPLC purity 90.4%. mp 77–78 $^\circ\text{C}$ (decomp).

Ethyl 2-(5-Aminopyridin-2-yloxy)acetate 79. Hydrogenation of **76** (1.46 g, 6.46 mmol) provided the title compound as an off-white solid (1.21 g, 95%). δ_{H} (400 MHz, $\text{DMSO}-d_6$) 7.42 (dd, 1H, $J = 0.5, 3.0$), 7.03 (dd, 1H, $J = 3.0, 8.5$), 6.63 (dd, 1H, $J = 0.5, 8.5$), 4.80 (s, 2H), 4.73 (s, 2H), 4.11 (q, 2H, $J = 7.0$), 1.17 (t, 2H, $J = 7.0$). δ_{C} (101 MHz, $\text{DMSO}-d_6$) 169.9, 154.4, 140.5, 131.0, 126.9, 110.6, 62.2, 60.6, 14.5. m/z (ES) 197 ($[\text{M} + \text{H}]^+$). HRMS, found 197.0930 ($\text{C}_9\text{H}_{13}\text{N}_2\text{O}_3$ requires 197.0926). HPLC purity 98.9%. mp 101–104 $^\circ\text{C}$.

One-Pot Synthesis of Indole-3-glyoxylamide Derivatives 5–35, 56–60, 62, and 64 (Scheme 1a): General Procedure. The appropriate starting indole **4a–o** (1.5 mmol) was dissolved in anhydrous THF (15 mL), then oxalyl chloride (144 μL , 209 mg, 1.65 mmol) was added. The solution was stirred at rt for 3 h, then DIPEA (610 μL , 452 mg, 3.5 mmol) added followed by the requisite amine ($\text{R}^2\text{-NH}_2$, 1.8 mmol) and DMAP (catalytic amount). The suspension was stirred at rt overnight then evaporated to dryness. The residue was extracted with EtOAc and water, then the organic layer evaporated once more to provide the crude product which was purified as specified in each case. Unless stated otherwise, purification was achieved by two successive recrystallizations: first from EtOAc/hexane, then from propan-2-ol/water. Characterization data, HPLC purity, and any additional purification details are provided for each example in the Supporting Information.

Synthesis of Indole-3-glyoxylate Methyl Esters 68a–j from Indoles 67a–j: General Procedure. The relevant indole compound **67a–j** was dissolved in anhydrous CH_2Cl_2 at a concentration of 0.1 M, then the solution was cooled to 0 $^\circ\text{C}$. AlCl_3 (typically 1.25 equiv) and methyl chlorooxacetate (typically 1.25 equiv) were added and the reaction continued at 0 $^\circ\text{C}$ until acceptable conversion was seen as

judged by TLC (reaction duration specified below for each case). Methanol was added to quench the reaction, then the mixture poured into satd NaHCO₃ and extracted thoroughly. If an emulsion resulted, the entire mixture was filtered under vacuum and the filtrate returned to the separating funnel. The organic layer was collected and the aqueous phase extracted with additional CH₂Cl₂. The combined organic extracts were dried over Na₂SO₄ and evaporated. Further purification was carried out by flash column chromatography on silica gel, using an eluent indicated in each case, to afford the desired product **68a–j**.

Methyl 2-(4-Chloro-1-isopropyl-1H-indol-3-yl)-2-oxoacetate 68a. Prepared from **67a** (520 μ L, 581 mg, 3.0 mmol), AlCl₃ (600 mg, 4.5 mmol), and methyl chlorooxoacetate (414 μ L, 551 mg, 4.5 mmol). Reaction duration 1 h. Column eluent 20 \rightarrow 33 \rightarrow 50% EtOAc/hexane. Title compound obtained as a yellow gum (280 mg, 33%). δ_{H} (400 MHz, CDCl₃) 8.28 (s, 1H), 7.38–7.21 (m, 3H), 4.71 (septet, 1H, $J = 6.5$), 3.96 (s, 3H), 1.60 (d, 6H, $J = 6.5$). δ_{C} (101 MHz, CDCl₃) 178.4, 164.5, 138.3, 135.7, 127.5, 124.5, 124.2, 113.6, 109.0, 52.7, 48.6, 22.4. m/z (ES) 280 (100%; [M(³⁵Cl) + H]⁺), 282 (30%; [M(³⁷Cl) + H]⁺). HRMS, found 280.0731 (C₁₄H₁₅ClNO₃ requires 280.0740). HPLC purity 98.6%.

Methyl 2-(5-Chloro-1-(2-methoxyethyl)-1H-indol-3-yl)-2-oxoacetate 68c. Prepared from **67c** (285 mg, 1.36 mmol), AlCl₃ (227 mg, 1.70 mmol), and methyl chlorooxoacetate (156 μ L, 208 mg, 1.70 mmol). Reaction duration 1 h. Column eluent 20 \rightarrow 33 \rightarrow 50 \rightarrow 67% EtOAc/hexane. Title compound obtained as a greasy, yellow solid (111 mg, 28%). δ_{H} (400 MHz, CDCl₃) 8.45 (s, 1H), 8.44 (dd, 1H, $J = 0.5, 2.0$), 7.35–7.28 (m, 2H), 4.33 (t, 2H, $J = 5.0$), 3.97 (s, 3H), 3.76 (t, 2H, $J = 5.0$), 3.34 (s, 3H). δ_{C} (101 MHz, CDCl₃) 176.9, 163.0, 141.0, 135.2, 129.6, 128.2, 124.5, 122.4, 112.6, 111.2, 70.6, 59.2, 52.8, 47.5. m/z (ES) 296 (100%; [M(³⁵Cl) + H]⁺), 298 (35%; [M(³⁷Cl) + H]⁺). HRMS, found 296.0694 (C₁₄H₁₅ClNO₄ requires 296.0690). HPLC purity 95.9%. mp 88–90 °C.

Methyl 2-(6-Chloro-1-isopropyl-1H-indol-3-yl)-2-oxoacetate 68d. Prepared using **67d** (347 μ L, 387 mg, 2.0 mmol), AlCl₃ (667 mg, 5.0 mmol), and methyl chlorooxoacetate (460 μ L, 613 mg, 5.0 mmol). Reaction duration 100 min (at rt). Column eluent 20 \rightarrow 30 \rightarrow 40% EtOAc/hexane. Title compound obtained as a crystalline yellow solid (142 mg, 25%). δ_{H} (400 MHz, CDCl₃) 8.49 (s, 1H), 8.38 (d, 1H, $J = 8.5$), 7.44 (s, 1H), 7.33 (d, 1H, $J = 8.5$), 4.66 (septet, 1H, $J = 6.5$), 3.98 (s, 3H), 1.64 (d, 6H, $J = 6.5$). δ_{C} (101 MHz, CDCl₃) 176.7, 163.2, 136.9, 136.4, 130.0, 125.8, 124.1, 123.9, 113.1, 110.5, 52.8, 48.7, 22.5. m/z (ES) 280 (100%; [M(³⁵Cl) + H]⁺), 282 (35%; [M(³⁷Cl) + H]⁺). HRMS, found 280.0742 (C₁₄H₁₅ClNO₃ requires 280.0740). HPLC purity 99.7%. mp 94–95 °C.

Methyl 2-(7-Chloro-1-isopropyl-1H-indol-3-yl)-2-oxoacetate 68e. Prepared using **67e** (441 mg, 2.28 mmol), AlCl₃ (380 mg, 2.85 mmol), and methyl chlorooxoacetate (262 μ L, 349 mg, 2.85 mmol). Reaction duration 1 h. Column eluent 15 \rightarrow 33 \rightarrow 50 \rightarrow 67% CH₂Cl₂/hexane then 20 \rightarrow 33% EtOAc/hexane. Title compound obtained as a waxy yellow solid (195 mg, 31%). δ_{H} (400 MHz, CDCl₃) 8.60 (s, 1H), 8.45 (dd, 1H, $J = 1.0, 8.0$), 7.32 (dd, 1H, $J = 1.0, 8.0$), 7.25 (t, 1H, $J = 8.0$), 5.73 (septet, 1H, $J = 6.5$), 3.98 (s, 3H), 1.64 (d, 6H, $J = 6.5$). δ_{C} (101 MHz, CDCl₃) 176.7, 163.2, 137.0, 132.1, 130.2, 126.4, 124.1, 121.6, 117.2, 113.1, 52.8, 49.6, 23.8. m/z (ES) 280 (100%; [M(³⁵Cl) + H]⁺), 282 (30%; [M(³⁷Cl) + H]⁺). HRMS, found 280.0734 (C₁₄H₁₅ClNO₃ requires 280.0740). HPLC purity 99.2%; mp 62 °C.

Methyl 2-(1-Isopropyl-4-methoxy-1H-indol-3-yl)-2-oxoacetate 68f. Prepared using **67f** (405 mg, 2.14 mmol), AlCl₃ (428 mg, 3.21 mmol), and methyl chlorooxoacetate (295 μ L, 393 mg, 3.21 mmol). Reaction duration 80 min. Column eluent 10 \rightarrow 20 \rightarrow 33 \rightarrow 50% EtOAc/pentanes. Title compound obtained as a bright-yellow gum (120 mg, 20%). δ_{H} (400 MHz, CDCl₃) 8.13 (s, 1H), 7.26 (t, 1H, $J = 8.0$), 7.07 (d, 1H, $J = 8.0$), 6.72 (d, 1H, $J = 8.0$), 4.68 (septet, 1H, $J = 6.5$), 3.95 (s, 3H), 3.94 (s, 3H), 1.59 (d, 6H, $J = 6.5$). δ_{C} (101 MHz, CDCl₃) 182.0, 165.6, 154.1, 138.3, 132.6, 124.4, 115.9, 113.5, 103.8, 103.4, 55.6, 52.3, 48.5, 22.6. m/z (ES) 276 ([M + H]⁺). HRMS, found 276.1232 (C₁₅H₁₈NO₄ requires 276.1236). HPLC purity 98.1%.

Methyl 2-(1-Isopropyl-5-methoxy-1H-indol-3-yl)-2-oxoacetate 68g. Prepared using **67g** (315 mg, 1.66 mmol), AlCl₃ (277 mg,

2.08 mmol), and methyl chlorooxoacetate (191 μ L, 255 mg, 2.08 mmol). Reaction duration 50 min. Column eluent 10 \rightarrow 20 \rightarrow 30 \rightarrow 40% EtOAc/hexane. Title compound obtained as a thick, orange oil (146 mg, 32%). δ_{H} (400 MHz, CDCl₃) 8.43 (s, 1H), 7.98 (d, 1H, $J = 2.5$), 7.33 (d, 1H, $J = 9.0$), 6.98 (dd, 1H, $J = 2.5, 9.0$), 4.67 (septet, 1H, $J = 6.5$), 3.97 (s, 3H), 3.93 (s, 3H), 1.61 (d, 6H, $J = 6.5$). δ_{C} (101 MHz, CDCl₃) 176.8, 163.6, 157.1, 135.7, 131.2, 128.3, 114.2, 112.8, 111.1, 104.3, 55.8, 52.7, 48.7, 22.6. m/z (ES) 276 ([M + H]⁺). HRMS, found 276.1226 (C₁₅H₁₈NO₄ requires 276.1236). HPLC purity 92.1%.

Methyl 2-(5-Methoxy-1-(2-methoxyethyl)-1H-indol-3-yl)-2-oxoacetate 68h. Prepared using **67h** (308 mg, 1.50 mmol), AlCl₃ (251 mg, 1.88 mmol), and methyl chlorooxoacetate (173 μ L, 230 mg, 1.88 mmol). Reaction duration 40 min. Column eluent 20 \rightarrow 40 \rightarrow 60 \rightarrow 80% EtOAc/hexane. Title compound obtained as a viscous, bright-yellow oil (134 mg, 31%) which crystallized on storage at –20 °C, giving a yellow solid. δ_{H} (400 MHz, CDCl₃) 8.38 (s, 1H), 7.97 (d, 1H, $J = 2.5$), 7.30 (d, 1H, $J = 9.0$), 6.98 (dd, 1H, $J = 2.5, 9.0$), 4.32 (t, 2H, $J = 5.0$), 3.97 (s, 3H), 3.93 (s, 3H), 3.76 (t, 2H, $J = 5.0$), 3.34 (s, 3H). δ_{C} (101 MHz, CDCl₃) 177.1, 163.5, 157.1, 147.1, 131.6, 128.2, 114.3, 112.9, 110.9, 104.3, 70.6, 59.1, 55.8, 52.7, 47.5. m/z (ES) 292 ([M + H]⁺). HRMS, found 292.1186 (C₁₅H₁₈ClNO₅ requires 292.1185). HPLC purity 97.8%. mp 80–82 °C.

Methyl 2-(1-Isopropyl-6-methoxy-1H-indol-3-yl)-2-oxoacetate 68i. Prepared using **67i** (348 mg, 1.84 mmol), AlCl₃ (307 mg, 2.30 mmol), and methyl chlorooxoacetate (212 μ L, 282 mg, 2.30 mmol). Reaction duration 70 min. Column eluent 15 \rightarrow 30 \rightarrow 40% EtOAc/hexane. Title compound obtained as a thick, yellow oil (175 mg, 35%) which crystallized on storage at –20 °C to give a yellow solid. δ_{H} (400 MHz, CDCl₃) 8.40 (s, 1H), 8.34 (d, 1H, $J = 8.5$), 7.00 (dd, 1H, $J = 2.0, 8.5$), 6.89 (d, 1H, $J = 2.0$), 4.64 (septet, 1H, $J = 6.5$), 3.96 (s, 3H), 3.90 (s, 3H), 1.62 (d, 6H, $J = 6.5$). δ_{C} (101 MHz, CDCl₃) 176.7, 163.5, 157.6, 137.4, 135.3, 123.6, 121.2, 113.2, 112.2, 94.6, 55.8, 52.6, 48.3, 22.4. m/z (ES) 276 ([M + H]⁺). HRMS, found 276.1243 (C₁₅H₁₈NO₄ requires 276.1236). HPLC purity 95.9%. mp 91 °C.

Methyl 2-(1-Isopropyl-7-methoxy-1H-indol-3-yl)-2-oxoacetate 68j. Prepared using **67j** (379 mg, 2.0 mmol), AlCl₃ (333 mg, 2.5 mmol), and methyl chlorooxoacetate (230 μ L, 306 mg, 2.5 mmol). Reaction duration 1 h. Column eluent 5 \rightarrow 10 \rightarrow 20 \rightarrow 30% EtOAc/pentanes. Title compound obtained as a viscous orange oil (150 mg, 27%). δ_{H} (400 MHz, CDCl₃) 8.46 (s, 1H), 8.09 (dd, 1H, $J = 1.0, 8.0$), 7.26 (t, 1H, $J = 8.0$), 6.82–6.79 (m, 1H), 5.46 (septet, 1H, $J = 6.5$), 3.98 (s, 3H), 3.97 (s, 3H), 1.58 (d, 6H, $J = 6.5$). δ_{C} (101 MHz, CDCl₃) 176.8, 163.6, 147.5, 135.8, 129.5, 126.2, 124.2, 115.3, 113.1, 105.4, 55.5, 52.7, 50.7, 23.6. m/z (ES) 276 ([M + H]⁺). HRMS, found 276.1232 (C₁₅H₁₈NO₄ requires 276.1236). HPLC purity 80.2%.

Synthesis of Azaindole-3-glyoxylate Methyl Esters 68k–o from Azaindoles 67k–o: General Procedure. The relevant azaindole compound **67k–o** was dissolved in anhydrous CH₂Cl₂ (30 mL/mmol), then AlCl₃ (5 equiv) was added and the suspension stirred for 1 h. Methyl chlorooxoacetate (5 equiv) was added and reaction continued for the duration specified in each case. Methanol was added to quench the reaction, then the mixture was evaporated to dryness under vacuum. Further purification was carried out by flash column chromatography on silica gel, using an eluent indicated in each case, to afford the desired product **68k–o**.

Methyl 2-(1-Isopropyl-1H-pyrrolo[3,2-b]pyridin-3-yl)-2-oxoacetate 68k. Prepared from **67k** (365 mg, 2.28 mmol), AlCl₃ (1.52 g, 11.4 mmol), and methyl chlorooxoacetate (1.05 mL, 1.40 mg, 11.4 mmol). Reaction duration 4.5 h. In this case, after quenching with MeOH, extraction between EtOAc and water was carried out and the organic layer collected and evaporated. Column eluent 2.5 \rightarrow 5 \rightarrow 10% MeOH/CHCl₃. Product obtained as a golden brown gum (40 mg, 7%). Given the poor recovery in this case, it is suspected the majority of material was either retained by the column or decomposed on silica. δ_{H} (400 MHz, CDCl₃) 8.71 (dd, 1H, $J = 1.5, 4.5$), 8.57 (s, 1H), 7.75 (dd, 1H, $J = 1.5, 8.5$), 7.24 (dd, 1H, $J = 4.5, 8.5$), 4.71 (septet, 1H, $J = 6.5$), 3.97 (s, 3H), 1.62 (d, 6H, $J = 6.5$). δ_{C} (101 MHz, CDCl₃) 177.4, 164.1, 146.6, 144.9, 136.7, 129.4, 118.2, 117.9, 112.6, 52.8, 49.1, 22.4. m/z (ES) 247 ([M + H]⁺). HRMS, found 247.1082 (C₁₃H₁₅N₂O₃ requires 247.1083). HPLC purity 95.8%.

Methyl 2-(1-Isopropyl-1H-pyrrolo[3,2-c]pyridin-3-yl)-2-oxoacetate 68f. Prepared from **67l** (320 mg, 2.0 mmol), AlCl_3 (1.33 g, 10 mmol), and methyl chlorooxoacetate (0.92 mL, 1.23 mg, 10 mmol). Reaction duration 2 h. Column eluent 0 \rightarrow 2 \rightarrow 4 \rightarrow 6 \rightarrow 8% MeOH/ CH_2Cl_2 . Product obtained as a waxy, off-white solid (191 mg, 39%). δ_{H} (400 MHz, CDCl_3) 9.66 (d, 1H, $J = 1.0$), 8.54 (s, 1H), 8.51 (d, 1H, $J = 6.0$), 7.36 (dd, 1H, $J = 1.0, 6.0$), 4.73 (septet, 1H, $J = 7.0$), 3.99 (s, 3H), 1.65 (d, 6H, $J = 7.0$). δ_{C} (101 MHz, CDCl_3) 176.6, 162.8, 145.9, 143.3, 140.4, 136.5, 123.6, 113.2, 105.5, 52.9, 48.9, 22.5. m/z (ES) 247 ($[\text{M} + \text{H}]^+$). HRMS, found 247.1081 ($\text{C}_{13}\text{H}_{15}\text{N}_2\text{O}_3$ requires 247.1083). HPLC purity 94.1%.

Methyl 2-(1-Isopropyl-1H-pyrrolo[2,3-c]pyridin-3-yl)-2-oxoacetate 68m. Prepared from **67m** (320 mg, 2.0 mmol), AlCl_3 (1.33 g, 10 mmol), and methyl chlorooxoacetate (0.92 mL, 1.23 mg, 10 mmol). Reaction duration 2 h. Column eluent 0 \rightarrow 1 \rightarrow 2 \rightarrow 4 \rightarrow 6% MeOH/ CH_2Cl_2 . Product obtained as a waxy, off-white solid (263 mg, 53%). δ_{H} (400 MHz, $\text{DMSO}-d_6$) 9.14 (d, 1H, $J = 1.0$), 8.71 (s, 1H), 8.42 (d, 1H, $J = 5.5$), 8.07 (dd, 1H, $J = 1.0, 5.5$), 5.04 (septet, 1H, $J = 6.5$), 3.92 (s, 3H), 1.58 (d, 6H, $J = 6.5$). δ_{C} (101 MHz, $\text{DMSO}-d_6$) 178.7, 163.8, 142.7, 140.0, 135.2, 133.5, 131.8, 116.0, 111.7, 53.2, 49.8, 22.6. m/z (ES) 247 ($[\text{M} + \text{H}]^+$). HRMS, found 247.1074 ($\text{C}_{13}\text{H}_{15}\text{N}_2\text{O}_3$ requires 247.1083). HPLC purity 97.4%.

Methyl 2-(1-Isopropyl-1H-pyrrolo[2,3-b]pyridin-3-yl)-2-oxoacetate 68n. Prepared from **67n** (320 mg, 2.0 mmol), AlCl_3 (1.33 g, 10 mmol), and methyl chlorooxoacetate (0.92 mL, 1.23 mg, 10 mmol). Reaction duration 2.5 h. Column eluent 67 \rightarrow 100% CH_2Cl_2 /hexane then 0.5 \rightarrow 1 \rightarrow 2% MeOH/ CH_2Cl_2 . Product obtained as a waxy, off-white solid (421 mg, 86%). δ_{H} (400 MHz, $\text{DMSO}-d_6$) 8.73 (s, 1H), 8.49 (dd, 1H, $J = 1.5, 8.0$), 8.45 (dd, 1H, $J = 1.5, 4.5$), 7.39 (dd, 1H, $J = 4.5, 8.0$), 5.15 (septet, 1H, $J = 7.0$), 3.92 (s, 3H), 1.56 (d, 6H, $J = 7.0$). δ_{C} (101 MHz, $\text{DMSO}-d_6$) 178.8, 163.8, 147.9, 145.3, 138.2, 130.4, 119.9, 119.1, 110.6, 53.2, 47.7, 22.4. m/z (ES) 247 ($[\text{M} + \text{H}]^+$). HRMS, found 247.1089 ($\text{C}_{13}\text{H}_{15}\text{N}_2\text{O}_3$ requires 247.1083).

Methyl 2-(1-(2-Methoxyethyl)-1H-pyrrolo[2,3-b]pyridin-3-yl)-2-oxoacetate 68o. Prepared from **67o** (325 μL , 352 mg, 2.0 mmol), AlCl_3 (1.33 g, 10 mmol), and methyl chlorooxoacetate (0.92 mL, 1.23 mg, 10 mmol). Reaction duration 5 h. Column eluent 0 \rightarrow 1 \rightarrow 2 \rightarrow 4% MeOH/ CH_2Cl_2 . Product obtained as a pale-yellow oil which crystallized on standing to a beige solid (324 mg, 62%). δ_{H} (400 MHz, CDCl_3) 8.68 (dd, 1H, $J = 1.5, 8.0$), 8.62 (s, 1H), 8.42 (dd, 1H, $J = 1.5, 5.0$), 7.30 (dd, 1H, $J = 5.0, 8.0$), 4.55 (t, 2H, $J = 5.0$), 3.98 (s, 3H), 3.80 (t, 2H, $J = 5.0$), 3.36 (s, 3H). δ_{C} (101 MHz, CDCl_3) 177.1, 162.8, 148.0, 145.0, 140.6, 131.2, 119.6, 119.4, 111.3, 70.6, 59.0, 52.8, 45.3. m/z (ES) 263 ($[\text{M} + \text{H}]^+$). HRMS, found 263.1038 ($\text{C}_{13}\text{H}_{15}\text{N}_2\text{O}_4$ requires 263.1032). HPLC purity 98.3%. mp 69–70 °C.

Conversion of Esters 68a and 68c–o into Amides 36, 38, and 40–51 (Scheme 1b): General Procedure. The starting ester, the relevant amine ($\text{R}^2\text{-NH}_2$, 1.2 equiv) and TBD (30 mol %) were combined in the minimum volume of toluene (typically 1–2 mL), then the mixture was heated at 85 °C overnight. The solvent was removed by rotary evaporation then the residue purified further. Unless stated otherwise, this was achieved as follows. Hexane was added to a solution of the crude material in boiling EtOAc, with continuing heating, until cloudiness persisted, at which point the mixture was left to stand for 1–2 min. A sticky film of brown gum (mostly unreacted amine component) quickly accumulated at the bottom of the flask from which the remainder of the suspension could readily be decanted into a separate flask, at which point, the mixture was evaporated to dryness. Recrystallization of the remaining residue from propan-2-ol/water provided the amide product, which was collected by filtration and dried. Characterization data, HPLC purity, and any additional purification details are provided for each example in the Supporting Information.

Synthesis of Alkynes 81–83 from 2-Bromopyridine: General Procedure. $\text{PdCl}_2(\text{PPh}_3)_2$ (2 mol %), triphenylphosphine (4 mol %), and CuI (4 mol %) were added in succession to a 0.5 M solution of 2-bromopyridine in TEA. The resulting suspension was stirred for 30 min, then the relevant alkyne (1.0 equiv) was added. The reaction mixture was then stirred overnight in the dark, quenched by addition of satd NH_4Cl , and evaporated under vacuum. The residual slurry was

extracted with EtOAc and water, the aqueous phase was extracted with more EtOAc, then the combined organic extracts washed with water then brine, and evaporated under vacuum. Flash column chromatography on silica gel, eluted as specified in each individual case, then afforded the pure alkyne products.

2-(Pentyn-1-yl)pyridine 81. Synthesized using 2-bromopyridine (954 μL , 1.58 g, 10 mmol), $\text{PdCl}_2(\text{PPh}_3)_2$ (140 mg, 0.2 mmol), PPh_3 (105 mg, 0.4 mmol), CuI (76 mg, 0.4 mmol), and pent-1-yne (986 μL , 10 mmol). Column eluent 10 \rightarrow 15 \rightarrow 20% EtOAc/hexane. Product obtained as an amber oil (1.13 g, 78%). δ_{H} (400 MHz, $\text{DMSO}-d_6$) 8.51 (d, 1H, $J = 5.0$), 7.76 (dt, 1H, $J = 2.0, 8.0$), 7.45 (d, 1H, $J = 8.0$), 7.35–7.31 (m, 1H), 2.43 (t, 2H, $J = 7.0$), 1.58 (sextet, 2H, $J = 7.0$), 1.00 (t, 3H, $J = 7.0$). δ_{C} (101 MHz, $\text{DMSO}-d_6$) 150.3, 143.4, 137.0, 127.3, 123.3, 90.8, 81.4, 21.9, 20.8, 13.8. m/z (ES) 146 ($[\text{M} + \text{H}]^+$). HRMS, found 146.0965 ($\text{C}_{10}\text{H}_{12}\text{N}$ requires 146.0970).

2-(4-Methylpent-1-ynyl)pyridine 82. Synthesized using 2-bromopyridine (3.81 mL, 6.32 g, 40 mmol), $\text{PdCl}_2(\text{PPh}_3)_2$ (562 mg, 0.8 mmol), PPh_3 (420 mg, 1.6 mmol), CuI (305 mg, 1.6 mmol), and 4-methylpent-1-yne (4.71 mL, 3.29 g, 40 mmol). Column eluent 5 \rightarrow 10 \rightarrow 15 \rightarrow 20 \rightarrow 25% EtOAc/hexane. Product obtained as a brown oil (4.48 g, 70%). δ_{H} (400 MHz, $\text{DMSO}-d_6$) 8.53 (d, 1H, $J = 4.5$), 7.75 (dt, 1H, $J = 2.0, 8.0$), 7.45 (d, 1H, $J = 8.0$), 7.33 (ddd, 1H, $J = 1.0, 4.5, 6.0$), 2.35 (d, 2H, $J = 6.5$), 1.85 (septet, 1H, $J = 6.5$), 0.98 (d, 6H, $J = 6.5$). δ_{C} (101 MHz, $\text{DMSO}-d_6$) 150.3, 143.5, 137.0, 127.3, 123.3, 89.8, 82.1, 27.94, 27.91, 22.2. m/z (ES) 160 ($[\text{M} + \text{H}]^+$). HRMS, found 160.1120 ($\text{C}_{11}\text{H}_{14}\text{N}$ requires 160.1126). HPLC purity 99.5%.

5-(Pyridin-2-yl)pent-4-yn-1-ol 83. Synthesized using 2-bromopyridine (2.38 mL, 3.95 g, 25 mmol), $\text{PdCl}_2(\text{PPh}_3)_2$ (351 mg, 0.5 mmol), PPh_3 (262 mg, 1.0 mmol), CuI (190 mg, 1.0 mmol), and pent-4-yn-1-ol (2.33 mL, 2.10 g, 25 mmol). Column eluent 2.5 \rightarrow 5 \rightarrow 10 \rightarrow 15% MeOH/ CH_2Cl_2 . Product obtained as a yellow oil (2.46 g, 61%). δ_{H} (400 MHz, $\text{DMSO}-d_6$) 8.52 (d, 1H, $J = 5.0$), 7.76 (dt, 1H, $J = 1.5, 7.5$), 7.44 (d, 1H, $J = 7.5$), 7.33 (ddd, 1H, $J = 1.5, 5.0, 5.5$), 4.59 (t, 1H, $J = 5.5$), 3.53 (q, 2H, $J = 5.5$), 2.50 (t, 2H, $J = 7.0$), 1.74–1.67 (m, 2H). δ_{C} (101 MHz, $\text{DMSO}-d_6$) 150.3, 143.5, 137.0, 127.3, 123.3, 90.9, 81.1, 59.9, 31.7, 15.6. m/z (ES) 162 ($[\text{M} + \text{H}]^+$). HRMS, found 162.0912 ($\text{C}_{10}\text{H}_{12}\text{NO}$ requires 162.0919). HPLC purity 99.0%.

2-(5-Methoxypent-1-ynyl)pyridine 84. By Methylation of **83** (Method A). Alcohol **83** (1.14 g, 7.08 mmol) and methyl iodide (0.53 mL, 1.21 g, 8.5 mmol) were dissolved in anhydrous DMF (25 mL) at 0 °C, then sodium hydride (60% dispersion in mineral oil, 0.34 g, 8.5 mmol) was added in small portions over 5 min. After stirring for 30 min at 0 °C, the cooling was removed and reaction continued at rt for 3 h. Water was added dropwise to quench any remaining NaH, then the mixture evaporated under vacuum. The residue was extracted between EtOAc and water, the aqueous phase extracted with more EtOAc, then the combined organic extracts washed with brine, water then brine, dried over Na_2SO_4 , filtered, and evaporated. The resulting brown oil was purified by preparative HPLC, using a gradient of 5–15% MeCN in water (containing 0.1% v/v TFA) over 20 min. After evaporation of pooled fractions, the remaining yellow oil was partitioned between EtOAc and satd NaHCO_3 to regenerate the free base form of the product. After separation of the layers, the aqueous phase was extracted again with EtOAc and the combined organics dried over Na_2SO_4 , filtered, and evaporated to dryness once more to afford the title compound as a yellow/orange oil (337 mg, 27%). δ_{H} (400 MHz, $\text{DMSO}-d_6$) 8.56–8.50 (m, 1H), 7.77 (dt, 1H, $J = 1.5, 7.5$), 7.45 (d, 1H, $J = 7.5$), 7.34 (dd, 1H, $J = 5.0, 7.5$), 3.44 (t, 2H, $J = 6.5$), 3.25 (s, 3H), 2.49 (t, 2H, $J = 6.5$), 1.78 (quintet, 2H, $J = 6.5$). δ_{C} (101 MHz, $\text{DMSO}-d_6$) 149.8, 142.9, 136.6, 126.8, 122.9, 89.8, 80.8, 70.4, 57.9, 27.9, 15.3. m/z (ES) 176 ($[\text{M} + \text{H}]^+$). HRMS, found 176.1075 ($\text{C}_{11}\text{H}_{14}\text{NO}$ requires 176.1075). HPLC purity 99.7%.

By Two-Step Synthesis from Pent-4-yn-1-ol (Method B). A solution of pent-4-yn-1-ol (3.26 mL, 2.94 g, 35 mmol) and methyl iodide (4.36 mL, 9.94 g, 70 mmol) in dry THF (60 mL) was cooled to 0 °C, then sodium hydride (60% dispersion in mineral oil, 1.68 g, 42 mmol) was added portionwise over 10 min. After 5 min more, the cooling was removed and the reaction mixture heated at 50 °C for 2.5 h. The suspension was poured carefully into ice-cold water (250 mL) then extracted twice with Et_2O . The combined extracts were washed

with water, dried over Na_2SO_4 , filtered, then evaporated slowly under vacuum, maintaining the water bath at 4 °C and using an air bleed to control the evaporation rate. Slow evaporation was necessary to prevent significant loss of the volatile intermediate, 5-methoxy-pent-1-yne. Once the solution of this crude alkyne had been concentrated to approximately 25 mL, it was used immediately as the alkyne component of a Sonogashira cross-coupling with 2-bromopyridine (3.34 mL, 5.53 g, 35 mmol), according to the general procedure described above, also using $\text{PdCl}_2(\text{PPh}_3)_2$ (491 mg, 0.7 mmol), PPh_3 (367 mg, 1.4 mmol), and CuI (267 mg, 1.4 mmol). Column eluent 0 \rightarrow 1 \rightarrow 2.5 \rightarrow 4 \rightarrow 6% MeOH/ CH_2Cl_2 . Title compound obtained as an orange/brown oil (1.11 g, 18% over 2 steps). Analytical data were in agreement with the sample prepared by method A.

Cyclization of 2-Alkynylpyridines 81, 82, and 84 to 3-Alkylindolizines 85–87: General Procedure. CuCl (1 equiv) was added to a 0.45 M solution of starting 2-alkynylpyridine in dry DMA/TEA (7:1). The mixture was stirred at rt for 10 min then heated to 130 °C for the duration specified in each case. The reaction mixture was poured into a 1:1 mixture of EtOAc and water, which was then extracted thoroughly. Following vacuum filtration to remove suspended solids, the filtrate was poured into a separating funnel and the layers separated. The aqueous layer was extracted twice more with EtOAc, repeating the filtration step as necessary. The combined extracts were washed with water then brine, dried over Na_2SO_4 , filtered, and evaporated. Purification was carried out by flash column chromatography on silica gel, using the eluent specified in each case, and making sure to run the column as quickly as possible to minimize decomposition of the indolizine product. After evaporation and drying, the indolizines were stored at –20 °C until further use.

3-Ethylindolizine 85. Prepared from alkyne **81** (500 mg, 3.44 mmol) and CuCl (341 mg, 3.44 mmol). Reaction duration 7.5 h. Column eluent 0 \rightarrow 10% EtOAc/hexane. Title compound obtained as a yellow oil (161 mg, 32%). δ_{H} (400 MHz, $\text{DMSO}-d_6$) 7.99 (d, 1H, $J = 7.0$), 7.40 (d, 1H, $J = 9.0$), 6.66–6.61 (m, 1H), 6.59–6.54 (m, 2H), 6.34 (d, 1H, $J = 4.0$), 2.80 (q, 2H, $J = 7.5$), 1.30 (t, 3H, $J = 7.5$). δ_{C} (101 MHz, $\text{DMSO}-d_6$) 132.1, 126.0, 122.7, 119.4, 115.8, 111.1, 110.3, 98.3, 18.9, 12.2. m/z (ES) 146 ($[\text{M} + \text{H}]^+$). HRMS, found 146.0972 ($\text{C}_{10}\text{H}_{12}\text{N}$ requires 146.0970).

3-Isopropylindolizine 86. Prepared from alkyne **82** (4.01 g, 25.2 mmol) and CuCl (2.49 g, 25.2 mmol). Reaction duration 6.5 h. Column eluent 0 \rightarrow 5 \rightarrow 10% EtOAc/hexane. Title compound obtained as a bright-yellow oil (1.24 g, 31%). δ_{H} (400 MHz, $\text{DMSO}-d_6$) 8.00 (d, 1H, $J = 7.0$), 7.40 (d, 1H, $J = 9.0$), 6.65–6.60 (m, 1H), 6.58–6.52 (m, 2H), 6.35 (d, 1H, $J = 4.0$), 3.24 (septet, 1H, $J = 7.0$), 1.28 (d, 6H, $J = 7.0$). δ_{C} (101 MHz, $\text{DMSO}-d_6$) 132.2, 130.7, 122.8, 119.6, 115.7, 110.2, 109.4, 98.4, 24.8, 21.6. m/z (ES) 160 ($[\text{M} + \text{H}]^+$). HRMS, found 160.1127 ($\text{C}_{11}\text{H}_{14}\text{N}$ requires 160.1126). HPLC purity 94.2%.

3-(2-Methoxyethyl)indolizine 87. Prepared from alkyne **84** (1.09 g, 6.22 mmol) and CuCl (616 mg, 6.22 mmol). Reaction duration 4 h. Column eluent 5 \rightarrow 10 \rightarrow 20% EtOAc/pentanes. Title compound obtained as a bright-yellow oil (591 mg, 54%). δ_{H} (400 MHz, $\text{DMSO}-d_6$) 8.06 (dd, 1H, $J = 1.0, 6.5$), 7.39 (dt, 1H, $J = 1.0, 9.0$), 6.64 (ddd, 1H, $J = 1.0, 6.5, 9.0$), 6.59 (d, 1H, $J = 4.0$), 6.55 (dt, 1H, $J = 1.0, 6.5$), 6.35 (d, 1H, $J = 4.0$), 3.65 (t, 2H, $J = 6.5$), 3.28 (s, 3H), 3.09 (t, 2H, $J = 6.5$). δ_{C} (101 MHz, $\text{DMSO}-d_6$) 132.2, 123.0, 121.9, 119.3, 115.9, 112.7, 110.3, 98.5, 70.8, 58.4, 26.2. m/z (ES) 176 ($[\text{M} + \text{H}]^+$). HRMS, found 176.1073 ($\text{C}_{11}\text{H}_{14}\text{NO}$ requires 176.1075). HPLC purity 99.1%.

Synthesis of Indolizine-1-glyoxylamides 52–55 (Scheme 4): General Procedure. These reactions were carried out using the same protocol as the one-pot indole-3-glyoxylamide syntheses described above, except the first step (reaction with oxalyl chloride) was carried out at 0 °C instead of rt. Characterization data, HPLC purity, and any additional purification details are provided for each example in the Supporting Information.

Preparation of 61, 63, and 65 via Ester Deprotection: General Procedure. These reactions were not run under N_2 . The starting ester, either **62**, **64**, or ethyl 2-(2-(3-(2-(6-methoxy-pyridin-3-ylamino)-2-oxoacetyl)-1H-indol-1-yl)-2-methylpropoxy)acetate (prepared from **4m** by the general procedure for one-pot indole-3-glyoxylamide

synthesis), was dissolved in 1:1 THF/water to a final concentration of approximately 0.1 M, then 5 M NaOH (2.5 equiv) was added. The reaction mixture was stirred at rt for 2 h. Complete reaction was confirmed by TLC, then the solution was adjusted to pH 7 with 1 M HCl and evaporated under vacuum. The residue was extracted with EtOAc and 1 M HCl, the aqueous layer extracted three times further with EtOAc, then the combined organic solutions dried over Na_2SO_4 , filtered, and evaporated. Purification was carried out by preparative HPLC, using the conditions specified in each case. Characterization data, HPLC purity, and full purification details are provided for each example in the Supporting Information.

HPLC Solubility Assay. The maximal aqueous solubility of compounds **12**, **13**, and **32** was estimated as follows: dilutions of compound from 10 mM DMSO stock solutions were made into water at final concentrations ranging from 1–100 μM (typically 1, 2, 4, 6, 10, 15, 20, 30, 50, and 100 μM). These solutions were mixed overnight at rt then centrifuged in a benchtop microcentrifuge at 13000 rpm (approximately 17000g) for 5 min to remove any suspended precipitate. Supernatants were analyzed by HPLC using a C_{18} 5 μm column, 4.6 mm \times 150 mm, and a gradient of 5–55% MeCN/water over 9 min; ramp to 100% MeCN over 4 min; hold at 100% MeCN for 5 min, with UV detection at 254 nm. Plots of peak area against concentration were constructed, and the point at which each plot deviated from linearity was estimated as the threshold aqueous solubility of the test compound (above which point the plot leveled off, indicating saturation).

Biology. Cell Lines and Culture. Cell lines were obtained from the American Type Culture Collection (FaDu, SCC-4, SK-MEL-28) or the European Collection of Cell Cultures (MES-SA, MES-SA/Dx5, SH-SY5Y, Caco-2) and cultured at 37 °C as recommended in each case, with the exception of FaDu, which was grown in RPMI-1640 medium supplemented with 2 mM L-glutamine. Additionally, all cell culture medium was supplemented with 100 IU/mL penicillin and 100 $\mu\text{g}/\text{mL}$ streptomycin.

Cytotoxicity (MTT) Assay. Cells were distributed into 96-well tissue culture plates (Greiner Bio-One) at an appropriate density in a volume of 100 $\mu\text{L}/\text{well}$ and incubated for 24 h to allow for cell attachment. Test compound solutions were prepared by dilution from 10 mM DMSO stock solutions into full growth medium at 2 \times the required final screening concentration and dosed in triplicate at 100 $\mu\text{L}/\text{well}$ (i.e., final assay volume \sim 200 $\mu\text{L}/\text{well}$). After incubation for 72 h, medium was removed from the wells, the cells were washed with PBS, and 100 $\mu\text{L}/\text{well}$ of a solution of MTT in PBS (0.5 mg/mL) was added. The plate was incubated once more for 45–60 min then the solution removed and 0.1 M HCl in 2-propanol added (40 $\mu\text{L}/\text{well}$). After gentle agitation to dissolve the formazan crystals, absorbance values at 570 nm were read using a microplate reader (reference wavelength 650 nm). Data was processed using Microsoft Excel, expressed as viability relative to vehicle control (DMSO only), and plotted in dose–response form using GraphPad Prism 6 (GraphPad Software, Inc.), allowing derivation of LC_{50} values by nonlinear regression.

Tubulin Polymerization Assay (OD₃₄₀ Method). Purified porcine brain tubulin and other reagents were obtained commercially in kit form (Cytoskeleton, Inc.). Assays were carried out in half-area 96-well plates at 37 °C and a final concentration of 3.6 mg/mL tubulin, 9.2% glycerol, and 900 μM GTP in 100 μL total volume. Test compounds were preplated at 10 \times final assay concentration in water (10 $\mu\text{L}/\text{well}$), then a solution of tubulin (4 mg/mL) in G-PEM buffer (80 mM PIPES pH 6.9, 2 mM MgCl_2 , 0.5 mM EGTA) containing 10.2% glycerol and 1 mM GTP was prepared freshly on ice and promptly distributed into reaction wells at 90 $\mu\text{L}/\text{well}$. Reactions were followed at 37 °C over 60 min, monitoring OD₃₄₀ at 1 min intervals. Data from each well was normalized relative to initial readings, and plots of $\Delta\text{OD}_{\text{max}}$ (final–initial values) against compound concentration, expressed relative to vehicle control (DMSO only), were used to calculate IC_{50} values (Supporting Information, Figure S1).

Tubulin Polymerization Assay (DAPI Fluorescence Method). Purified tubulin and other reagents were sourced in kit form (Cytoskeleton, Inc.) as above. Assays were run in a total volume of

55 μL , in half-area 96-well black plates at 37 $^{\circ}\text{C}$ in G-PEM buffer containing 1.45 mg/mL tubulin, 900 μM GTP, 4.97 μM DAPI, and 13.75% glycerol. Reactions were monitored by measuring DAPI fluorescence (excitation 360 nm, emission 450 nm) once per minute over a period of 60 min. Data was normalized and processed as per the OD₃₄₀ method (see Supporting Information, Figures S2,S3).

Tubulin Competitive Binding Assay. Assays were performed in 96-well plates in duplicate. Biotinylated porcine tubulin (750 ng/well, >99% purity, Cytoskeleton Inc.) was incubated with tritiated tubulin binders (0.1 μM [³H]-colchicine (PerkinElmer), 0.2 μM [³H]-vinblastine (ARC Inc.), or 0.05 μM [³H]-paclitaxel (BioTrend)) and test compounds at various concentrations in 200 μL G-PEM buffer containing 1 mM GTP at a final DMSO concentration of 3% and a total volume of 200 μL /well. For the [³H]-colchicine binding assay, the plate was incubated for 2 h at 37 $^{\circ}\text{C}$, after which 79.2 μg /well streptavidin yttrium silicate SPA beads (PerkinElmer) was added in 20 μL of G-PEM buffer (final volume 220 μL) then samples incubated for a further 45 min at 37 $^{\circ}\text{C}$ before bound radioactivity was determined using a Wallac 1450 Microbeta (PerkinElmer). For the [³H]-vinblastine binding assay, SPA beads were added together with the other assay components and the plate incubated for 15 min at rt before reading. For the [³H]-paclitaxel binding assay, biotinylated tubulin was precoupled to the SPA beads for 30 min at 4 $^{\circ}\text{C}$, before the addition of test compounds and radiolabel, after which the plate was incubated for a further 25 min at rt before reading. Inhibition at each compound concentration was calculated according to eq 1, where CPM = counts per minute, CPM_[NSB] is the reading obtained in the presence of a 1000-fold molar excess of unlabeled ligand, and CPM_[TB] is the reading for vehicle control (3% DMSO).

$$\% \text{inhibition} = 100 - \left[\frac{\text{CPM}_{[\text{sample}]} - \text{CPM}_{[\text{NSB}]}}{\text{CPM}_{[\text{TB}]} - \text{CPM}_{[\text{NSB}]}} \right] \times 100 \quad (1)$$

IC₅₀ values were determined from seven-point semilog concentration–inhibition curves in XLfit (ID Business Solutions) or GraphPad Prism 6 (GraphPad Software, Inc.) using a four-parameter inhibition model.

Cell Cycle Analysis. FaDu cells were seeded into 12-well plates at 10⁵ cells/well in 1 mL of full growth medium, then incubated overnight to allow for cell attachment. Test compounds were prepared at 2 \times final screening concentration in full growth medium then dosed at 1 mL/well (final assay volume \sim 2 mL), after which plates were incubated at 37 $^{\circ}\text{C}$ for 24 h. Medium was removed and cells washed with PBS (500 μL /well) then harvested by detachment with 0.05% trypsin–EDTA (500 μL /well) followed by centrifugation (2000g, 5 min) in 1.5 mL microcentrifuge tubes. The cells were washed with flow cytometry buffer (100 mM PBS pH 7.4, 0.1% w/v BSA, 0.1% w/v Na₂S₂O₃; 500 μL) and centrifuged once more. Buffer was removed and each cell pellet fixed by dropwise addition of ice-cold 70% ethanol (1.0 mL) with mixing using a vortex mixer. Samples were kept on ice for 30 min then centrifuged (2000g, 5 min) and the fixing solution removed. After washing with flow cytometry buffer as above, samples were treated with RNase A (100 μg /mL in PBS, 50 μL) at rt for at least 15 min, then propidium iodide (50 μg /mL in PBS, 200 μL) was added and incubation continued overnight, in the dark. Samples were analyzed by flow cytometry using a FACSCalibur instrument (BD Biosciences), collecting a minimum of 10000 events per sample and data was then analyzed using Flowing Software 2.5.1 (www.flowingsoftware.com).

Immunofluorescence Staining. FaDu cells were seeded onto glass coverslips in 24-well plates at 15000 cells/well in 500 μL of full growth medium, then incubated for 24 h to allow for cell attachment. Test compounds were prepared at 2 \times final assay concentration in full growth medium then added at 500 μL /well and the plate incubated for 24 h. Medium was removed by aspiration and the cells washed with PBS, then treated for 3 min with PHEM buffer (60 mM PIPES, 25 mM HEPES, 10 mM EGTA, 2 mM MgCl₂, pH 6.9) containing 0.5% v/v Triton X-100 and 10 μM paclitaxel (this treatment removes unassembled tubulin dimers while preserving intact microtubules⁴⁰). Each culture was fixed by treatment with PHEM containing 8% w/v paraformaldehyde and 0.3% w/v glutaraldehyde on ice for 10 min. The

fixative was removed and the cells washed three times with PBS, then blocked by treatment with 2% FCS and 1% BSA in PBS for 30 min. The blocking solution was removed and the samples incubated with FITC-conjugated mouse anti- α -tubulin antibody (clone DM1A, Sigma, 1:500) in PBS for 40 min. The cells were washed three times with PBS then incubated with DAPI (5 μg /mL in PBS) for 5 min. After a further three PBS washes, coverslips were removed from the assay plate and slide mounted using ProLong Diamond Antifade Mountant (ThermoFisher Scientific). Slides were subsequently imaged using a spinning disc confocal microscope (Olympus IX81, PerkinElmer, UK) by capturing confocal z-stack images in 0.5 μm increments at 100 \times magnification.

Mouse Mitochondrial Stability Assay. Stock solutions of test compounds (2 mM in DMSO) were diluted to 0.1 mM with MeCN, and these solutions further diluted to 1.25 μM in 50 mM potassium phosphate buffer (pH 7.4) containing 0.63 mg/mL micromosomal protein from pooled CD-1 (male) mouse liver microsome preparation (20 mg/mL; BD Biosciences). An aliquot of the resultant solution (80 μL) was preincubated for 5 min at 37 $^{\circ}\text{C}$ in a shaking incubator before reaction was initiated by addition of NADPH (5 mM in potassium phosphate buffer, 20 μL) or buffer alone (for no cofactor control, 20 μL). Parallel reactions were stopped at 0 and 30 min time points by the addition of two volumes of ice-cold acetonitrile. The quenched samples were centrifuged (3000g, 30 min, 4 $^{\circ}\text{C}$) and the resultant supernatants analyzed for parent compound by LC-MS/MS, monitoring ion transitions for parent and daughter ions. Results of determinations carried out in duplicate are reported as mean percent parent compound remaining at 30 min. Final incubation conditions were 1 μM test compound, 0.5 mg/mL microsomal protein, and 1 mM NADPH.

Bidirectional Caco-2 Permeability Assay. Caco-2 cells were seeded onto 24-well transwell plates at 20000 cells/well and used as confluent monolayers after a 21 day culture. Test and control compounds (propranolol, vinblastine) were prepared at 10 μM in HBSS supplemented with 25 mM HEPES, pH 7.4, at a final DMSO concentration of 0.1%. These solutions were added to donor compartments for both apical to basolateral (A \rightarrow B) and basolateral to apical (B \rightarrow A) measurements. After incubation at 37 $^{\circ}\text{C}$ for 60 min, samples were analyzed by mass spectrometry using an analytical internal standard. Apparent permeability (P_{app}) values, expressed as $\times 10^{-6}$ cm s⁻¹, were determined according to eq 2 where V_{acceptor} and V_{donor} are the volumes of the transwell compartments (apical 125 μL , basolateral 600 μL), T is the incubation time (in min), A is the area of cells exposed (in cm²), and the concentrations are relative mass spectroscopic responses normalized to the internal standard:

$$P_{\text{app}} = \left\{ \left(\frac{[\text{acceptor}_{\text{final}}] \times V_{\text{acceptor}}}{[\text{donor}_{\text{initial}}] \times V_{\text{donor}}} \right) / (T \times 60) \right\} \times \frac{V_{\text{donor}}}{A} \times 10^6 \quad (2)$$

Lucifer yellow was added to the apical buffer in each well to assess cell viability as a control for integrity of the monolayer. Results from any well with a lucifer yellow $P_{\text{app}} > 10 \times 10^{-6}$ cm s⁻¹ were rejected. Efflux ratios are expressed as $P_{\text{app}}(\text{B} \rightarrow \text{A})/P_{\text{app}}(\text{A} \rightarrow \text{B})$. Values for control compounds were as expected: propranolol $P_{\text{app}}(\text{A} \rightarrow \text{B})$ 66.7 $\times 10^{-6}$ cm s⁻¹, efflux ratio 0.7; vinblastine $P_{\text{app}}(\text{A} \rightarrow \text{B}) < 0.2 \times 10^{-6}$ cm s⁻¹, efflux ratio >288.

Multicellular Tumor Spheroid Cytotoxicity Screen. Multicellular tumor spheroids were prepared from the FaDu cell line using the forced-floating method, in 100 μL /well full growth medium in 96-well tissue culture plates, as described previously.⁹⁵ After spheroids had formed, test compounds were dosed essentially as for the 2D cytotoxicity assay but using $n = 6$ rather than triplicates, accommodating a nine-point dose–response experiment with vehicle control (DMSO) on each plate. Images were captured at regular intervals (0, 1, 2, 3, 4, and 7 days postdosing) using a Zeiss Axiovert 200 M light microscope with AxioCam MRm camera and AxioVision 4.6 software (Carl Zeiss Inc., Germany) and size measurements made using AxioVision. These values were converted into spheroid volume expressed relative to DMSO control and EC₅₀ values determined by

nonlinear regression using GraphPad Prism 6 (GraphPad Software, Inc.), as above.

Mouse Xenograft Model. Male CD1 athymic mice (aged 7–8 weeks, stock number 000711; Charles River UK) were kept in ventilated cages with food and water provided ad libitum. FaDu cells, verified mycoplasma free, were suspended in PBS (pH 7.4) at a density of 5×10^7 mL⁻¹ and each animal received a subcutaneous injection of 5×10^6 cells (100 μ L) from this suspension. Once xenografts were established, tumors were measured with a digital caliper and the volume calculated as (length \times width²)/2. Mice with palpable tumors (100–300 mm³) were assigned randomly into groups ($n = 9$) before beginning the treatment schedule. The control group received 200 μ L vehicle (95:5 water/glycerol containing 0.25% v/v Tween-20 and 2.3% v/v DMSO) by oral gavage once daily for 10 days, with the treatment groups receiving either 33 (10 mg/kg), 59 (10 mg/kg), or 59 (20 mg/kg) diluted from stock solutions in 100% DMSO in 200 μ L of the same formulation, by the same route and schedule. In a parallel experiment to compare the effect of vinblastine treatment, two groups received either vehicle (200 μ L PBS) or vinblastine (3 mg/kg in 200 μ L PBS) by the intraperitoneal route on days 1, 4, and 7 only. For all groups, tumor volumes were monitored regularly, and mice were culled when tumors reached the maximum permitted size (15 mm diameter). All animal procedures were conducted in accordance with the UK Home Office Regulations under the Animals (Scientific Procedures) Act 1986 and the awarded project license number under which these protocols were performed is PPL:40/3424. In addition, the University of Sheffield Animal Welfare and Ethical Review Body approved all the in vivo experiments used in this study.

■ ASSOCIATED CONTENT

Supporting Information

The Supporting Information is available free of charge on the ACS Publications website at DOI: 10.1021/acs.jmedchem.5b01312.

Characterization data, purification details, and HPLC purity for all screening compounds; NMR spectra for all screening compounds and synthetic intermediates (PDF) Molecular formula strings (CSV)

■ AUTHOR INFORMATION

Corresponding Authors

*For M.J.T.: phone +44 (0)114 222 9364; E-mail: m.j.thompson@sheffield.ac.uk.

*For H.E.C.: phone +44 (0)114 271 7966; E-mail: h.colley@sheffield.ac.uk.

Author Contributions

^VM.J.T. wrote the manuscript with assistance from the other authors specified (H.E.C., M.W., E.J.G., and M.M.). All authors have approved the manuscript prior to submission.

Notes

The authors declare no competing financial interest.

■ ACKNOWLEDGMENTS

We gratefully acknowledge funding from Weston Park Hospital Cancer Charity (grant refs SG110 to M.J.T., H.E.C., and S.J.D.; CA135 to M.J.T., M.M., H.E.C., and S.J.D.), Sheffield Healthcare Gateway Faculty Innovation Fund (University of Sheffield, to H.E.C. and M.J.T.), and the University of Sheffield Early Career Researcher Scheme (grants to M.J.T. and H.E.C.). We thank Michael Briggs, Sharon Wicks, Lisa Strong, Richard Newman, Roshini Markandu, and Lynsey Crowley (Charles River) for their contributions to in vitro ADME work, and also Drs. David Clark, Steve Price, and Mark Albertella (Charles River) for helpful collaboration; Simon Thorpe (University of

Sheffield) for assistance with mass spectrometry, and Dr. Simon Tazzyman (University of Sheffield) for valuable help with confocal microscopy.

■ ABBREVIATIONS USED

ABCG2, ATP-binding cassette subfamily G member 2; Akt, RAC- α serine/threonine-protein kinase; BCRP, breast cancer resistance protein; DAPI, 4',6-diamidino-2-phenylindole; DIPEA, *N,N*-diisopropylethylamine; DLS, dynamic light scattering; 5-FU, 5-fluorouracil; GTP, guanosine 5'-triphosphate; HBSS, Hanks' Balanced Salt Solution; HNC, head and neck cancer; LC₅₀, lethal concentration for 50% of the population; MCTS, multicellular tumor spheroid; MMPA, matched molecular pair analysis; MRP1, multidrug resistance-associated protein 1; MRP2, multidrug resistance-associated protein 2; MTA, microtubule-targeting agent; mTor, mammalian target of rapamycin; PAINS, pan-assay interference compounds; P-gp, P-glycoprotein; PN, peripheral neuropathy; SEM, standard error of the mean; TBD, 1,5,7-triazabicyclo[4.4.0]dec-5-ene

■ REFERENCES

- (1) Nitika, V.; Kapil, K. Microtubule targeting agents: a benchmark in cancer therapy. *Curr. Drug Ther.* **2014**, *8*, 189–196.
- (2) Risinger, A. L.; Giles, F. J.; Mooberry, S. L. Microtubule dynamics as a target in oncology. *Cancer Treat. Rev.* **2009**, *35*, 255–261.
- (3) Stanton, R. A.; Gernert, K. M.; Nettles, J. H.; Aneja, R. Drugs that target dynamic microtubules: a new molecular perspective. *Med. Res. Rev.* **2011**, *31*, 443–481.
- (4) Barbier, P.; Tsvetkov, P. O.; Breuzard, G.; Devred, F. Deciphering the molecular mechanisms of anti-tubulin plant derived drugs. *Phytochem. Rev.* **2014**, *13*, 157–169.
- (5) Rohena, C. C.; Mooberry, S. L. Recent progress with microtubule stabilizers: new compounds, binding modes and cellular activities. *Nat. Prod. Rep.* **2014**, *31*, 335–355.
- (6) Jordan, M. A.; Horwitz, S. B.; Lobert, S.; Correia, J. J. Exploring the mechanisms of action of the novel microtubule inhibitor vinflunine. *Semin. Oncol.* **2008**, *35*, S6–S12.
- (7) Field, J. J.; Kanakkanthara, A.; Miller, J. H. Microtubule-targeting agents are clinically successful due to both mitotic and interphase impairment of microtubule function. *Bioorg. Med. Chem.* **2014**, *22*, 5050–5059.
- (8) Zasadil, L. M.; Andersen, K. A.; Yeum, D.; Rocque, G. B.; Wilke, L. G.; Tevaarwerk, A. J.; Raines, R. T.; Burkard, M. E.; Weaver, B. A. Cytotoxicity of paclitaxel in breast cancer is due to chromosome missegregation on multipolar spindles. *Sci. Transl. Med.* **2014**, *6*, 229ra43.
- (9) Ogden, A.; Rida, P. C. G.; Reid, M. D.; Aneja, R. Interphase microtubules: chief casualties in the war on cancer? *Drug Discovery Today* **2014**, *19*, 824–829.
- (10) Fürst, R.; Vollmar, A. M. A new perspective on old drugs: non-mitotic actions of tubulin-binding drugs play a major role in cancer treatment. *Pharmazie* **2013**, *68*, 478–483.
- (11) Mitchison, T. J. The proliferation rate paradox in antimetabolic chemotherapy. *Mol. Biol. Cell* **2012**, *23*, 1–6.
- (12) Seligmann, J.; Twelves, C. Tubulin: an example of targeted chemotherapy. *Future Med. Chem.* **2013**, *5*, 339–352.
- (13) Kavallaris, M. Microtubules and resistance to tubulin-binding agents. *Nat. Rev. Cancer* **2010**, *10*, 194–204.
- (14) Katsetos, C. D.; Draber, P. Tubulins as therapeutic targets in cancer: from bench to bedside. *Curr. Pharm. Des.* **2012**, *18*, 2778–2792.
- (15) Murray, S.; Briassoulis, E.; Linardou, H.; Bafaloukos, D.; Papadimitriou, C. Taxane resistance in breast cancer: mechanisms, predictive biomarkers and circumvention strategies. *Cancer Treat. Rev.* **2012**, *38*, 890–903.

- (16) Gan, P. P.; Kavallaris, M. Tubulin-targeted drug action: functional significance of class II and class IVb β -tubulin in *Vinca* alkaloid sensitivity. *Cancer Res.* **2008**, *68*, 9817–9824.
- (17) Carlson, K.; Ocean, A. J. Peripheral neuropathy with microtubule-targeting agents: occurrence and management approach. *Clin. Breast Cancer* **2011**, *11*, 73–81.
- (18) Canta, A.; Chiorazzi, A.; Cavaletti, G. Tubulin: a target for antineoplastic drugs into the cancer cells but also in the peripheral nervous system. *Curr. Med. Chem.* **2009**, *16*, 1315–1324.
- (19) Dumontet, C.; Jordan, M. A. Microtubule-binding agents: a dynamic field of cancer therapeutics. *Nat. Rev. Drug Discovery* **2010**, *9*, 790–803.
- (20) Kingston, D. G. I.; Snyder, J. P. The quest for a simple bioactive analog of paclitaxel as a potential anticancer agent. *Acc. Chem. Res.* **2014**, *47*, 2682–2691.
- (21) Gerullis, H.; Ecke, T.; Eimer, C.; Wishahi, M.; Otto, T. Vinflunine as second-line treatment in platin-resistant metastatic urothelial carcinoma: a review. *Anti-Cancer Drugs* **2011**, *22*, 9–17.
- (22) Gourmelon, C.; Frenel, J. S.; Campone, M. Eribulin mesylate for the treatment of late-stage breast cancer. *Expert Opin. Pharmacother.* **2011**, *12*, 2883–2890.
- (23) Preston, J. N.; Trivedi, M. V. Eribulin: a novel cytotoxic chemotherapy agent. *Ann. Pharmacother.* **2012**, *46*, 802–811.
- (24) Cortes, J.; Montero, A. J.; Glück, S. Eribulin mesylate, a novel microtubule inhibitor in the treatment of breast cancer. *Cancer Treat. Rev.* **2012**, *38*, 143–151.
- (25) Brogdon, C. F.; Lee, F. Y.; Canetta, R. M. Development of other microtubule-stabilizer families: the epothilones and their derivatives. *Anti-Cancer Drugs* **2014**, *25*, 599–609.
- (26) Edelman, M. J.; Shvartsbeyn, M. Epothilones in development for non-small-cell lung cancer: novel anti-tubulin agents with the potential to overcome taxane resistance. *Clin. Lung Cancer* **2012**, *13*, 171–180.
- (27) Sadeghi, S.; Olevsky, O.; Hurvitz, S. A. Profiling and targeting HER2-positive breast cancer using trastuzumab emtansine. *Pharmacogenomics Pers. Med.* **2014**, *7*, 329–338.
- (28) Coen van Hasselt, J. G.; Gupta, A.; Hussein, Z.; Beijnen, J. H.; Schellens, J. H. M.; Huijtema, A. D. R. Population pharmacokinetic–pharmacodynamic analysis for eribulin mesylate-associated neutropenia. *Br. J. Clin. Pharmacol.* **2013**, *76*, 412–424.
- (29) Valero, V. Managing ixabepilone adverse events with dose reduction. *Clin. Breast Cancer* **2013**, *13*, 1–6.
- (30) Ebenezer, G. J.; Carlson, K.; Donovan, D.; Cobham, M.; Chuang, E.; Moore, A.; Cigler, T.; Ward, M.; Lane, M. E.; Ramnarain, A.; Vahdat, L. T.; Polydefkis, M. Ixabepilone-induced mitochondria and sensory axon loss in breast cancer patients. *Ann. Clin. Transl. Neurol.* **2014**, *1*, 639–649.
- (31) Vahdat, L. T.; Garcia, A. A.; Vogel, C.; Pellegrino, C.; Lindquist, D. L.; Iannotti, N.; Gopalakrishna, P.; Sparano, J. A. Eribulin mesylate versus ixabepilone in patients with metastatic breast cancer: a randomized phase II study comparing the incidence of peripheral neuropathy. *Breast Cancer Res. Treat.* **2013**, *140*, 341–351.
- (32) Wozniak, K. M.; Nomoto, K.; Lapidus, R. G.; Wu, Y.; Carozzi, V.; Cavaletti, G.; Hayakawa, K.; Hosokawa, S.; Towle, M. J.; Littlefield, B. A.; Slusher, B. S. Comparison of neuropathy-inducing effects of eribulin mesylate, paclitaxel and ixabepilone in mice. *Cancer Res.* **2011**, *71*, 3952–3962.
- (33) LaPointe, N. E.; Morfini, G.; Brady, S. T.; Feinstein, S. C.; Wilson, L.; Jordan, M. A. Effects of eribulin, vincristine, paclitaxel and ixabepilone on fast axonal transport and kinesin-1 driven microtubule gliding: implications for chemotherapy-induced peripheral neuropathy. *Neurotoxicology* **2013**, *37*, 231–239.
- (34) Polastro, L.; Aftimos, P. G.; Awada, A. Eribulin mesylate in the management of metastatic breast cancer and other solid cancers: a drug review. *Expert Rev. Anticancer Ther.* **2014**, *14*, 649–665.
- (35) Laughney, A. M.; Kim, E.; Sprachman, M. M.; Miller, M. A.; Kohler, R. H.; Yang, K. S.; Orth, J. D.; Mitchison, T. J.; Weissleder, R. Single-cell pharmacokinetic imaging reveals a therapeutic strategy to overcome drug resistance to the microtubule inhibitor eribulin. *Sci. Transl. Med.* **2014**, *6*, 261ra152.
- (36) Lu, Y.; Chen, J.; Xiao, M.; Li, W.; Miller, D. D. An overview of tubulin inhibitors that interact with the colchicine binding site. *Pharm. Res.* **2012**, *29*, 2943–2971.
- (37) Patil, S. A.; Patil, R.; Miller, D. D. Indole molecules as inhibitors of tubulin polymerization: potential new anticancer agents. *Future Med. Chem.* **2012**, *4*, 2085–2115.
- (38) Kaur, R.; Kaur, G.; Gill, R. K.; Soni, R.; Bariwal, J. Recent developments in tubulin polymerization inhibitors: an overview. *Eur. J. Med. Chem.* **2014**, *87*, 89–124.
- (39) Liu, Y.-M.; Chen, H.-L.; Lee, H.-Y.; Liou, J.-P. Tubulin inhibitors: a patent review. *Expert Opin. Ther. Pat.* **2014**, *24*, 69–88.
- (40) Wienecke, A.; Bacher, G. Indibulin, a novel microtubule inhibitor, discriminates between mature neuronal and nonneuronal tubulin. *Cancer Res.* **2009**, *69*, 171–177.
- (41) Desai, A.; Ratain, M. J.; Moshier, K.; Tipton, M.; Dooley, W.; Hocknell, K.; Dahl, T.; Sherman, M.; Limentani, S. A phase I, dose-escalation trial of STA-5312, a microtubule inhibitor with a novel binding site, in advanced or metastatic solid malignancies. *J. Clin. Oncol.* **2006**, *24*, 13040, 2006 ASCO Annual Meeting Proceedings Part I.
- (42) (a) STA-5312 administered on alternate weekdays every two weeks to patients with hematologic malignancies and patients with solid tumors, NCT00088101. www.clinicaltrials.gov (accessed December 30, 2014). (b) A phase I study of STA-5312 in subjects with advanced or metastatic solid tumors, NCT00276913. www.clinicaltrials.gov (accessed December 30, 2014).
- (43) Bacher, G.; Nickel, B.; Emig, P.; Vanhoefer, U.; Seeber, S.; Shandra, A.; Klenner, T.; Beckers, T. D-24851, a novel synthetic microtubule inhibitor, exerts curative antitumoral activity in vivo, shows efficacy toward multidrug-resistant tumor cells, and lacks neurotoxicity. *Cancer Res.* **2001**, *61*, 392–399.
- (44) Kuppens, I. E. L. M.; Witteveen, P. O.; Schot, M.; Schuessler, V. M.; Daehling, A.; Beijnen, J. H.; Voest, E. E.; Schellens, J. H. M. Phase I dose-finding and pharmacokinetic trial of orally administered Indibulin (D-24851) to patients with solid tumors. *Invest. New Drugs* **2007**, *25*, 227–235.
- (45) Oostendorp, R. L.; Witteveen, P. O.; Schwartz, B.; Vainchtein, L. D.; Schot, M.; Nol, A.; Rosing, H.; Beijnen, B. H.; Voest, E. E.; Schellens, J. H. M. Dose-finding and pharmacokinetic study of orally administered Indibulin (D-24851) to patients with advanced solid tumors. *Invest. New Drugs* **2010**, *28*, 163–170.
- (46) Semenova, M. N.; Kiselyov, A. S.; Titov, I. Y.; Raihstat, M. M.; Molodtsov, M.; Grishchuk, E.; Spiridonov, I.; Semenov, V. V. *In vivo* evaluation of indolyl glyoxylamides in the phenotypic sea urchin embryo assay. *Chem. Biol. Drug Des.* **2007**, *70*, 485–490.
- (47) (a) Ritchie, T. J.; Macdonald, S. J. F. The impact of aromatic ring count on compound developability – are too many aromatic rings a liability in drug design? *Drug Discovery Today* **2009**, *14*, 1011–1020. (b) Ritchie, T. J.; Macdonald, S. J. F.; Young, R. J.; Pickett, S. D. The impact of aromatic ring count on compound developability: further insights by examining carbo- and hetero-aromatic and -aliphatic ring types. *Drug Discovery Today* **2011**, *16*, 164–171.
- (48) Lovering, F.; Bikker, J.; Humblet, C. Escape from flatland: increasing saturation as an approach to improving clinical success. *J. Med. Chem.* **2009**, *52*, 6752–6756.
- (49) Ishikawa, M.; Hashimoto, Y. Improvement in aqueous solubility in small molecule drug discovery programs by disruption of molecular planarity and symmetry. *J. Med. Chem.* **2011**, *54*, 1539–1554.
- (50) Mok, N. Y.; Maxe, S.; Brenk, R. Locating sweet spots for screening hits and evaluating pan-assay interference filters from the performance analysis of two lead-like libraries. *J. Chem. Inf. Model.* **2013**, *53*, 534–544.
- (51) Hennemann, B. Palliative chemotherapy of head and neck cancer: present status and future development. *Laryngorhinootologie* **2006**, *85*, 172–178.
- (52) Cullen, K. J.; Schumaker, L.; Nikitakis, N.; Goloubeva, O.; Tan, M.; Sarlis, M. J.; Haddad, R. I.; Posner, M. R. β -Tubulin-II expression strongly predicts outcome in patients receiving induction chemotherapy for locally advanced squamous carcinoma of the head and

neck: a companion analysis of the TAX 324 trial. *J. Clin. Oncol.* **2009**, *27*, 6222–6228.

(53) Schena, M.; Barone, C.; Birocco, N.; Dongiovanni, D.; Numico, G.; Colantonio, I.; Bertetto, O. Weekly cisplatin paclitaxel and continuous infusion fluorouracil in patients with recurrent and/or metastatic head and neck squamous cell carcinoma: a phase II study. *Cancer Chemother. Pharmacol.* **2005**, *55*, 271–276.

(54) Pointreau, Y.; Garaud, P.; Chapet, S.; Sire, C.; Tuchais, C.; Tortochaux, J.; Faivre, S.; Guerrif, S.; Alfonsi, M.; Calais, G. Randomized trial of induction chemotherapy with cisplatin and 5-fluorouracil with or without docetaxel for larynx preservation. *J. Natl. Cancer Inst.* **2009**, *101*, 498–506.

(55) Paccagnella, A.; Ghi, M. G.; Loreggian, L.; Buffoli, A.; Koussis, H.; Mione, C. A.; Bonetti, A.; Campostrini, F.; Gardani, G.; Ardizzoia, A.; Dondi, D.; Guaraldi, M.; Cavallo, R.; Tomio, L.; Gava, A. Concomitant chemoradiotherapy versus induction docetaxel, cisplatin and 5-fluorouracil (TPF) followed by concomitant chemoradiotherapy in locally advanced head and neck cancer: a phase II randomized study. *Ann. Oncol.* **2010**, *21*, 1515–1522.

(56) Theile, D.; Ketabi-Kiyanvash, N.; Herold-Mende, C.; Dyckhoff, G.; Efferth, T.; Bertholet, V.; Haefeli, W. E.; Weiss, J. Evaluation of drug transporters' significance in for multidrug resistance in head and neck squamous cell carcinoma. *Head Neck* **2011**, *33*, 959–968.

(57) (a) Jacobs, C.; Lyman, G.; Velez-Garcia, E.; Sridhar, K. S.; Knight, W.; Hochster, H.; Goodnough, L. T.; Mortimer, J. E.; Einhorn, L. H.; Schacter, L. A phase III randomized study comparing cisplatin and fluorouracil as single agents and in combination for advanced squamous cell carcinoma of the head and neck. *J. Clin. Oncol.* **1992**, *10*, 257–263. (b) Forastiere, A. A.; Metch, B.; Schuller, D. E.; Ensley, J. F.; Hutchins, L. F.; Triozzi, P.; Kish, J. A.; McClure, S.; VonFeldt, E.; Williamson, S. K. Randomized comparison of cisplatin plus fluorouracil and carboplatin plus fluorouracil versus methotrexate in advanced squamous-cell carcinoma of the head and neck: a Southwest Oncology Group study. *J. Clin. Oncol.* **1992**, *10*, 1245–1251.

(58) Lee, J.; Moon, C. Current status of experimental therapeutics for head and neck cancer. *Exp. Biol. Med.* **2011**, *236*, 375–389.

(59) Machiels, J. P.; Schmitz, S. New advances in targeted therapies for squamous cell carcinoma of the head and neck. *Anti-Cancer Drugs* **2011**, *22*, 626–633.

(60) Matta, A.; Ralhan, R. Overview of current and future biologically based targeted therapies in head and neck squamous cell carcinoma. *Head Neck Oncol.* **2009**, *1*, 6.

(61) Raza, S.; Kornblum, N.; Kancharla, V. P.; Baig, M. A.; Singh, A. B.; Kavalari, M. Emerging therapies in the treatment of locally advanced squamous cell carcinomas of the head and neck. *Recent Pat. Anti-Cancer Drug Discovery* **2011**, *6*, 246–257.

(62) Denaro, N.; Russi, E. G.; Colantonio, I.; Adamo, V.; Merlano, M. C. The role of antiangiogenic agents in the treatment of head and neck cancer. *Oncology* **2012**, *83*, 108–116.

(63) (a) Faller, B.; Ertl, P. Computational approaches to determine drug solubility. *Adv. Drug Delivery Rev.* **2007**, *59*, 533–545. (b) Delaney, J. S. Predicting aqueous solubility from structure. *Drug Discovery Today* **2005**, *10*, 289–295.

(64) (a) Tetko, I. V.; Tanchuk, V. Y.; Kasheva, T. N.; Villa, A. E. Estimation of aqueous solubility of chemical compounds using E-state indices. *J. Chem. Inf. Model.* **2001**, *41*, 1488–1493. (b) Tetko, I. V.; Gasteiger, J.; Todeschini, R.; Mauri, A.; Livingstone, D.; Ertl, P.; Palyulin, V. A.; Radchenko, E. V.; Zefirov, N. S.; Makarenko, A. S.; Tanchuk, V. Y.; Prokopenko, V. V. Virtual computational chemistry laboratory – design and description. *J. Comput.-Aided Mol. Des.* **2005**, *19*, 453–463. (c) VCCLAB; Virtual Computational Chemistry Laboratory; <http://www.vcclab.org>, (accessed October 17, 2015).

(65) Tetko, I. V.; Tanchuk, V. Y.; Kasheva, T. N.; Villa, A. E. P. Internet software for the calculation of the lipophilicity and aqueous solubility of chemical compounds. *J. Chem. Inf. Model.* **2001**, *41*, 246–252.

(66) (a) Leach, A. G.; Jones, H. D.; Cosgrove, D. A.; Kenny, P. W.; Ruston, L.; MacFaul, P.; Wood, J. M.; Colclough, N.; Law, B. Matched molecular pairs as a guide in the optimization of pharmaceutical

properties: a study of aqueous solubility, plasma protein binding and oral exposure. *J. Med. Chem.* **2006**, *49*, 6672–6682. (b) Gleeson, P.; Bravi, G.; Modi, S.; Lowe, D. ADMET rules of thumb II: a comparison of the effects of common substituents on a range of ADMET parameters. *Bioorg. Med. Chem.* **2009**, *17*, 5906–5919. (c) Griffen, E.; Leach, A. G.; Robb, G. R.; Warner, D. J. Matched molecular pairs as a medicinal chemistry tool. *J. Med. Chem.* **2011**, *54*, 7739–7750.

(67) Fishburn, C. S. Attenuating attrition. *SciBX* **2013**, *6*(26), doi:10.1038/scibx.2013.647.

(68) Hussain, J.; Rea, C. Computationally efficient algorithm to identify matched molecular pairs (MMPs) in large data sets. *J. Chem. Inf. Model.* **2010**, *50*, 339–348.

(69) Warner, D. J.; Griffen, E.; St-Galley, S. A. WizePairZ: a novel algorithm to identify, encode, and exploit matched molecular pairs with unspecified cores in medicinal chemistry. *J. Chem. Inf. Model.* **2010**, *50*, 1350–1357.

(70) Papadatos, G.; Alkauri, M.; Gillet, V. J.; Willett, P.; Kadirkamanathan, V.; Luscombe, C. N.; Bravi, G.; Richmond, N. J.; Pickett, S. D.; Hussain, J.; Pritchard, J. M.; Cooper, A. W. J.; Macdonald, S. J. F. Lead optimization using matched molecular pairs: inclusion of contextual information for enhanced prediction of hERG inhibition, solubility and lipophilicity. *J. Chem. Inf. Model.* **2010**, *50*, 1872–1886.

(71) Thompson, M. J.; Louth, J. C.; Ferrara, S.; Jackson, M. P.; Sorrell, F. J.; Cochrane, E. J.; Gever, J.; Baxendale, S.; Silber, M. B.; Roehl, H. H.; Chen, B. Discovery of 6-substituted indole-3-glyoxylamides as lead antiprion agents with enhanced cell line activity, improved microsomal stability and low toxicity. *Eur. J. Med. Chem.* **2011**, *46*, 4125–4132.

(72) Zhang, Z.; Yang, Z.; Wong, H.; Zhu, J.; Meanwell, N. A.; Kadow, J. F.; Wang, T. An effective procedure for the acylation of azaindoles at C-3. *J. Org. Chem.* **2002**, *67*, 6226–6227.

(73) Sabot, C.; Kumar, K. A.; Meunier, S.; Mioskowski, C. A convenient aminolysis of esters catalyzed by 1,5,7-triazabicyclo[4.4.0]dec-5-ene (TBD) under solvent-free conditions. *Tetrahedron Lett.* **2007**, *48*, 3863–3866.

(74) Tsuritani, T.; Strotman, N. A.; Yamamoto, Y.; Kawasaki, M.; Yasuda, N.; Mase, T. N-Cyclopropylation of indoles and cyclic amides with copper(II) reagent. *Org. Lett.* **2008**, *10*, 1653–1655.

(75) Nguyen, T. M.; Duong, H. A.; Richard, J.-A.; Johannes, C. W.; Pincheng, F.; Ye, D. K. J.; Shuying, E. L. Cascade fluorofunctionalization of 2,3-unsubstituted indoles by means of electrophilic fluorination. *Chem. Commun.* **2013**, *49*, 10602–10604.

(76) (a) Conner, S. E.; Gossett, L. S.; Green, J. E.; Jones, W. D., Jr.; Mantlo, N. B.; Matthews, D. P.; Mayhugh, D. R.; Smith, D. L.; Vance, J. A.; Wang, X.; Warshawsky, A. M.; Winneroski, L. L., Jr.; Xu, Y.; Zhu, G. Preparation of sulfonamide derivatives, in particular *N,N*-benzo[*b*]thiophene sulfonamides, as PPAR modulators, especially PPAR agonists. (Eli Lilly & Co., USA) WO 2004073606 A2, September 2, 2004; *SciFinder Scholar* AN 2004:718289;. (b) Wilson, D.; Fanning, L. T. D.; Sheth, U.; Martinborough, E.; Termin, A.; Neubert, T.; Zimmermann, N.; Knoll, T.; Whitney, T.; Katarikar, A.; Lehsten, D.; Stamos, D.; Zhou, J.; Arumugam, V.; Gutierrez, C. Heterocyclic derivatives as modulators of ion channels and their preparation, pharmaceutical compositions and use in the treatment of diseases. (Vertex Pharmaceuticals Inc., USA) WO 2007075892 A2, July 5, 2007; *SciFinder Scholar* AN 2007:730896.

(77) Yeom, C.-E.; Kim, M. J.; Kim, B. M. 1,8-Diazabicyclo[5.4.0]-undec-7-ene (DBU)-promoted efficient and versatile aza-Michael reaction. *Tetrahedron* **2007**, *63*, 904–909.

(78) Amato, G.; Roeloffs, R.; Rigdon, G. C.; Antonio, B.; Mersch, T.; McNaughton-Smith, G.; Wickenden, A. G.; Fritch, P.; Suto, M. J. *N*-Pyridyl and pyrimidine benzamides as KCNQ2/Q3 potassium channel openers for the treatment of epilepsy. *ACS Med. Chem. Lett.* **2011**, *2*, 481–484.

(79) Kel'in, A. V.; Sromek, A. W.; Gevorgyan, V. A novel Cu-assisted cycloisomerization of alkynyl imines: efficient synthesis of pyrroles and pyrrole-containing heterocycles. *J. Am. Chem. Soc.* **2001**, *123*, 2074–2075.

- (80) Li, H.; Xia, Z.; Chen, S.; Koya, K.; Ono, M.; Sun, L. Development of a practical synthesis of STA-5312, a novel indolizine oxalylamide microtubule inhibitor. *Org. Process Res. Dev.* **2007**, *11*, 246–250.
- (81) Debnar, T.; Dreisigacker, S.; Menche, D. Highly regioselective opening of zirconacyclopentadienes by remote coordination: concise synthesis of the furan core of the leupyrins. *Chem. Commun.* **2013**, *49*, 725–727.
- (82) Chen, Y.-J.; Huang, W.-C.; Wei, Y.-L.; Hsu, S.-C.; Yuan, P.; Lin, H. Y.; Wistuba, I. I.; Lee, J. J.; Yen, C.-J.; Su, W.-C.; Chang, K.-Y.; Chang, W.-C.; Chou, T.-C.; Chou, C.-K.; Tsai, C.-H.; Hung, M.-C. Elevated BCRP/ABCG2 expression confers acquired resistance to gefitinib in wild-type EGFR-expressing cells. *PLoS One* **2011**, *6*, e21428.
- (83) (a) Shelanski, M. L.; Gaskin, F.; Cantor, C. R. Microtubule assembly in the absence of added nucleotides. *Proc. Natl. Acad. Sci. U. S. A.* **1973**, *70*, 765–768. (b) Lee, J. C.; Timasheff, S. N. In vitro reconstitution of calf brain microtubules: effects of solution variables. *Biochemistry* **1977**, *16*, 1754–1764.
- (84) Bonne, D.; Heusèle, C.; Simon, C.; Pantaloni, D. 4',6-Diamidino-2-phenylindole, a fluorescent probe for tubulin and microtubules. *J. Biol. Chem.* **1985**, *260*, 2819–2825.
- (85) Cortese, F.; Bhattacharyya, B.; Wolff, J. Podophyllotoxin as a probe for the colchicine binding site of tubulin. *J. Biol. Chem.* **1977**, *252*, 1134–1140.
- (86) Wallner, B. P.; Schwartz, B. E.; Komarnitsky, P. B.; Bacher, G.; Kutscher, B.; Raab, G. Use of indolyl-3-glyoxylic acid derivatives including indibulin, alone or in combination with further agents for treating cancer. (Ziopharm Oncology Inc., USA) WO 2008066807 A1, Jun 5, 2008; *SciFinder Scholar* AN 2008:673085.
- (87) Yamada, H. Y.; Gorbsky, G. J. Spindle checkpoint function and cellular sensitivity to antimetabolic drugs. *Mol. Cancer Ther.* **2006**, *5*, 2963–2969.
- (88) Harker, W. G.; Sikic, B. I. Multidrug (pleiotropic) resistance in doxorubicin-selected variants of the human sarcoma cell line MES-SA. *Cancer Res.* **1985**, *45*, 4091–4096.
- (89) Chen, G.; Jaffrézou, J.-P.; Fleming, W. H.; Durán, G. E.; Sikic, B. I. Prevalence of multidrug resistance related to activation of the *Mdr1* gene in human sarcoma mutants derived by single-step doxorubicin selection. *Cancer Res.* **1994**, *54*, 4980–4987.
- (90) Nakamura, T.; Sakaeda, T.; Ohmoto, N.; Tamura, T.; Aoyama, N.; Shirakawa, T.; Nakamura, T.; Kim, K. I.; Kim, S. R.; Kuroda, Y.; Matsuo, M.; Kasuga, M.; Okumura, K. Real-time quantitative polymerase chain reaction for MDR1, MRP1, MRP2 and CYP3A-mRNA levels in Caco-2 cell lines, human duodenal enterocytes, normal colorectal tissues, and colorectal adenocarcinomas. *Drug Metab. Dispos.* **2002**, *30*, 4–6.
- (91) Gutmann, H.; Fricker, G.; Török, M.; Michael, S.; Beglinger, C.; Drewe, J. Evidence for different ABC-transporters in Caco-2 cells modulating drug uptake. *Pharm. Res.* **1999**, *16*, 402–407.
- (92) Xia, C. Q.; Liu, N.; Yang, D.; Miwa, G.; Gan, L.-S. Expression, localization and functional characteristics of breast cancer resistance protein in Caco-2 cells. *Drug Metab. Dispos.* **2005**, *33*, 637–643.
- (93) Breslin, S.; O'Driscoll, L. Three-dimensional cell culture: the missing link in drug discovery. *Drug Discovery Today* **2013**, *18*, 240–249.
- (94) Hirschhaeuser, F.; Menne, H.; Dittfeld, C.; West, J.; Mueller-Klieser, W.; Kunz-Schughart, L. A. Multicellular tumor spheroids: an underestimated tool is catching up again. *J. Biotechnol.* **2010**, *148*, 3–15.
- (95) Colley, H. E.; Hearnden, V.; Avila-Olias, M.; Cecchin, D.; Canton, I.; Madsen, J.; MacNeil, S.; Warren, N.; Hu, K.; McKeating, J. A.; Armes, S. P.; Murdoch, C.; Thornhill, M. H.; Battaglia, G. Polysome-mediated delivery of combination anticancer therapy to head and neck cancer cells: 2D and 3D *in vitro* evaluation. *Mol. Pharmaceutics* **2014**, *11*, 1176–1188.
- (96) (a) Kadletz, L.; Heiduschka, G.; Domayer, J.; Schmid, R.; Enzenhofer, E.; Thurnher, D. Evaluation of spheroid head and neck squamous cell carcinoma cell models in comparison to monolayer cultures. *Oncol. Lett.* **2015**, *10*, 1281–1286. (b) Tupper, J.; Greco, O.; Tozer, G. M.; Dachs, G. U. Analysis of the horseradish peroxidase/indole-3-acetic acid combination in a three-dimensional tumor model. *Cancer Gene Ther.* **2004**, *11*, 508–513.
- (97) Huang, T.-H.; Chiu, S.-J.; Chiang, P.-H.; Chiou, S.-H.; Li, W.-T.; Chen, C.-T.; Chang, C. A.; Chen, J.-C.; Lee, Y.-J. Antiproliferative effects of *N*-heterocyclic indole glyoxylamide derivatives on human lung cancer cells. *Anticancer Res.* **2011**, *31*, 3407–3416.
- (98) Li, W.-T.; Yeh, T.-K.; Song, J.-S.; Yang, Y.-N.; Chen, T.-W.; Lin, C.-H.; Chen, C.-P.; Shen, C.-C.; Hsieh, C.-C.; Lin, H.-L.; Chao, Y.-S.; Chen, C.-T. BPROC305, and orally active microtubule-disrupting anticancer agent. *Anti-Cancer Drugs* **2013**, *24*, 1047–1057.
- (99) Hu, C.-B.; Chen, C.-P.; Yeh, T.-K.; Song, J.-S.; Chang, C.-Y.; Chu, J.-J.; Tung, F.-F.; Ho, P.-Y.; Chen, T.-W.; Lin, C.-H.; Wang, M.-H.; Chang, K.-Y.; Huang, C.-L.; Lin, H.-L.; Li, W.-T.; Hwang, D.-R.; Chern, J.-H.; Hwang, L.-L.; Chang, J.-Y.; Chao, Y.-S.; Chen, C.-T. BPROC261 is a novel orally active antitumor agent with antimetabolic and anti-angiogenic activities. *Cancer Sci.* **2011**, *102*, 182–191.
- (100) Li, W.-T.; Hwang, D.-R.; Chen, C.-P.; Shen, C.-W.; Huang, C.-L.; Chen, T.-W.; Lin, C.-H.; Chang, Y.-L.; Chang, Y.-Y.; Lo, Y.-K.; Tseng, H.-Y.; Lin, C.-C.; Song, J.-S.; Chen, H.-C.; Chen, S.-J.; Wu, S.-H.; Chen, C.-T. Synthesis and biological evaluation of *N*-heterocyclic indolyl glyoxylamides as orally active anticancer agents. *J. Med. Chem.* **2003**, *46*, 1706–1715.
- (101) Thompson, M. J.; Louth, J. C.; Ferrara, S.; Sorrell, F. J.; Irving, B. J.; Cochrane, E. J.; Meijer, A. J. H. M.; Chen, B. Structure–activity relationship refinement and further assessment of indole-3-glyoxylamides as a lead series against prion disease. *ChemMedChem* **2011**, *6*, 115–130.
- (102) Baell, J. B. Screening-based translation of public research encounters painful problems. *ACS Med. Chem. Lett.* **2015**, *6*, 229–234.
- (103) Fitton, A. O.; Hill, J.; Jane, D. E.; Millar, R. Synthesis of simple oxetanes carrying reactive 2-substituents. *Synthesis* **1987**, *1987*, 1140–1142.